Spring 2017

Optimal precoder design for wireless communication and power transfer from distributed arrays

Sairam Goguri
University of Iowa

OPTIMAL PRECODER DESIGN FOR WIRELESS COMMUNICATION AND POWER TRANSFER FROM DISTRIBUTED ARRAYS

by

Sairam Goguri

A thesis submitted in partial fulfillment of the
requirements for the Doctor of Philosophy
degree in Electrical and Computer Engineering
in the Graduate College of
The University of Iowa

May 2017

Thesis Supervisors: Professor Raghuraman Mudumbai
Professor Soura Dasgupta

Graduate College
The University of Iowa
Iowa City, Iowa

CERTIFICATE OF APPROVAL

PH.D. THESIS

This is to certify that the Ph.D. thesis of

Sairam Goguri

has been approved by the Examining Committee for the thesis requirement for the Doctor of Philosophy degree in Electrical and Computer Engineering at the May 2017 graduation.

Thesis Committee: _____
Raghu Mudumbai, Thesis Supervisor

_____
Soura Dasgupta, Thesis Supervisor

_____
Sudhakar Reddy

_____
Mathews Jacob

_____
David Love

To my mother Manjula Goguri, my father Shankar Reddy Goguri, my brother Satyapal Reddy Goguri and my sister-in-law Srujana Reddy Vangala.

ACKNOWLEDGEMENTS

I would like to take this opportunity to offer my sincere gratitude to my advisors Professor Raghuraman Mudumbai and Professor Soura Dasgupta, who have always been a source of inspiration and will always hold them in high regard. I am highly indebted for their immense support and constant guidance that have ensured continuous progress and completion of this thesis.

I would like to express my sincere thanks to Professor Sudhakar Reddy, without whom I would not have come to the University of Iowa for pursuing my Ph.D. and also for his constant guidance throughout the program and even before joining the University of Iowa. I would like to thank my committee members Professor Jacob Mathews and, Professor David Love from Purdue University for sharing their perspective. I would also like to extend my sincere thanks to Professor Anton Kruger for his constant support and encouragement in performing experiments that were of immense help to my thesis. I am also thankful to our collaborators in other universities, Professor Upamanyu Madhow and Professor Rick Brown, for their help and feedback.

I would like to thank the support of the faculty of Department of Electrical and Computer Engineering, the University of Iowa for sharing their knowledge and Ms. Cathy Kern and Dina Blanc for their support throughout the program. I would also like extend my sincere thanks to Mr. Navin Rao, an alumnus of Department of Electronics and Communication Engineering, Osmania University for introducing me

to Professor Sudhakar Reddy.

I would like to thank Tomohiro Arakawa from Purdue University for conducting one of the experiments that were of immense help to this work. I would like to extend my sincere thanks to seniors, Dr. Achanta Hema, Dr. Henry Baidoo Williams for their support and guidance throughout the program and lab mates, in particular to Meheli Basu and Benjamin Peiffer for the frequent conversations and help. I would also like to thank my long time friend Phani Krishna for his constant support. I would also like to thank Laxmi Shanthi Chede, Sriram Hemachandran, and Sayan Bandyapadhyay for all the help they extended to me in my stay away from home.

ABSTRACT

Distributed MIMO (DMIMO) communications and specifically the idea of distributed transmit beamforming involves multiple transmitters coordinating among themselves to form a virtual antenna array and steer a beam to one or more receivers. Recent works have successfully demonstrated this concept of beamforming with narrowband, frequency-flat wireless channels. We consider the generalization of this concept to wideband, frequency selective channels and propose two Figures of Merit (FOMs), namely, communication capacity and received power to measure the performance of beamforming.

We formulate the precoder design that maximizes the two FOMs as optimization problems and derive general properties of the optimal precoders. The two metrics are equivalent with frequency-flat channels, whereas, they result in vastly different optimal criteria with wideband channels. The capacity maximizing solution also differs from classical water-filling due to the per-transmitter power constraints of the distributed beamforming setting, whereas, the power maximizing solution involves the array nodes concentrating their power in a small, finite set of frequencies resulting in an overall received signal consisting of a small number of sinusoidal tones. We have not been able to derive closed-form solutions for the optimal precoders, but we provide fixed point algorithms that efficiently computes these precoders numerically. We show using simulations that solution to both these maximization problems can yield substantially better performance as compared to simple alternatives such as equal

power allocation. The fixed point algorithms also suggest a distributed implementation where each node can compute these precoders on their own iteratively using feedback from a cooperating receiver. We also establish the relationship between various precoders.

The idea of maximizing received power suggests a natural application of wireless power transfer(WPT). However, the large-scale propagation losses associated with radiative fields makes antennas unattractive for WPT systems. Motivated by this observation, we also consider the problem of optimizing the efficiency of WPT to a receiver coil from multiple transmitters using near-field coupling. This idea of WPT using near-field coupling is not new; however, the difficulty of constructing tractable and realistic circuit models has limited the ability to accurately predicting and optimizing the performance of these systems. We present a new simple theoretical model and take the more abstract approach of modeling the WPT system as a linear circuit whose input-output relationship is expressed in terms of a small number of unknown parameters. We present a simple derivation of the optimal voltage excitations to be applied at the transmitters to maximize efficiency, and also some general properties of the optimal solution. Obviously, the optimal solution is a function of unknown parameters, and we describe a procedure to estimate these parameters using a set of direct measurements. We also present a series of experimental results, first, with two transmitter coils and a receiver coil in a variety of configurations and then with four transmitter coils and two receiver coils to illustrate our approach and the efficiency increase achieved by using the calculated optimal solution from our model.

PUBLIC ABSTRACT

Multiple antenna communication (MIMO) systems have well-known advantages such as increased spectral and energy efficiency through *spatial multiplexing* and *beamforming*. However, the applicability of MIMO systems is often limited by physical constraints such as size and dimensions. One approach to overcome these limitations is by using Distributed MIMO (DMIMO), where a group of single small antenna transmitting devices form a virtual antenna array emulating the functionality of centralized MIMO systems. The idea of *beamforming* is to ensure that the transmissions of the individual array nodes combine constructively at the intended receiver and successful demonstration of distributed transmit narrowband beamforming leads to a natural problem of wideband beamforming. This work deals with the specific problem of wideband beamforming and proposes two natural Figures of Merit, namely, capacity and received power to measure the performance of beamforming.

The idea of maximizing received power suggests a natural application of wireless power transfer(WPT). However, the use of antennas for WPT is not a viable option because of high propagation losses associated with radiative fields and hence, most WPT systems use near-field coupling. Recent applications of WPT systems for wireless charging of mobile devices, biomedical implants has drawn a lot of interest from researchers. We also deal with the problem of maximizing the WPT efficiency to a single receiver coil from multiple transmit coils to overcome some of the limitations of existing work by using a more abstract approach.

TABLE OF CONTENTS

LIST OF TABLES

Table

LIST OF FIGURES

Figure

LIST OF ALGORITHMS

Algorithm

CHAPTER 1
INTRODUCTION

Recent advancements in WiFi and Cellular standards such as 802.11n, 802.11ac, Long-Term Evolution (LTE) have MIMO (Multiple-Input Multiple-Output) as an integral part. However, the applicability of MIMO is often limited by physical and economic constraints. For example, mobile devices because of their form factor can only support a small number of antennas. Even for infrastructure nodes such as base stations, MIMO transceivers with a large number of antennas can result in bulky systems [3]. One approach to overcome these limitations is by using Distributed MIMO (DMIMO), which envisions the cooperation of a group of distributed transmitters to form a virtual antenna array emulating the functionality of centralized MIMO systems, as shown in Fig. 1.1. This concept can enable cooperation between a number of small, single antenna wireless devices to obtain the benefits of multi-antenna communication techniques such as increased spectral and energy efficiency through *spatial multiplexing* and *beamforming* on a potentially large scale. Recently, this concept of DMIMO in general [3, 4] and the idea of distributed transmit beamforming in particular [4], has captured the attention of researchers.

The idea of *beamforming* is to ensure that the transmissions of the individual array nodes combine constructively at the intended receiver; this has the effect of *focusing* the transmitted energy of the distributed array spatially in the direction of the intended receiver. The directivity increases linearly with the array size n, which given a power constraint on each individual transmitter translates to a factor of n^2

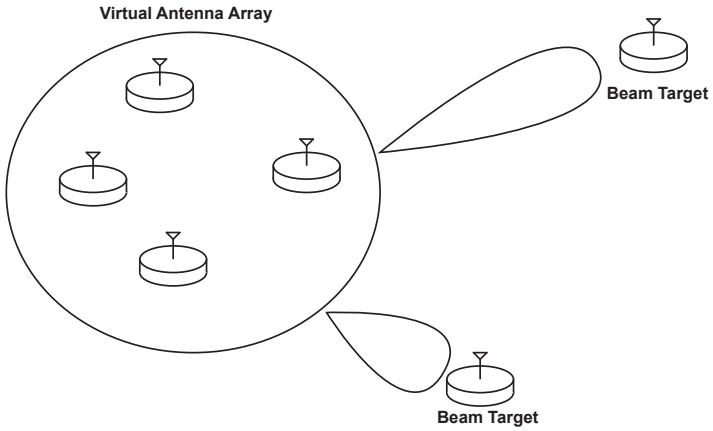

Figure 1.1: The concept system includes a distributed transmit antenna array which consists of a large number of cooperating nodes that form a virtual antenna array and external beam targets

increase in the received power, which can be substantial for large arrays.

Prior work on distributed transmit beamforming has focused on narrowband beamforming, where the wireless propagating channels are assumed to be frequency-flat. This work deals with the problem of broadband or wideband beamforming, where the wireless channels are frequency selective.

1.1 Motivation

In the case of narrowband beamforming, since the wireless channels are frequency flat, each channel can be represented by a single complex number. Let h_i denote the complex channel gain between the i-th node and the receiver. Assuming that all the nodes in the array are pre-synchronized (zero phase and frequency-offset

between nodes), the complex baseband signal at the receiver which is the superposition of signals from each node in the transmit array, in the absence of noise is given by:

$$y(t) = \sum_{i=1}^{n} h_i g_i x(t) \tag{1.1}$$

where g_i is the *precoding weight* applied by the i-th node and $x(t)$ is the common message signal transmitted from all the nodes in the transmit array.

With precoding weights of $g_i = \alpha_i e^{-j\angle h_i}$ for some real-valued $\alpha_i > 0$ at the i-th node, individual signals from each node arrive with zero phase and hence add constructively to form a beam at the receiver. The values of α_i are chosen to satisfy power constraints at each node.

We can see that this choice of precoding weights maximizes the signal power and hence, maximizes the *signal to noise ratio* or SNR at the receiver assuming that the transmit power at each node is constrained. In this case, maximizing SNR also maximizes the total communication capacity of the distributed array to the receiver.

For wideband systems, we denote the frequency selective channel between the i-th node and the receiver by $H_i(f)\ \forall f \in \mathcal{B}$, where $\mathcal{B}$ is the bandwidth available for transmission. The signal at the receiver, similar to the case of narrowband beamforming is the superposition of signals from each node,

$$Y(f) = \sum_{i=1}^{n} H_i(f) G_i(f) X(f) \tag{1.2}$$

where $G_i(f)$ is the *precoding filter* or *precoder* applied by the i-th node at frequency f and $X(f)$ is the Fourier transform of the common message signal.

Similar to narrowband beamforming, choosing the phase response of the precoding filter to be the opposite of the channel phase for each user over the entire frequency band, i.e., $\angle G_i(f) = -\angle H_i(f)\ \forall\ i$ and $f \in \mathcal{B}$, ensures that the signals arrive with zero phase and form a beam at the receiver over the entire frequency band, $\mathcal{B}$.

Thus, for the transmissions of distributed array to be coherent at the receiver, the phase response of the precoding filter is fully determined, unlike the magnitude response which can be chosen to optimize various figures of merit. The magnitude response of the precoder basically dictates how the total transmit power at each array node is allocated across the frequency band and each node faces a tradeoff between concentrating all its power in the frequency band where it has the strongest channel to the receiver and using its power to augment the transmissions of other nodes. It turns out that different optimality criteria lead to vastly different power allocating strategies in the case of wideband beamforming.

1.2 Relation between capacity and power maximization

As mentioned before, beamforming maximizes capacity and received power for narrowband distributed arrays. We now argue that the relationship is much more interesting with wideband arrays. We start by considering the simple case of a single transmitter (not a distributed array) and receiver with a frequency selective channel. In this case, to maximize received power, the optimal solution is to concentrate all the power at a single frequency at which channel is the strongest. However, the capacity

maximizing solution is to spread the power equally across the frequency band at high SNR, which is exactly the opposite of power maximizing solution and at low SNR, the maximizing capacity solution obeys waterfilling [5]. As the SNR asymptotically approaches zero, the capacity maximizing and the power maximizing solution turn out to be equivalent. Thus, even with a single transmitter the relationship between capacity and power maximizing can be very different depending on the SNR.

With distributed arrays, it is easy to construct an example where it is sub-optimal in terms of received power for all the nodes to concentrate all the power in a single frequency. Consider a distributed array with 2 nodes, where one of the nodes has a strong channel in the first half of the frequency band and the second node has a strong channel in another half of the frequency band. In this case, it is easy to see that maximum received power is obtained when each node individually tries to maximize its own power at the receiver which means concentrating power in 2 frequencies. Again with arrays as with a single transmitter, the nature of capacity maximizing solution varies a lot with SNR. At high SNR, we again expect that it is nearly-optimal for all nodes to spread their power equally across the frequency band and at low SNR, we expect the capacity maximizing solution to approach the power maximizing solution.

1.3 Background and contribution

We now present a quick overview of the previous work related to distributed beamforming. A key feature of this is the recognition that classical MIMO methods

designed for centralized arrays are not directly applicable to distributed arrays as these methods do not account for clock offsets arising from separate oscillators on the nodes [6]. Novel synchronization methods have been developed which allow distributed array nodes to synchronize themselves [7–10], and determine a set of array weights that steer beams and *nulls (nullforming)* to specific receivers [11]. Recent experimental demonstrations of beamforming [12–16] and nullforming [17] using explicit [18], implicit channel feedback [19], retrodirective techniques [20] and spatial multiplexing [21] from distributed arrays in a variety of configurations e.g. Access Points in WiFi networks [22], cellular Base Stations [23] have shown tremendous promise about the practical feasibility of these methods. Most of these works on distributed beamforming have focused on the narrowband case, except [24] which presents preliminary results on extending feedback-based algorithms to frequency selective channels. The tremendous experimental and conceptual progress on narrowband beamforming motivates a generalization to wideband beamforming.

The problem of wideband capacity maximization is well studied for single transmitter single receiver where the optimal solution follows the well-known method of waterfilling [5]. The capacity maximization problem is also well studied for MIMO systems with centralized arrays and for vector multiple-access channels [1, 25]. In both the cases, the optimal solution still follows waterfilling. Distributed arrays are characterized by individual transmit power constraint on each node and differ from centralized arrays which have aggregate total transmit power constraint [2]. Also, distributed arrays, unlike Multiple Access Channel (MAC) sources, allow transmitter

nodes to cooperatively send a shared message signal. In other words, distributed arrays are *more constrained than centralized arrays, but are more flexible than MAC channel sources*. Therefore, MAC channels and centralized arrays provide lower and upper bounds respectively, to the performance of distributed arrays.

The problem of maximizing the total received power from a centralized array is quite trivial as all the nodes can coordinate and pick a strong channel. However, the problem we consider [26] of maximizing received power subject to per-transmitter power constraints on each array node is novel. The main contribution of this work is to determine this optimal precoding solution and develop some insights into how it depends on the channel responses.

1.4 Maximizing wireless power transfer efficiency

We also consider the problem of optimizing the power transfer efficiency of a MISO WPT system that transfers power from multiple transmitting coils to a single receiver. The idea of maximizing received power naturally suggests the application of wireless power transfer(WPT). However, the large propagation losses associated with radiative fields results in small power transfer efficiency making antennas a poor choice for building WPT systems. Hence, most of the WPT systems use near-field inductive coupling to transfer power from a single or multiple transmitting coils to a single or multiple receivers.

The physical principle behind inductive-coupled WPT systems is very simple and has been known now for 150 years: applying AC voltages to drive currents in

the transmitter coils produces induced currents in a receiver coil which can then supply power to a resistive load without any wired power supply. However, some of the transmitted power is also unavoidably dissipated to various loss mechanisms e.g. radiation, parasitic resistances and undesired eddy currents in conducting surfaces near the transmitter coils. Fundamentally, the problem of designing efficient WPT systems can be thought of as the problem of minimizing these losses, so that as much of the transmitted power is conveyed to the receiver as possible.

The attractions of wireless power transfer technology are especially obvious given the recent proliferation of powerful mobile computing platforms e.g., smartphones, watches, and fitness trackers. There now exist international standards [27] for inductive WPT and commercial products supporting these standards are widely available. However, present-day devices are still mostly limited to short-range and low power applications [28,29] and their efficiency can often be quite low [30]. As a result, wireless power transfer remains an area of very active research and development.

Many methods have been proposed in recent work to achieve efficient WPT systems. One such technique is resonant coupling where the transmitter and receiver are both designed to resonate with high Q at the same frequency; this technique has been used for instance to light up a 60 W lightbulb with around 50% efficiency at a distance of a few feet [31], which is significantly better than the performance of non-resonant coupled systems. However, the performance of resonant coupled systems is sensitive to the presence of other conducting objects near the coils and the geometry of the coils [32, 33], and it is challenging in practice to keep the system in

resonance [32, 34, 35].

Another recently proposed idea is to use multiple transmitter coils [36, 37] to focus the energy of the magnetic field towards the receiver. This idea is superficially similar to beamforming from phased array antennas and the analogy can be useful [38]. However, it is important to keep in mind that the physics of radiative electromagnetic fields from antennas is very different from that of magnetic near-fields. Indeed, we illustrate in our experimental results that beamforming at the receiver - is not necessarily optimal for WPT systems.

A common challenge in all of the previous work on WPT systems is the difficulty of building accurate models that can predict the power transfer efficiency well enough to tune and optimize the system. The most common approach in previous work is to model WPT systems as lumped RLMC circuits which can then be analyzed using standard circuits solving techniques. The problem is that an accurate and realistic circuit model requires a complex circuit that captures the many different loss mechanisms in WPT systems; furthermore, the L and M circuit elements require rather complex numerical calculations, and the M values are very sensitive to small changes in the geometry of the system. Some previous work has also used models for WPT systems based on coupled-mode theory [31], this approach, however, has been shown to be equivalent [39] to the RLMC circuit model and suffers from similar difficulties.

1.4.1 Our approach

Our approach is most easily explained using an analogy with wireless channel modeling. Just as in WPT systems, wireless communication engineers have long faced the problem that it is extremely difficult to accurately calculate the frequency response of the propagation channel from the physics of EM fields in space, especially in non-Line of Sight situations. Instead, the channel response is typically estimated in real-time at the receiver using known training sequences or other a-priori knowledge about the signal emitted by the transmitter e.g. a constant envelope property.

This is exactly what we propose to do for WPT systems. Specifically, we assume that the WPT system is represented by an unknown multi-terminal linear circuit; we consider the transmitter terminals as inputs and receiver as the output and express the input-output relationship between the terminal voltages and currents using a minimal number of unknown impedance and transconductance parameters [40]. We propose to directly estimate these parameters using a series of simple measurements. Calculating the input excitations to this MISO system that yields maximum power transfer efficiency is then a simple analytical exercise.

1.5 Outline

In chapter 2, we formulate the optimization problems of maximizing communication capacity, received power and derive properties of the resulting optimal solutions. We also present a systematic analysis of the properties of the various precoders. In chapter 3, we present fixed point algorithms to numerically compute the

capacity and power maximizing precoders and describe how aggregate feedback from a cooperating receiver can be used to compute these precoders in a distributed fashion at each node. In chapter 4, we formulate the problem of maximizing the efficiency of wireless power transfer (WPT) system using multiple transmitting coils to a single receiver coil and also present experimental results. Chapter 5 concludes and presents some potential future research direction.

CHAPTER 2
FORMULATION OF PRECODERS TO MAXIMIZE CAPACITY AND RECEIVED POWER

In this chapter, we formulate the optimization problems that maximize the two FOMs with wideband beamforming. First, we look at the problem of maximizing communication capacity followed by the problem of maximizing received power and finally, derive the relationship between various precoders.

2.1 Overview

Consider a distributed transmit array with n transmitters indexed by $i \in \{1, \cdots, n\}$ with complex channels to the receiver with a frequency response $H_i(f), \forall i \in \{1, 2, ..., n\}$ and $f \in \mathcal{B}$, where $\mathcal{B}$ is the total bandwidth available for transmission. Suppose each transmitter transmits a common message signal $X(f)$ over $\mathcal{B}$ after precoding by the complex gain $G_i(f)$, the aggregate signal at the receiver is given by,

$$Y(f) = \sum_i Y_i(f), \text{ where } Y_i(f) = G_i(f)H_i(f)X(f)$$

We divide the frequency band of bandwidth $\mathcal{B}$ into a discrete set of subcarriers centered around the frequencies f_k, $k \in \{1, 2, \ldots, K\}$, and the number of these subcarriers or subchannels are $K = \mathcal{B} \times T$, where $\mathcal{B}$ and T are the total two-sided bandwidth and duration of the signal to be transmitted respectively. We lose no essential generality when we consider a discretized frequency space; we can choose T as large as necessary to increase the frequency resolution, and taking the limit $T \to \infty$ will yield the continuous frequency space. The complex baseband channel seen by the

i-th transmitter on the k-th subchannel centered around frequency f_k is denoted by $H_i(f_k)$ while the precoding filter applied by i-th transmitter on the k-th subchannel is denoted by $G_i(f_k)$. The aggregate received signal on the k-th subchannel is

$$y(f_k) = x(f_k) \sum_{i=1}^{n} G_i(f_k) H_i(f_k) \tag{2.1}$$

and the corresponding power in the received signal on the k-th subchannel is

$$\begin{aligned} P_R(f_k) = E\left(|y(f_k)|^2\right) &= E\left(|x(f_k)|^2\right) \left| \sum_{i=1}^{n} G_i(f_k) H_i(f_k) \right|^2 \\ &= P_x(f_k) \left| \sum_{i=1}^{n} G_i(f_k) H_i(f_k) \right|^2 \end{aligned}$$

where $P_x(f_k) \doteq E\left(|x_k|^2\right)$. Without loss of generality, we assume that the message signal has unit power,i.e.,

$$P_x(f_k) = 1 \tag{2.2}$$

Hence, the received signal power on the k-th subchannel further reduces to

$$P_R(f_k) = E\left(|y(f_k)|^2\right) = \left| \sum_{i=1}^{n} G_i(f_k) H_i(f_k) \right|^2 \tag{2.3}$$

The aim is to design a set of precoding filters $G_i(f)$ that maximize a considered FOM subject to *per-transmitter power constraints on each array node*, which implies that the total transmitted power by each node, $P_{T,i}$ is a constant. The total transmitted power by the i-th transmitter is $P_{T,i} = \sum_{k=1}^{K} P_x(f_k) \left|G_i(f_k)\right|^2 \ \forall i \in \{1, 2, ..., n\}$ and with (2.2), the total transmitted power reduces to

$$P_{T,i} = \sum_{k=1}^{K} \left|G_i(f_k)\right|^2 \ \forall i \in \{1, 2, ..., n\} \tag{2.4}$$

In both maximization problems, we assume that each transmitter transmits unit power, i.e, $P_{T,i} = 1 \ \forall i \in \{1, 2, ..., n\}$. We also note that the maximum received power on target scales linearly with P_T where $P_{T,i} = P_T \ \forall i \in \{1, 2, ..., n\}$, unlike maximum communication capacity.

To avoid trivialities we make the following assumption.

Assumption 2.1

$$h_i(f_k) \neq 0, \ \forall \ i \in \{1, \cdots, n\}, k \in \{0, \cdots, K\} \tag{2.5}$$

2.2 Precoder for maximizing capacity

The communication capacity of the MISO channel in the presence of white noise with a unit power spectral density can be written as:

$$\sum_{k=1}^{K} \log_2 \left(1 + \left| \sum_{i=1}^{n} G_i(f_k) H_i(f_k) \right|^2 \right) \tag{2.6}$$

Note: In general, capacity of the MISO channel in the presence of colored noise is given by:

$$\sum_{k=1}^{K} \log_2 \left(1 + \frac{\left| \sum_{i=1}^{n} G_i(f_k) H_i(f_k) \right|^2}{\sigma_k^2} \right) \tag{2.7}$$

where σ_k^2 is the noise variance in the k-th subchannel. As a consequence of the data processing inequality, the capacity would be unchanged if the received signal is passed through a reversible *whitening filter*, $H_w(f)$, as shown in Fig. 2.1, i.e., the capacity of the system shown in Fig. 2.1 is the same as that given by (2.7). We also note that colored noise $w_c(t)$ can be thought of as the output of a *coloring filter* with white noise as the input as shown in Fig. 2.1. We observe that the position of the whitening

filter in Fig. 2.1 can be changed to result in a new system as shown in Fig. 2.2 that is equivalent to the system in Fig. 2.1. As a result of this change, the received signal is corrupted by white noise and the capacity of the system shown in 2.2 is given by (2.6) for which the channels, $H_i(f)$ are given by the *whitened channels*, $H_i(f)H_w(f)$. Hence, using the equivalence between systems shown in Figs. 2.1 and 2.2, we argue that the capacity equation given by (2.6) covers the more general case of capacity with colored noise.

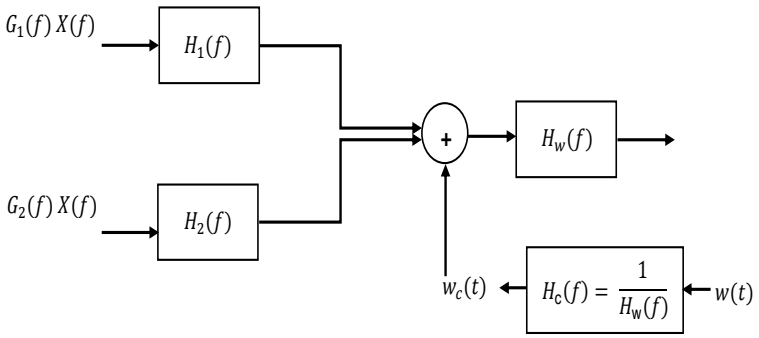

Figure 2.1: A model for a distributed transmit array consisting of 2 nodes with frequency selective channels and colored noise

2.2.1 Simplification and optimization problems

Let $H_i(f_k) = h_i(f_k)e^{j\angle H_i(f_k)}$, where $h_i(f_k)$ describes the magnitude response. It is easy to see that the maximizing solution of (2.6) obeys $G_i(f_k) = g_i(f_k)e^{-j\angle H_i(f_k)}$, i.e., beamforming is necessary and hence, the phase response of the precoder must be

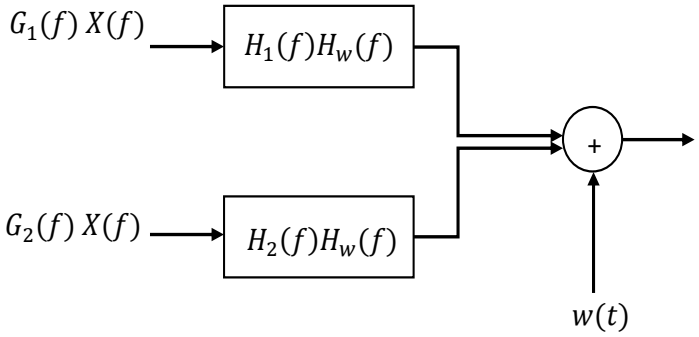

Figure 2.2: Equivalent model to the system represented by Fig. 2.1 with white noise

set to achieve coherence with the other transmitters at every frequency. Therefore, the communication capacity of the MISO channel can be modified as:

$$\sum_{k=1}^{K} \log_2 \left(1 + \left(\sum_{i=1}^{n} g_i(f_k) h_i(f_k) \right)^2 \right) \tag{2.8}$$

Now we present the optimization problems that helps us quantify the best achievable capacity using beamforming for both distributed and centralized setting. As noted earlier, the solution to the centralized system provides an upper bound on maximum achievable capacity with distributed beamforming.

The problem for distributed capacity maximization can be formulated as follows:

Problem 2.1 *Given real non-negative scalars $h_i(f_k)$, find real non-negative scalars $g_i(f_k)$ that maximize*

$$\sum_{k=1}^{K} \log_2 \left(1 + \left(\sum_{i=1}^{n} g_i(f_k) h_i(f_k) \right)^2 \right) \tag{2.9}$$

subject to:

$$\sum_{k=1}^{K} g_i^2(f_k) = 1, \ \forall \ i \in \{1, \cdots, n\} \tag{2.10}$$

The centralized capacity maximization problem with the same definitions can be formulated as:

Problem 2.2 *Given real non-negative scalars $h_i(f_k)$, find real non-negative scalars $g_i(f_k)$ to maximize (2.9) subject to:*

$$\sum_{i=1}^{n} \sum_{k=1}^{K} g_i^2(f_k) = n. \tag{2.11}$$

2.2.2 Optimal criteria for centralized and distributed beamforming

We now derive the optimal criteria for precoders in both centralized and distributed setting.

2.2.2.1 Centralized beamforming

First, we present the capacity maximizing solution of centralized beamforming described by Problem 2.2, and omit details due to its similarity to the traditional water filling methods.

Define the vectors of precoders and SNRs over the k-th subchannel to be respectively

$$\boldsymbol{g}(f_k) = \left[g_1(f_k), \cdots, g_n(f_k)\right]^T \text{ and } \boldsymbol{h}(f_k) = \left[h_1(f_k), \cdots, h_n(f_k)\right]^T. \tag{2.12}$$

Then (2.9) and (2.11) respectively reduce to

$$\sum_{k=1}^{K} \log_2 \left(1 + \left(\boldsymbol{h}^T(f_k)\boldsymbol{g}(f_k)\right)^2\right) \text{ and } \sum_{k=1}^{K} ||\boldsymbol{g}(f_k)||^2 = n.$$

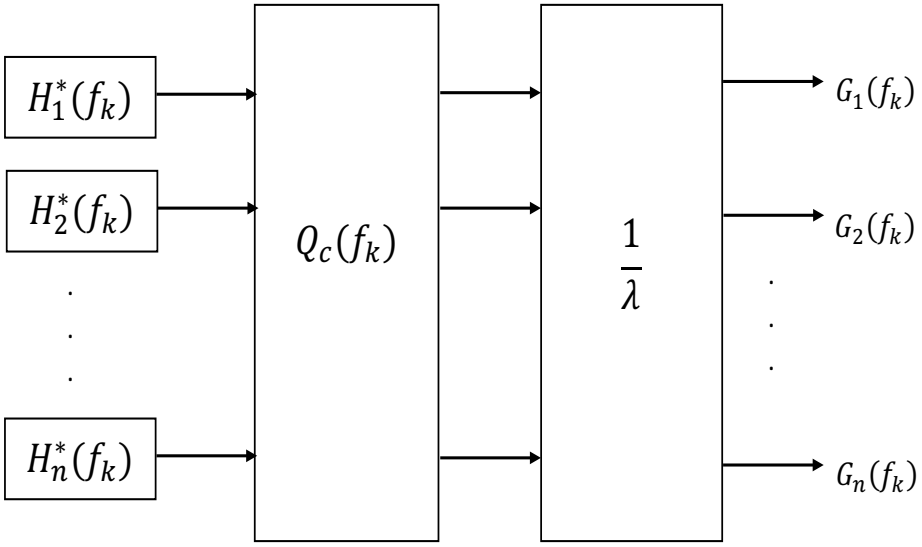

Figure 2.3: Criterion for capacity maximization with centralized beamforming

Thus by the Cauchy-Schwarz inequality, for some real non-negative scalar $Q(f_k)$, the optimizing $\mathbf{g}_k$ obey:

$$\mathbf{g}(f_k) = Q(f_k)\mathbf{h}(f_k), \tag{2.13}$$

Figure 2.3 illustrates the structure of the optimal precoder at every frequency, f_k. We note that the phase of the precoder is set by choosing the complex conjugate of the channel and ensures beamforming for optimality. The pulse-shaping filter, $Q_c(f_k)$ is a function of the channel gains and is common to all the nodes in the array at a given frequency and determines the amount of power allocated by each node. Since, in the centralized scenario, the nodes can coordinate and distribute the total power amongst themselves unlike in the distributed scenario, there is just one total power constraint which determines the scaling constant, λ. We now present the solution

to the scaled version of the pulse-shaping filter, $Q(f_k)$ and using (2.13) Problem 2.2 reduces to: find real non-negative scalar $Q(f_k)$ that maximize

$$\sum_{k=1}^{K} \log_2 \left(1 + Q^2(f_k)||\boldsymbol{h}(f_k)||^4\right)$$

subject to

$$\sum_{k=1}^{K} Q^2(f_k)||\boldsymbol{h}(f_k)||^2 = n.$$

Effectively, the Kn variable complex optimization problem 2.2 has been reduced to an K variable real constrained optimization problem. Arrange the $\boldsymbol{h}(f_k)$ to obey $\|\mathbf{h}(f_k)\| \geq \|\mathbf{h}(f_{k+1})\|$. Suppose L is the largest integer for which

$$\frac{1}{L}\left(n + \sum_{l=0}^{L-1} \frac{1}{\|\mathbf{h}(f_k)\|^2}\right) > \frac{1}{\| \mathbf{h}(f_{L-1})\|^2}. \tag{2.14}$$

Then it can be shown that the optimizing $\mathbf{g}(f_k)$ obey:

$$\mathbf{g}(f_k) = \begin{cases} \frac{\mathbf{h}(f_k)}{\|\mathbf{h}(f_k)\|}\sqrt{\frac{1}{L}\left(n + \sum_{l=0}^{L-1} \frac{1}{\|\mathbf{h}(f_l)\|^2}\right) - \frac{1}{\| \mathbf{h}(f_k)\|^2}} & 0 \leq k \leq L \\ 0 & \text{else} \end{cases}. \tag{2.15}$$

This is in the vein of most classical water filling solutions. Larger n and/or large SNRs means fewer subchannels are silent.

2.2.2.2 Distributed beamforming

We now present the capacity maximizing solution of distributed beamforming described by Problem 2.1. The summation in each logarithm term in (2.9) is over the channel index k, while the constraints in (2.10) are summations in the transmitter index i. Hence, we cannot conclude that the matched filtering condition (2.13) results in optimality. However, as (2.10) only involves the magnitudes of the $G_i(f_k)$,

maximization requires that for some real non-negative $Q_i(f_k)$,

$$g_i(f_k) = Q_i(f_k)h_i(f_k). \tag{2.16}$$

and Problem 2.1 becomes:

Problem 2.3 *Given real non-negative scalar $h_i(f_k)$, find real non-negative scalar $Q_i(f_k)$ to maximize*

$$\sum_{k=1}^{K} \log_2 \left(1 + \left(\sum_{i=1}^{n} Q_i(f_k)h_i^2(f_k)\right)^2\right) \tag{2.17}$$

subject to:

$$\sum_{k=1}^{K} Q_i^2(f_k)h_i^2(f_k) = 1, \ \forall \ i \in \{1, \cdots, n\} \tag{2.18}$$

We now derive the optimality criteria and the separation property.

Theorem 2.1 ***Separation Property:*** *Consider Problem 2.3, with Assumption 2.1 in force. Then there exist real non-negative scalars a_i, $i \in \{1, \cdots, n\}$ and $Q_d(f_k)$, $k \in \{0, \cdots, K\}$, such that at the optimum:*

$$Q_i(f_k) = a_i Q_d(f_k). \tag{2.19}$$

Proof: Consider the Lagrangian with Lagrange multipliers λ_i,

$$\mathcal{L} = \sum_{k=1}^{K} \log_2 \left(1 + \left(\sum_{i=1}^{n} Q_i(f_k)h_i^2(f_k)\right)^2\right) - \sum_{i=1}^{n} \lambda_i \left(\sum_{k=1}^{K} Q_i^2(f_k)h_i^2(f_k) - 1\right) \tag{2.20}$$

The partial derivatives of the Lagrangian at every frequency f_k are:

$$\frac{\partial \mathcal{L}}{\partial Q_i(f_k)} = 2\frac{\sum_{i=1}^{n} Q_i(f_k)h_i^2(f_k)}{1 + \left(\sum_{i=1}^{n} Q_i(f_k)h_i^2(f_k)\right)^2} h_m^2(f_k) - 2\lambda_m Q_i(f_k)h_m^2(f_k)$$

$$\frac{\partial \mathcal{L}}{\partial \lambda_m} = \sum_{k=1}^{K} Q_i^2(f_k)h_i^2(f_k) - 1$$

Under Assumption 2.1, equating the partial derivatives to zero, we get,

$$Q_p(f_q) = \frac{1}{\lambda_p} \frac{\sum_{i=1}^{n} Q_i(f_q) h_i^2(f_q)}{1 + \left(\sum_{i=1}^{n} Q_i(f_q) h_i^2(f_q)\right)^2}. \tag{2.21}$$

Thus $Q_p(f_q)$ is a product of two terms, indexed just by p and q alone.

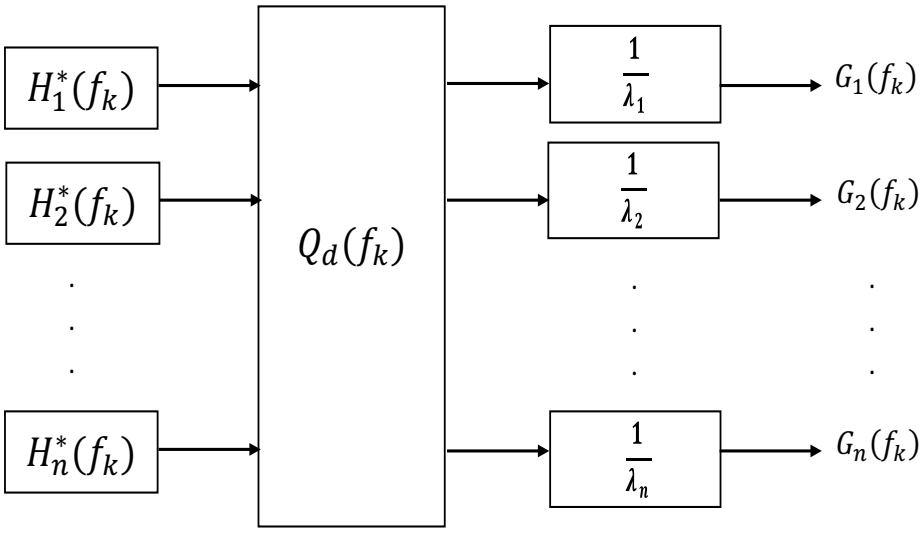

Figure 2.4: Criterion for capacity maximization with distributed beamforming

As a result of separation property, condition (2.16) reduces into a product of two one-variable functions as shown in Fig. 2.4, which illustrates the structure of the optimal precoder at every subchannel frequency. Similar to the centralized case, the phase of the precoder is set by choosing the complex conjugate of the channel that ensures beamforming is achieved for optimality. Even in this case, the pulse-shaping filter, $Q_{\mathrm{d}}(f_k)$ is a function of the channel gains which is common to all the nodes

in the array at a given frequency. Unlike in the centralized scenario, in distributed beamforming, each node has an individual power constraint and hence, there are n power constraints which determine the n scaling constants, λ_i.

Consequence of the separation property: With Assumption 2.1 in force, suppose for some $i \in \{1, \cdots, n\}$ and $k \in \{0, \cdots, K\}$, the optimizing $Q_i(f_k) = 0$. Then for this k and all $l \in \{1, \cdots, n\}$, the optimizing $Q_l(f_k) = 0$. This is so because, from Fig. 2.4 we note that $Q_i(f_k) = 0$ results in the pulse-shaping filter at the frequency f_k is zero, i.e., $Q_{\mathrm{d}}(f_k) = 0$ as the channel is non-zero. Since, the pulse shaping is common to all the nodes, $Q_{\mathrm{d}}(f_k) = 0$ results in $Q_l(f_k) = 0 \ \ \forall l \in \{1, \cdots, n\}$. Hence, if a transmitter is silent on a given subchannel, then *all* transmitters must be silent on this same subchannel.

2.3 Precoder for maximizing received power

The received power on target in each subchannel is given by (2.3) and the total received power is

$$P_R = \sum_{k=1}^{K} P_R(f_k) = \sum_{k=1}^{K} \left| \sum_{i=1}^{n} G_i(f_k) H_i(f_k) \right|^2 \tag{2.22}$$

In this case of maximizing receiver power, the optimization goal is still to find $G_i(f_k)$ that maximize (2.22) subject to the total transmitted power by each transmitter being equal to unity. The optimization problem is as follows:

Problem 2.4 *Given complex scalar $H_i(f_k)$, find complex scalars $G_i(f_k)$ to maximize*

$$\sum_{k=1}^{K} \left| \sum_{i=1}^{n} G_i(f_k) H_i(f_k) \right|^2 \tag{2.23}$$

subject to:

$$\sum_{k=1}^{K} |G_i(f_k)|^2 = 1, \forall\ i = 1, 2, ..., K \tag{2.24}$$

2.3.1 Simplification

Let $H_i(f_k) = h_i(f_k)e^{j\angle H_i(f_k)}$, where $h_i(f_k)$ describes the magnitude response. Similar to the problem of maximizing capacity, the maximum solution obeys $G_i(f_k) = g_i(f_k)e^{-j\angle H_i(f_k)}$, i.e., beamforming is necessary.

Therefore, the optimization problem can be re-formulated as an optimization over just the magnitude responses of the precoders as:

Problem 2.5 *Given $h_i(f_k)$, find $g_i(f_k)$ to maximize*

$$\sum_{k=1}^{K} \left(\sum_{i=1}^{n} g_i(f_k)h_i(f_k) \right)^2$$

subject to:

$$\sum_{k=1}^{K} g_i^2(f_k) = 1 \quad \forall i = 1, 2, ..n$$

The Lagrangian for Problem 2.5 is:

$$\mathcal{L}(\mathbf{g}, \lambda) = \sum_{k=1}^{K} \left(\sum_{i=1}^{n} g_i(f_k)h_i(f_k) \right)^2 - \sum_{i=1}^{n} \lambda_i \left(\sum_{k=1}^{K} g_i^2(f_k) - 1 \right) \tag{2.25}$$

where λ_i are the Lagrange multipliers and $\lambda = [\lambda_1, \lambda_2, \ldots, \lambda_n]$, $\mathbf{g} = [g_1, g_2, \ldots, g_n]$.

2.3.2 Properties of the power maximizing precoder

The partial derivatives of the Lagrangian in (2.25) are:

$$\frac{\partial \mathcal{L}}{\partial g_m} = 2 \left(\sum_{i=1}^{n} g_i(f_k)h_i(f_k) \right) h_m(f_k) - 2\lambda_m g_m(f_k)$$

$$\frac{\partial \mathcal{L}}{\partial \lambda_m} = \sum_{k} g_m^2(f_k) - 1$$

Equating the partial derivatives to zero, we get,

$$\left(\sum_{i=1}^{n} g_i(f_k)h_i(f_k)\right) h_m(f_k) = \lambda_m g_m(f_k),\ \forall f_k \in \mathcal{B}$$

$$\Rightarrow g_m(f_k) = \frac{1}{\lambda_m} S(f_k)h_m(f_k) \tag{2.26}$$

$$\text{where } S(f_k) = \sum_{i=1}^{n} g_i(f_k)h_i(f_k) \tag{2.27}$$

$$\text{and } \sum_{k} g_m^2(f_k) = 1,\ \forall m = 1 \ldots K \tag{2.28}$$

We now present some properties of the power maximizing solution for the precoding filter $g_i(f_k)$.

Property 2.1 *The optimizing precoding filters $g_m(f_k)$ are all identically zero everywhere except a finite set of no more than n frequencies.*

Proof: Multiplying (2.26) by $h_m(f_k)$ and summing over all transmitter nodes, using (2.27) we have

$$\sum_{m=1}^{n} g_m(f_k)h_m(f_k) \equiv S(f_k) = \sum_{m=1}^{n} \frac{h_m^2(f_k)}{\lambda_m} S(f_k)$$

$$\text{or } S(f_k)\left(\sum_{m=1}^{n} \frac{h_m^2(f_k)}{\lambda_m} - 1\right) = 0,\ \forall f_k \in \mathcal{B} \tag{2.29}$$

Equation (2.29) requires that for all frequencies k, either $S_k = 0$ or $\sum_{m=1}^{n} \frac{h_m^2(f_k)}{\lambda_m} = 1$. Note that the latter equation can be thought of as a set of linear equations in the n variables $\frac{1}{\lambda_m}$. This set of equations can generically be satisfied at no more than n frequencies for almost all realizations of the channel gains $h_i(f_k)$, which proves the result.

Note: Similar to capacity maximizing solution, the optimality criterion for power maximizing precoder described by (2.26) also obeys the separation property and as

a consequence of the separation property, if a user is silent on any subchannel, then all the users are silent on that particular subchannel. Furthermore, as a result of property 2.1, we observe that this consequence of the separation property holds true for atleast n subchannels.

Property 2.2 *The optimizing precoding filters $g_m(f_k)$ and the corresponding Lagrange multipliers λ_m satisfy:*

$$g_m(f_k) = \frac{\sum_{i \neq m} g_i(f_k) h_i(f_k)}{\lambda_m - h_m^2(f_k)}, \quad \forall k \tag{2.30}$$

Proof: Equation (2.30) is simply a rearrangement of (2.26) using (2.27).

Property 2.3 *When the transmit power is 1, the maximum power at the receiver is the sum of the maximizing value of the Lagrangian multipliers λ_m, i.e., $P_{R,max} = \sum_{i=1}^{n} \lambda_i$, where λ_i satisfy (2.26).*

Proof: Multiply both sides of (2.26) with $g_m(f_k)$, we get

$$\lambda_m g_m^2(f_k) = g_m(f_k) h_m(f_k) \left(\sum_{i=1}^{n} g_i(f_k) h_i(f_k) \right)$$

$$\Rightarrow \sum_{m=1}^{n} \lambda_m g_m^2(f_k) = \left(\sum_{m=1}^{n} g_m(f_k) h_m(f_k) \right)^2 \tag{2.31}$$

Summing the above equation over k, we get

$$\sum_{m=1}^{n} \lambda_m = \sum_{k} \left(\sum_{m=1}^{n} g_m(f_k) h_m(f_k) \right)^2 \equiv P_{R,max} \tag{2.32}$$

The Property 2.3 invites an interpretation of the maximizing value of λ_m as representing the contribution of the m-th transmitter to the total received power. Note

that multiplying (2.26) by $g_m(f_k)$ and using (2.28) that the maximizing λ_m satisfy:

$$\lambda_m = \sum_{k=1}^{K} S(f_k) g_m(f_k) h_m(f_k) \tag{2.33}$$

Property 2.4 *Scale-invariance of power maximizing solution. Let* $\mathbf{G}^{opt} = [g_i(f_k)]_{ik}$ *represent the set of precoders that achieve maximum received power when the transmit power constraint is* $P_{T,i} = 1 \ \forall i \in \{1, 2, ..., n\}$. *Then* $\sqrt{P}\mathbf{G}^{opt}$ *achieves maximum received power when the transmit power constraint is* $P_{T,i} = P \ \forall i \in \{1, 2, ..., n\}$.

Proof: The property follows readily from the following simple observation. Let $\mathbf{G_1}$, $\mathbf{G_2}$ represent a set of precoders that satisfy transmit power constraint of $P_{T,i} = 1 \ \forall i \in \{1, 2, ..., n\}$ and let their corresponding received power for a given set of channel responses be p_1, p_2, where $p_1 > p_2$. We note that the two sets of precoders $\sqrt{P}\mathbf{G_1}$, $\sqrt{P}\mathbf{G_2}$ each satisfy transmit power $P_{T,i} = P \ \forall i \in \{1, 2, ..., n\}$, and their corresponding received powers are Pp_1, Pp_2 and $Pp_1 > Pp_2$.

2.4 Relation between optimal precoders

In the previous sections, we looked at the optimal criteria for precoders that maximize the two FOMs. In this section, we explore the relationship between the various precoders for two FOMs and also establish the relationship between sum-rate capacity of MAC channel and distributed beamforming. The following results establish these relationships in detail.

1. **Comparison with MAC channel capacity**: We compare the maximum achievable capacity of distributed beamforming with that of the maximum sum-rate capacity of Gaussian multiple-access channel (MAC) and as mentioned

before, we expect the following:

Result: The maximum achievable capacity with beamforming is always greater than the maximum sum-rate capacity of the MAC channel or in other words, the maximum sum-rate capacity of MAC channel provides a strict lower bound on distributed beamforming capacity.

We prove the above result in two steps: in the first step, we show the result in the case of narrowband channels and in the second step, we generalize to wideband channels using the fact that we divide the wideband channel into a number of narrowband channels.

First, we deal with narrowband channels and present the following Lemma.

Lemma 2.1 *The input power distribution that maximizes the sum-rate capacity of a cooperative Gaussian MAC channel is also Gaussian, whose covariance matrix has rank 1. Additionally, beamforming solution maximizes the capacity of this channel.*

A detailed proof is provided in the Appendix. From the above Lemma, since the input covariance matrix has rank 1, the maximum sum-rate capacity of the MAC channel where the nodes send different messages is always less than that of capacity achieved by transmitting the same message signal in the narrowband scenario.

To generalize the result to wideband channels, we present the following Lemma.

Lemma 2.2 *The sum-rate capacity of a single user wideband MAC channel is*

maximized if independent message signals are transmitted on different subchannels, i.e., the covariance matrix of message signals is diagonal.

Proof: The capacity of the single user wideband MAC channel is [1]

$$C_{\text{MAC}} = \log \left| \mathbf{I} + \mathbf{HSH^H} \right| \tag{2.34}$$

where $\mathbf{S}$ is the covariance matrix of message signals on various narrowband subchannels.

Note: We obtain the above equation for the sum-rate capacity of wideband single user MAC channel by pretending that multiple antennas on each node in [1] as if they are antennas for each narrowband subchannel.

With the above observation, the channel matrix $\mathbf{H}$ is diagonal with the diagonal elements being the complex channel gains on each sub-channel. In [41], using Hadamard's inequality, it is shown that the maximizing covariance matrix, $\mathbf{S}$ is diagonal and follows the well-known solution of water-filling.

As we divide the wideband channel into K narrowband channels, the total capacity of the wideband channel is given by the sum of capacities on each narrowband channel and to maximize the wideband capacity, using Lemma 2.2; we assert that the message signals from all the nodes are independent on each narrowband channel, i.e.,

$$E\left[\mathbf{x_i x_i^H}\right] = \begin{bmatrix} P_i(f_1) & & \\ & \ddots & \\ & & P_i(f_K) \end{bmatrix} \quad \forall i \tag{2.35}$$

where $\mathbf{x_i} = [\mathrm{x_i}(f_1), \mathrm{x_i}(f_2), ..., \mathrm{x_i}(f_K)]^T$. Now, on each narrowband channel, using Lemma 2.1, we argue that the maximum sum-rate capacity of MAC channel,

$C_{\text{MAC}}(f_k)$ is always less than the capacity achieved by beamforming, $C_{\text{beam}}(f_k)$ i.e.,

$$C_{\text{MAC}}(f_k) < C_{\text{beam}}(f_k) \Rightarrow \sum_k C_{\text{MAC}}(f_k) < \sum_k C_{\text{beam}}(f_k)$$

which proves the result.

We now present empirical results and for the purpose of simulations, we assume that there are 4 users and 4 subchannels. The 4 subchannels are chosen from a Gaussian distribution with variances $20, 15, 10, 5$ dB across all users. Each channel is scaled by a constant β to change the average SNR. For example, with $\beta = 0.05$, the average SNR on these 4 subchannels are $-6, -11, -16, -21$ dB, and from Fig. 2.5, it can be observed that the capacity is approximately 3 times larger with wideband distributed beamforming as compared to MAC channel capacity. Even at high SNR, there is almost a constant gap between the maximum achievable capacity of MAC channel and distributed beamforming, confirming the strict lower bound provided by the maximum sum-rate capacity of MAC channel on maximum distributed beamforming capacity.

2. **Comparison between various power allocation schemes**:

   We intend to compare the maximum capacity of distributed beamforming with that of the capacity achieved by equal power allocation precoder which distributes the total available power uniformly across frequency and whose phase response is still chosen to achieve beamforming at the receiver. We state the following theorem:

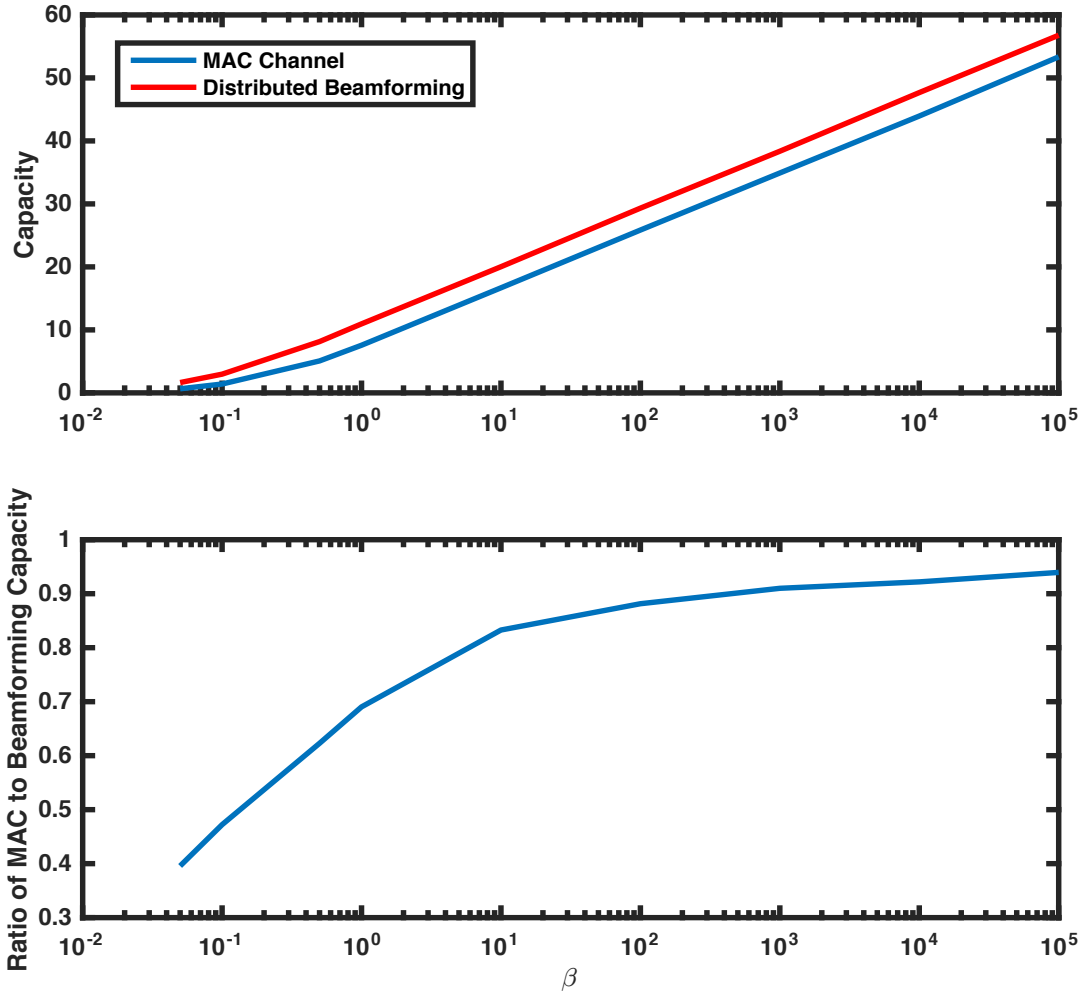

Figure 2.5: Capacity for MAC channel [1] and distributed beamforming [2] with 4 nodes and 4 subchannels. Also, the ratio of these capacities is plotted

Theorem 2.2 *Let* $C_{\max}(\boldsymbol{H})$ *and* $C_{\text{eq}}(\boldsymbol{H})$ *denote the maximum capacity with distributed beamforming and equal power beamforming, respectively. Then,*

$$\text{Lim}_{\gamma\to\infty}\ \frac{C_{\max}(\gamma\boldsymbol{H})}{C_{\text{eq}}(\gamma\boldsymbol{H})} = 1$$

A detailed proof of the above is given Appendix.

The above theorem states that at sufficiently *high SNR*, the equal power beamforming precoder is nearly optimal for maximizing the capacity with distributed beamforming.

3. **The relation between precoders that maximize capacity and power**: As mentioned in chapter 1, we expect the power maximizing precoder to also maximize the capacity at low SNR for wideband beamforming. Hence, we state the following theorem:

Theorem 2.3 *With distributed beamforming, let* $C_{\text{pow}}(\boldsymbol{H})$ *denote the achievable capacity with power maximizing precoder and* $C_{\max}(\boldsymbol{H})$ *denote the maximum achievable capacity. Then,*

$$\text{Lim}_{\gamma\to 0}\ \frac{C_{\text{pow}}(\gamma\boldsymbol{H})}{C_{\max}(\gamma\boldsymbol{H})} = 1$$

A detailed proof is presented in Appendix.

As a corollary to this theorem, we also show that the precoders that maximize the FOMs are equivalent at low SNR.

CHAPTER 3
FIXED POINT ALGORTIHMS FOR COMPUTING PRECODERS AND DISTRIBUTED IMPLEMENTATION

In this chapter, we present fixed point algorithms which help us numerically compute the capacity or power maximizing precoders. At the end of this chapter, we show that with the help of feedback from a cooperating receiver node, we can avoid the need for any central node coordination to compute these precoders, or in other words, the availability of feedback from receiver helps us compute these precoders in a distributed manner at each node. We define,

$$S(f_k) = \sum_{i=1}^{n} G_i(f_k)H_i(f_k) = \sum_{i=1}^{n} g_i(f_k)h_i(f_k) \tag{3.1}$$

a quantity that is extensively used and we describe its significance later in the chapter.

Since we assume that each node has prior channel knowledge from itself to the receiver, the phase response of the precoder at each node can be computed in a straightforward manner, as $\angle G_i(f_k) = -\angle H_i(f_k)\ \forall i$ and k. Hence, we use the fixed point algorithms to compute the magnitude response of the precoders at each node.

3.1 Capacity maximizing precoder

We can pictorially represent the capacity maximizing precoder as shown in Fig. 3.1 and this follows from Fig. 2.4 as the pulse-shaping filter, $Q_d(f_k)$ can be expressed in terms of $S(f_k)$,

$$Q_d(f_k) = \frac{S(f_k)}{1 + S^2(f_k)}$$

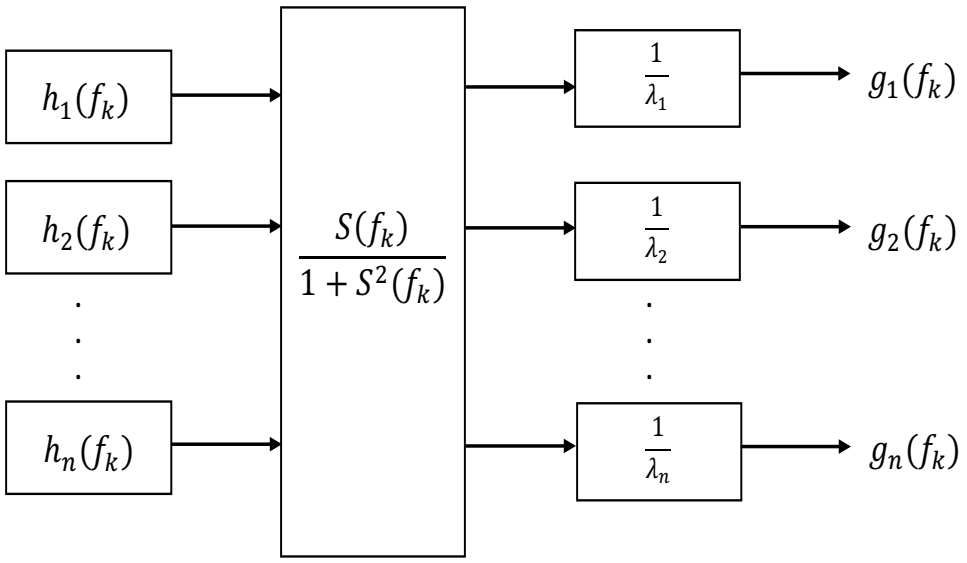

Figure 3.1: Pictorial representation of optimal criterion for capacity maximizing precoder using distributed beamforming

Hence, from Fig. 3.1, we have

$$g_p(f_q) = \frac{1}{\lambda_p} \frac{S(f_q)}{1 + S^2(f_q)} h_p(f_q) \tag{3.2}$$

Also, the optimum Lagrangian multiplier satisfies the constraint that each transmitter transmits unit power,

$$\sum_{k=1}^{N} g_i^2(f_k) = 1 \ \forall i \in \{1, 2, ..., n\} \tag{3.3}$$

3.1.1 Algorithm

We now present the fixed point algorithm to determine the precoder which follows from Fig. 3.6. The algorithm is based on the iteration:

$$S^{(l+1)}(f_k) = \sum_{i=1}^{N} g_i^{(l)}(f_k) h_i(f_k),$$

$$\lambda_i^{(l+1)} = \sqrt{\sum_{k=0}^{N-1} \left(\frac{S^{(l+1)}(f_k) h_i(f_k)}{1 + \left(S^{(l+1)}(f_k)\right)^2} \right)^2}$$

$$g_i^{(l+1)}(f_k) = \frac{1}{\lambda_i^{(l+1)}} \frac{S^{(l+1)}(f_k)}{1 + \left(S^{(l+1)}(f_k)\right)^2} h_i(f_k)$$

with the initialization $g_i^{(0)}(f_k) = h_i(f_k)$.

We can see that if the above iterations converge, the converged values indeed satisfy the optimality conditions (3.2), (3.3). The resulting algorithm is described in pseudocode form in Algorithm 3.1.

3.1.2 Simulations

We present simulation results for two scenarios corresponding to low and high SNR and consider three different power allocation strategies:

1. *Total power constraint or centralized beamforming*: constraint on average total power summed across transmitters,
2. *Per transmitter constraint or distributed beamforming*: separate constraint on the average power of each transmitter, where the precoder is computed using the fixed point method outlined in Algorithm 3.1, and
3. *Equal power allocation filter*: the power is distributed across the frequency band uniformly for each node regardless of the channels, and the phase response is

Algorithm 3.1 Fixed point algorithm for computing maximizing capacity precoder

1: Assign $r_i^{(0)}(f_k) = h_i(f_k) \quad \forall i$ and k

2: Find $\lambda_i^{(0)}$ such that, $\lambda_i^{(0)} \sum_k \left(r_i^{(0)}(f_k) \right)^2 = 1 \quad \forall i$

3: $g_i^{(0)}(f_k) \leftarrow \lambda_i^{(0)} r_i^{(0)}(f_k) \quad \forall i$

4: $S^{(0)}(f_k) \leftarrow \sum_{i=1}^{n} g_i^{(0)}(f_k) h_i(f_k)$

5: Define $m = 1$

6: **repeat**

7: $\quad r_i^{(m)}(f_k) \leftarrow \frac{S^{(m-1)}(f_k)}{1+\left(S^{(m-1)}(f_k)\right)^2} h_i(f_k) \quad \forall i$

8: $\quad$ Find $\lambda_i^{(m)}$ such that, $\lambda_i^{(m)} \sum_k \left(r_i^{(m)}(f_k) \right)^2 = 1 \quad \forall i$

9: $\quad g_i^{(m)}(f_k) \leftarrow \lambda_i^{(m)} r_i^{(m)}(f_k) \quad \forall i$

10: $\quad G_i^{(m)}(f_k) = g_i^{(m)}(f_k) e^{-\angle H_i(f_k)}$

11: $\quad S^{(m)}(f_k) \leftarrow \sum_{i=1}^{N} G_i^{(m)}(f_k) H_i(f_k)$

12: $\quad m \leftarrow m + 1;$

13: **until** $m \leq m_{max}$

14: $g_i(f_k) = g_i^{(m_{max})}(f_k)$ and $G_i(f_k) = g_i(f_k) e^{-\angle H_i(f_k)} \quad \forall i$

chosen to achieve perfect coherence at all frequencies.

For the "low SNR" case we consider $N = 4$ subchannels with the channel gains for each user on each channel chosen iid $\sim CN(0, \sigma_l^2)$, where $\sigma_l^2 = -20, -13, -10$ and -7 dB for the first, second, third and fourth channel respectively. Receiver noise level is 0 dB.

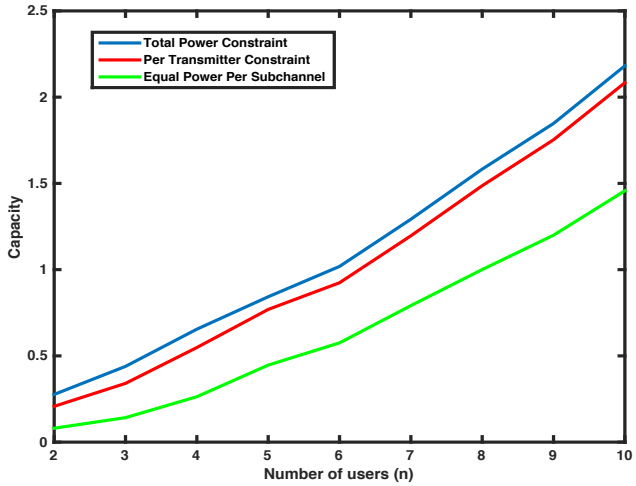

Figure 3.2: Capacity as a function of number of users with four subchannels at low SNR

Figure 3.2 depicts capacity as a function of n, the number of users, and shows that while the performance loss from the centralized to the decentralized case is modest, the disparity of both from the equal power allocation case is very substantial and grows with n. It also depicts the monotonic increase of capacity with n. This is

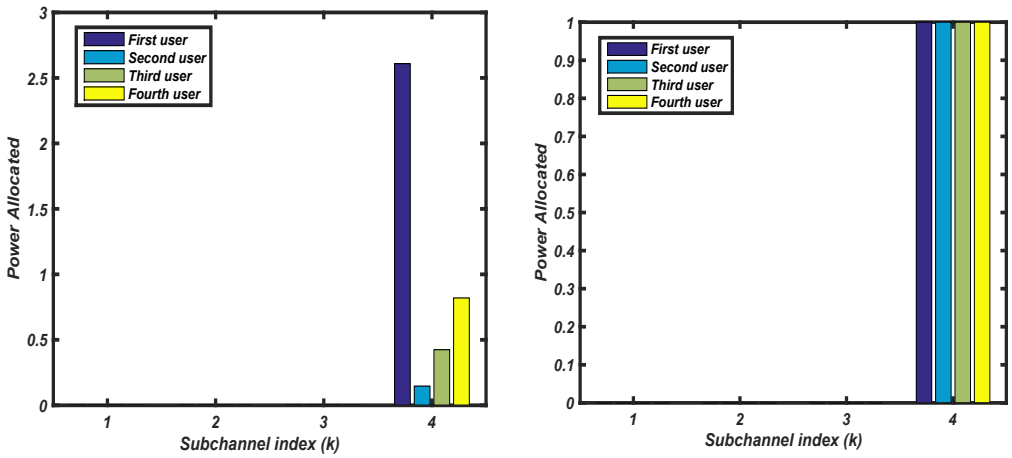

(a) Total power constraint (b) Per transmitter constraint

Figure 3.3: Power allocated to subchannels by each user at low SNR

expected as the average received SNR scales as n^2.

For small n and low SNRs, (2.15) suggests that in the centralized case users should be silent on weaker subchannels. This is confirmed by Fig. 3.3a which shows that with four users all power is allocated by each to the strongest subchannel. Figure 3.3b shows that this is true even in the decentralized case, confirming a consequence of the separation property that should a user be silent on a particular subchannel then all users are silent on this subchannel.

Figure 3.4 considers the high SNR case with four subchannels, chosen for each user as iid $\sim CN(0, \sigma_h^2)$, with $\sigma_h^2 = 40, 47, 50$ and 53 dB for the first, second, third and fourth channel respectively. We see from Fig. 3.4 that the capacity increases with increasing n in a concave (logarithmic) manner, as we expect. The decentralized

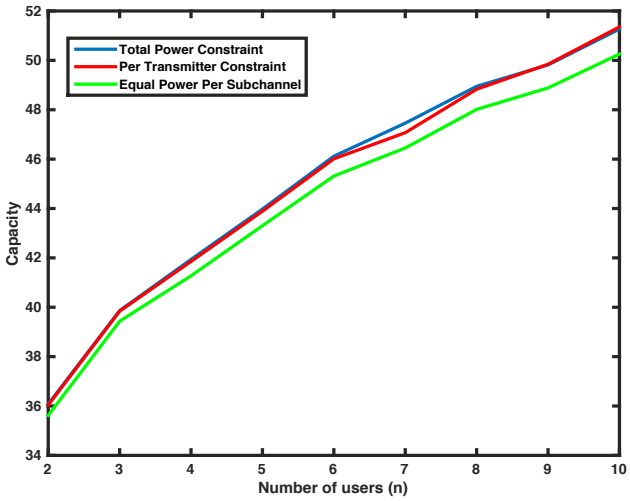

Figure 3.4: Capacity as a function of number of users with four subchannels at high SNR

performance is virtually indistinct from the centralized case, while the disparity with the equal power allocation case still persists but is less pronounced. As shown in Figures 3.5a and 3.5b, at this high SNR case no subchannel is silent. This is evident from (2.15) for the centralized case and this also manifests in the decentralized case.

3.2 Power maximizing precoder

We now present the fixed point algorithm to determine the power maximizing precoder. We note that similar to the capacity maximizing precoder, the optimal power maximizing precoder given by

$$g_m(f_k) = \frac{1}{\lambda_m} S(f_k) h_m(f_k)$$

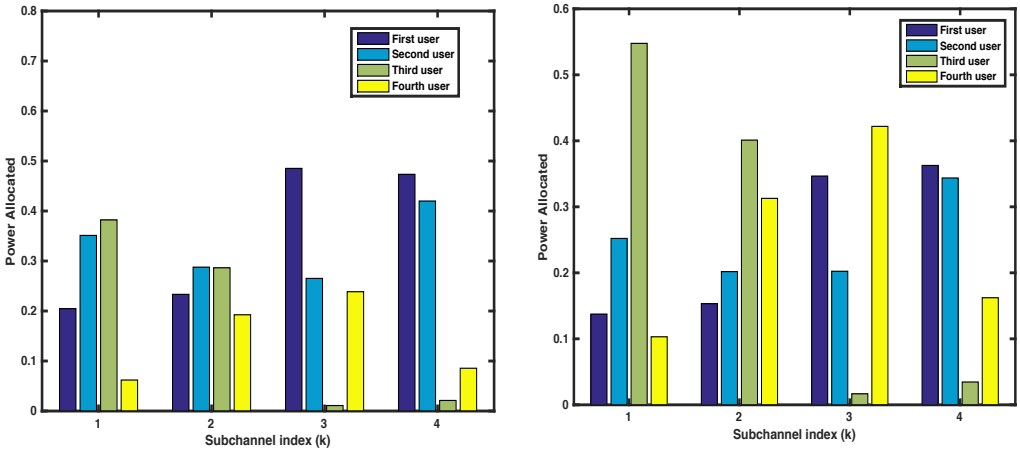

(a) Total power constraint. (b) Per transmitter constraint.

Figure 3.5: Power allocated to subchannels by each user at high SNR

satisfies the separation property, i.e., it is a product of terms indexed by m and k. The separation property along with the definition of $S(f_k)$, can be used to pictorially represent the optimal power maximizing precoder, as shown in Fig. 3.6.

3.2.1 Algorithm

The algorithm for computing the magnitude response of the power maximizing precoder is based on Fig. 3.6 and the iterations are as follows:

$$\begin{aligned} S_k^{(l+1)} &= \sum_{i=1}^{n} g_i^{(l)}(f_k) h_i(f_k), \\ \lambda_i^{(l+1)} &= \sqrt{\sum_{k=0}^{K-1} \left(S^{(l+1)}(f_k) h_i(f_k)\right)^2} \\ g_i^{(l+1)}(f_k) &= \frac{1}{\lambda_i^{(l+1)}} S^{(l+1)}(f_k) h_i(f_k) \end{aligned} \tag{3.4}$$

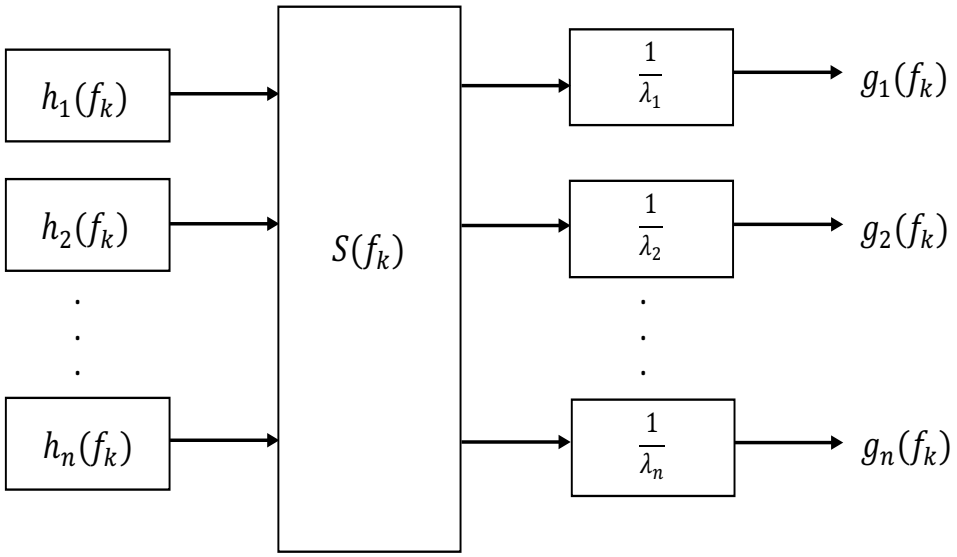

Figure 3.6: Pictorial representation of optimal criterion for power maximizing precoder using distributed beamforming

with the initialization $g_i^{(0)}(f_k) = h_i(f_k)$. We can see that if the above iterations converge, the converged values indeed satisfy the optimality conditions (2.26), (2.27) and (2.28). The resulting algorithm is described in pseudocode form in Algorithm 3.2.

3.2.2 Simulations

We now present simulation results where we used Algorithm 3.2 to calculate the power maximizing precoder for a variety of simulated channel responses. We compare the optimal precoders performance against two other precoding filters, namely,

1. *Matched Filter*: each node uses $G_i(f_k) = \alpha H_i^*(f_k)$, α is determined by power

Algorithm 3.2 Fixed point algorithm for computing power maximizing precoder

1: Assign $r_i^{(0)}(f_k) = h_i(f_k) \quad \forall i$ and k

2: Find $\lambda_i^{(0)}$ such that, $\sum_k \lambda_i^{(0)} \left(r_i^{(0)(f_k)} \right)^2 = 1 \quad \forall i$

3: $g_i^{(0)}(f_k) \leftarrow \lambda_i^{(0)} r_i^{(0)}(f_k) \quad \forall i$

4: $S^{(0)}(f_k) \leftarrow \sum_{i=1}^{n} g_i^{(0)}(f_k) h_i(f_k)$

5: Define $m = 1$

6: **repeat**

7: $\quad r_i^{(m)}(f_k) \leftarrow S^{(m-1)}(f_k) h_i(f_k) \quad \forall i$

8: $\quad$ Find $\lambda_i^{(m)}$ such that, $\sum_k \lambda_i^{(m)} \left(r_i^{(m)}(f_k) \right)^2 = 1 \quad \forall i$

9: $\quad g_i^{(m)}(f_k) \leftarrow \lambda_i^{(m)} r_i^{(m)}(f_k) \quad \forall i$

10: $\quad G_i^{(m)}(f_k) = g_i^{(m)}(f_k) e^{-\angle H_i(f_k)} \quad \forall i$

11: $\quad S^{(m)}(f_k) \leftarrow \sum_{i=1}^{n} G_i^{(m)}(f_k) H_i(f_k)$

12: $\quad m \leftarrow m + 1;$

13: **until** $m \leq m_{max}$

14: $g_i(f_k) = g_i^{(m_{max})}(f_k)$ and $G_i(f_k) = g_i(f_k) e^{-\angle H_i(f_k)} \quad \forall i$

constraint and

2. *Equal Power Allocation Filter*: power is distributed across the frequency band uniformly for each node regardless of the channels, and the phase response is chosen to achieve perfect coherence at all frequencies i.e. $G_i(f_k) = g_0 e^{-j\angle h_i(f_k)}$ where the constant g_0 is determined by the transmit power constraint.

Note that all three filters achieve distributed beamforming at all frequencies and differ only in the way the transmit power of the nodes is divided up across frequencies. For our simulations, we took $K = 128$ frequency bins. We simulated frequency-selective channels by choosing the channel impulse responses randomly to fit an exponential power delay profile. More precisely, the channels are chosen as follows:

$$h_i[l] \sim CN(0, \Sigma) \quad \forall i \text{ and } 0 \leq l \leq M$$

where M is the number of taps modeled, and

$$\Sigma_{r,c} = \begin{cases} e^{-l\sigma}, & \text{if } r = c = l \\ 0, & \text{otherwise} \end{cases}$$

and σ is the *rate of decay*, with a small σ corresponding to a large number of taps.

We take $\sigma = 0.25$ which corresponds to approximately $M = 15$ significant channel taps and $n = 2$ transmitting nodes. This choice of σ gives a fair amount of frequency selectivity in the channel responses as seen in Fig. 3.7. The individual and sum of the individual absolute channel gains at each frequency known as sum channel to receiver node are shown in Fig. 3.7.

It can also be seen from Fig. 3.7 that the precoding filter chooses two frequen-

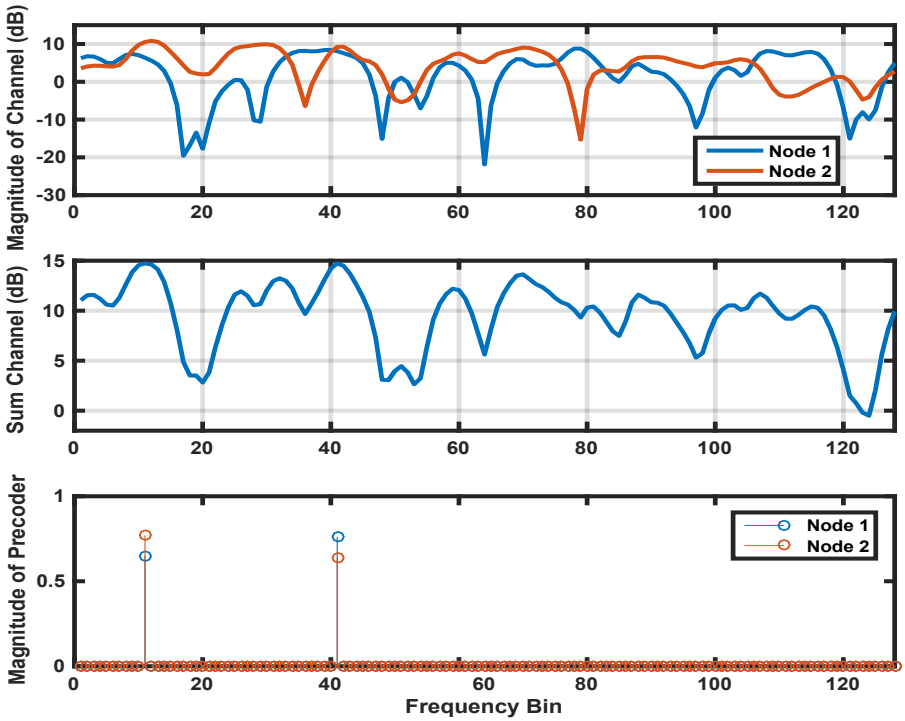

Figure 3.7: Individual node to receiver channel and the sum of the individual absolute channel gains at each frequency along with magnitude response of the precoder for each node

cies to transmit and one of the frequencies selected is the frequency at which the sum channel gain is maximum.

Other simulations confirm that similar results hold for larger arrays. For $n = 6$ transmitting nodes, as can be seen from Fig. 3.8, the power maximizing precoding filters choose a set of 4 active frequencies to achieve maximum received power.

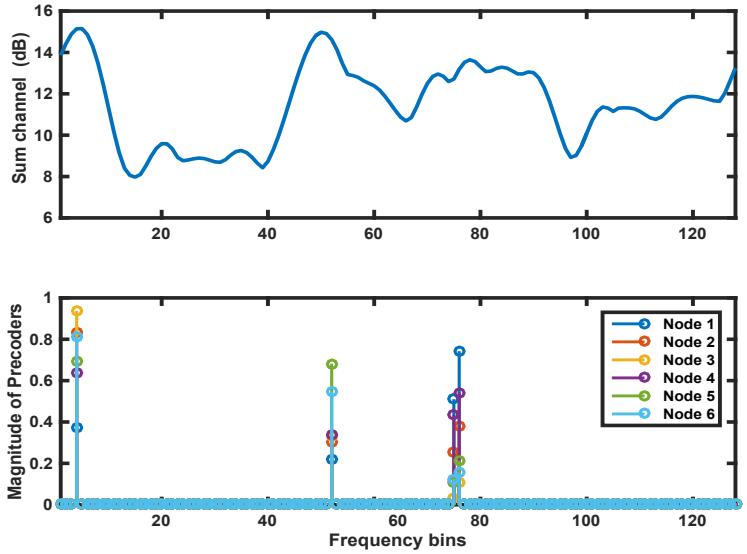

Figure 3.8: The absolute sum of the channel gains for 6 nodes across frequency and the magnitude response of individual precoder

The variation of the received power as a function of nodes is shown in Fig. 3.9. Since, as noted earlier, all the three precoding filters achieve beamforming at the receiver at all frequencies, we expect the received power with each of the precoders to increase approximately as n^2 because of the beamforming gain and therefore, the

received power plotted in dB, should increase logarithmically with n.

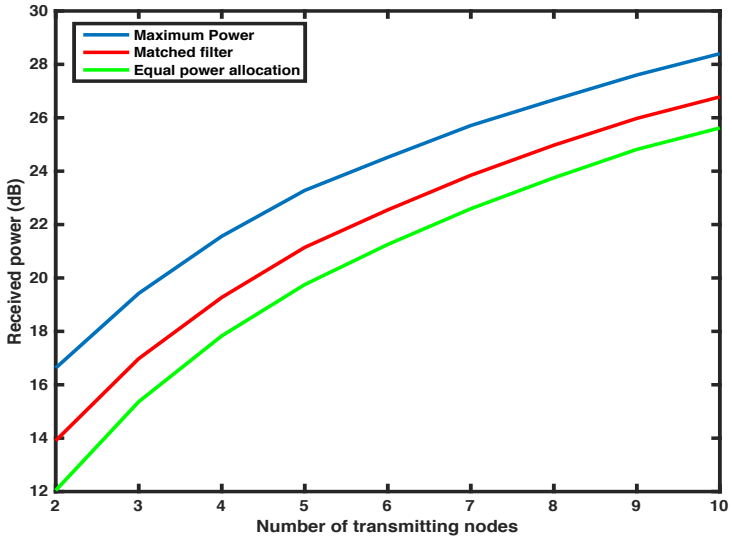

Figure 3.9: Received power as a function of number of nodes

This logarithmic increase is indeed observed in Fig. 3.9. For the power maximizing precoding filter, the received power with $n = 10$ nodes is 12 dB greater than that with $n = 2$ which compares with the estimate of 14 dB from the simple n^2 estimate. With $n = 2$ transmitter nodes, the averaged maximum power at the receiver is approximately 2.5 dB higher than the power achieved by the Matched Filter, and approximately 4.5 dB higher than Equal Power Allocation Filter, and this difference slightly reduces as the number of nodes increases.

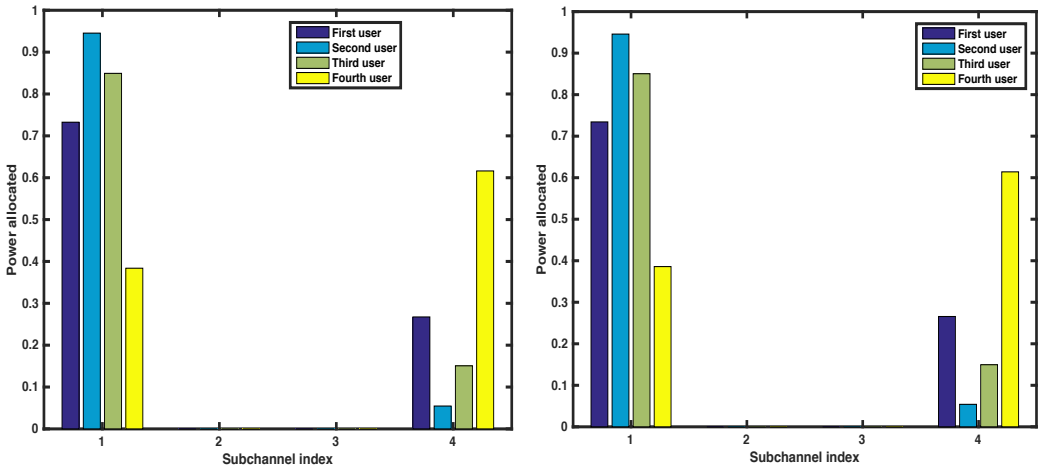

(a) Capacity maximizing precoder (b) Power maximizing precoder

Figure 3.10: Power allocated to subchannels by the power and capacity maximizing precoders by each user at low SNR

3.3 Performance comparison of precoders based on SNR

We now present simulation results that compare the performance of various precoders based on SNR. First, we consider the case of low SNR and show the equivalence of capacity and received power maximizing precoder. For the purpose of simulation, we consider 4 users and $K = 4$ subchannels, with the complex channel gains for each user on each subchannel is chosen iid $\sim CN(0, \sigma_l^2)$, where $\sigma_l^2 = -30, -25, -20$ and -15 dB for the first, second, third and fourth channel respectively. Receiver noise level is chosen to be 0 dB.

We consider a set of channels for which both the precoders are non-trivial, i.e., when the precoders are different from picking the strong sub-channel and this arises

because the capacity maximizing precoder might be silent on certain subchannels at low SNR. Figure 3.10a and 3.10b shows the power allocated by the capacity and power maximizing precoder to various subchannels respectively, and we observe that the power allocated by both the optimizing precoders to various subchannels is almost similar, confirming the equivalence of power and capacity maximizing precoder at low SNR.

Now, we scale the above channels by a factor of 10 and the resulting channels have average strengths of $\sigma_l^2 = -10, -5, 0$ and 5 dB for the first, second, third and fourth channel respectively, resulting in "medium SNR". We note that the power maximizing precoder is unchanged by the scaling as a virtue of the scale independence property mentioned in property 2.4 in section 2.3.1.

Figure 3.11a and 3.11b shows the power allocation across various subchannels by centralized and distributed beamforming and we observe that all the subchannels are used for maximizing capacity. Also, we can observe from Fig. 3.11 that the precoder for maximizing capacity is different from the power maximizing precoder, confirming the suboptimality of power maximizing precoder for capacity at medium SNR. The ratio of capacity achieved by equal power beamforming precoder and maximum achievable capacity with distributed beamforming is 0.95 confirming suboptimality of equal power beamforming for maximizing capacity.

We now compare the performance of precoders at high SNR and to generate channels for high SNR, we further scale the channels by a factor of 100 to result in average strengths of $\sigma_l^2 = 30, 35, 40$ and 45 dB for the first, second, third and fourth

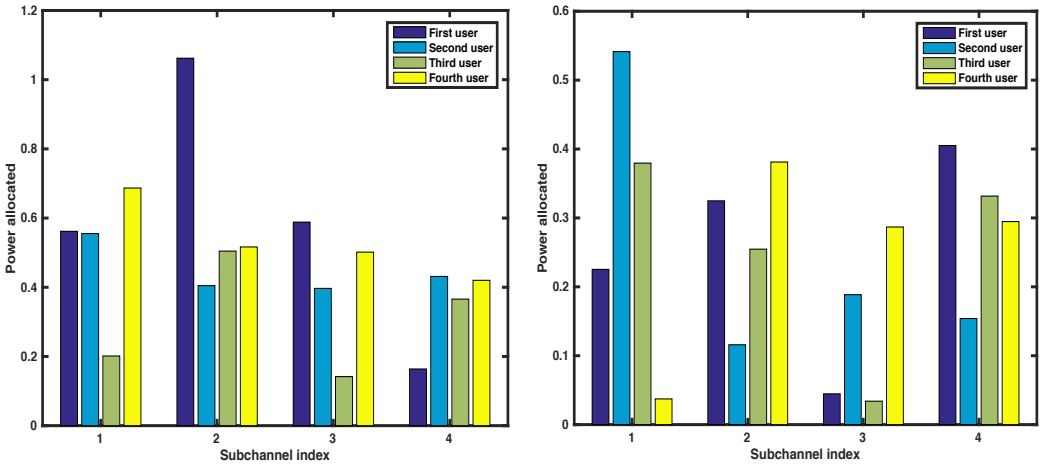

(a) Centralized beamforming (b) Distributed beamforming

Figure 3.11: Power allocated to subchannels by the power and capacity maximizing precoders by each user at medium SNR

channel respectively. Even in this case, the power maximizing precoder is unchanged because of scaling as a virtue of the scale independence property mentioned in section 2.3.1.

Figure 3.12a and 3.12b shows the power allocation across various subchannels by capacity maximizing precoder with centralized and distributed beamforming and we observe that all the subchannels are used for maximizing capacity. Although, the optimal precoders have power distribution that is different from equal power allocation, the ratio of capacity achieved by equal power beamforming precoder and maximum achievable capacity with distributed beamforming is 0.99, confirming the near-optimality of equal power beamforming at high SNR for maximizing capacity.

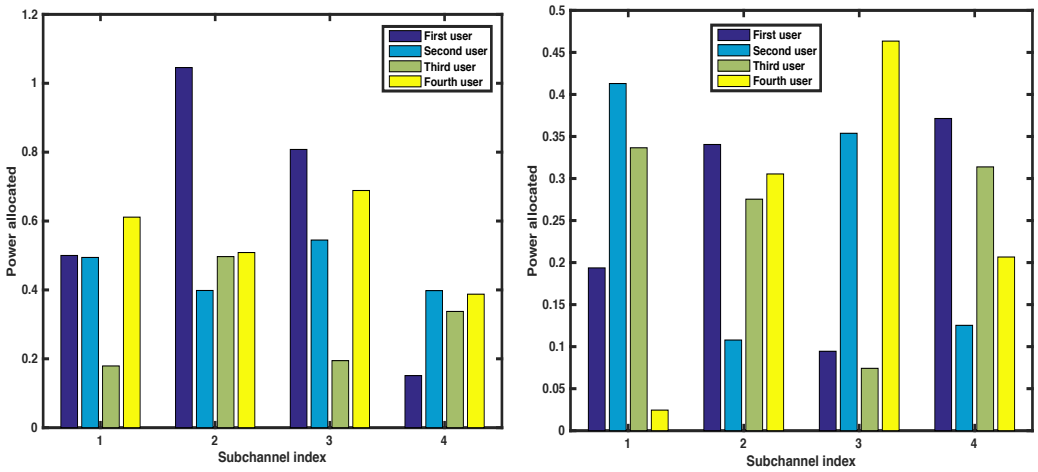

(a) Centralized beamforming (b) Distributed beamforming

Figure 3.12: Power allocated to subchannels by the power and capacity maximizing precoders by each user at high SNR

This is so because all the channels have high strength and the effect of power allocation mismatch between the optimal and equal power precoder has a marginal effect on capacity.

3.4 Distributed implementation using feedback

To compute the precoders using Algorithms 3.1 and 3.2, it can be seen from Fig. 3.1 and 3.6 that each node needs the following information at every iteration: CSI, the value of λ_i and knowledge of $S(f_k)$. The parameter λ_i is a scaling constant which ensures that the transmitted power is 1; hence, each node can compute these individually. Since we assume the *a-priori* knowledge of CSI, we explore ways of obtaining $S(f_k)$ at every iteration. We also note that in both the algorithms $S(f_k)$

is common to all the nodes in the transmit array, hence, none of the nodes need any specialized information to implement the precoders. One of the ways to obtain $S(f_k)$ is to have a centralized coordinator, which collects the CSI and precoder information from each node at every iteration, computes $S(f_k)$ and then broadcasts to all the nodes in the array. However, we aim to have no central coordination and implement these algorithms in a distributed manner. We show that this can be achieved by using *aggregate feedback* from a cooperating receiver.

The received signal on the k-th subchannel is $y_k = x_k \sum_{i=1}^{n} G_i(f_k)H_i(f_k)$ and assuming that the message signal on the k-th subchannel, x_k contains a known preamble, the receiver node can determine the aggregate complex channel gain,

$$S(f_k) = \sum_{i=1}^{n} G_i(f_k)H_i(f_k)$$

from the array nodes to itself. The receiver can quantize, encode and broadcast the complex number $S(f_k)$, also known as *aggregate feedback* back to nodes in the array. This approach eliminates the need for central node coordination and helps us implement the algorithms in a distributed fashion at each node. The idea of aggregate feedback has some compelling advantages. Specifically, we note two such properties:

1. *Scale independence.* The amount of feedback sent by the receiver is just a few bits per timeslot, independent of the size of the array.
2. *Adaptivity to network changes.* The algorithm automatically and continuously adjusts the precoding weights during any changes e.g. nodes joining or leaving the array, changes in channel gains because of motion.

CHAPTER 4
OPTIMIZING WIRELESS POWER TRANSFER EFFICIENCY WITH MULTIPLE TRANSMIT COILS

In this chapter, we present the optimization problem of maximizing the wireless power transfer efficiency from multiple transmit coils to a single receiver coil using near-field coupling and derive the efficiency-maximizing excitation for the transmit coils. We also present a practical real-time procedure to estimate the parameters that determine the optimal excitation and a series of experiments to illustrate our approach.

4.1 An abstract general model for WPT systems

Our abstract circuit model for the WPT system is illustrated in Fig. 4.1. In this model, a set of N voltage sources connected to N input terminals with voltages $v_1, v_2, ..., v_N$ represent the transmitters. These transmitters aim to deliver maximum power to a receiver which is modeled as a load as shown. The current delivered by each source is denoted by $i_1, i_2, ..., i_N$ and the load voltage and current are denoted by v_0 and i_0 respectively. We assume that all the elements in the circuit are linear, and the N sources are the only active elements. Beyond that, we make no assumptions about the interconnections between the different terminals and the complexity of the circuit.

For simplicity, we limit ourselves to a single-frequency AC circuit, where phasor voltages and currents are represented by complex numbers and the linear load by a

complex impedance Z_0. The generalization of the *circuit model* to arbitrary time-varying non-sinusoidal voltages and currents is interesting, however, is beyond the scope of this work.

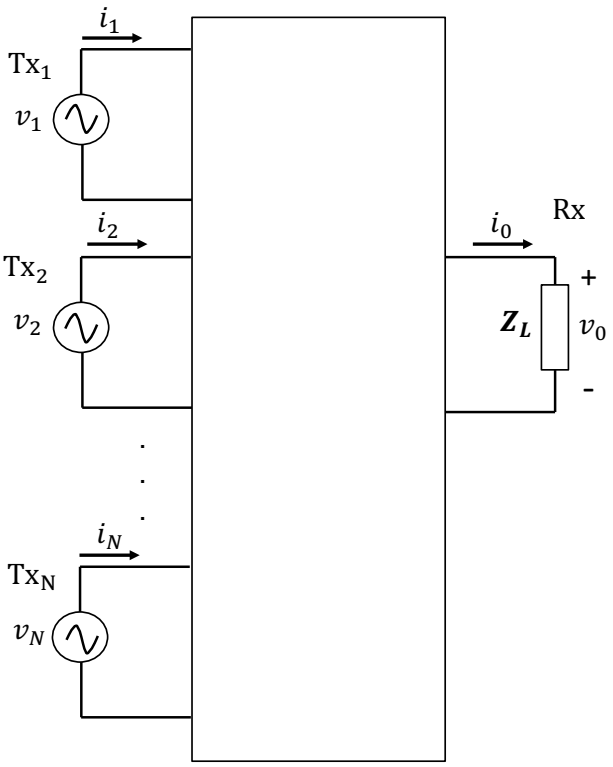

Figure 4.1: An abstract circuit model for inductive WPT systems

Under the linearity assumption mentioned above, the total voltage (v) and current (i) across any circuit element can be computed using the superposition principle as sum of contributions proportional to each of the v_i's:

$$v = a_1^* v_1 + a_2^* v_2 + \ldots + a_N^* v_N \equiv \mathbf{a^H v} \tag{4.1}$$

$$\text{and} \quad i = b_1^* v_1 + b_2^* v_2 + \ldots + b_N^* v_N \equiv \mathbf{b^H v} \tag{4.2}$$

where $\mathbf{v} = [v_1, v_2, ..., v_N]^T$ and so on.

Using (4.1) and (4.2), the power consumed by any circuit element with voltage v across its terminals and current i flowing across it is given by:

$$P = \Re(v^* i) = \frac{1}{2}\left(v^* i + i^* v\right) = \frac{1}{2}\mathbf{v^H}\left(\mathbf{ab^H} + \mathbf{ba^H}\right)\mathbf{v} \tag{4.3}$$

Now consider specifically the load terminal where the voltage and current obey Ohm's law:

$$i_0 = \frac{v_0}{Z_0} = \mathbf{b_0^H v} \text{ and } v_0 = \mathbf{a_0^H v}$$

for some "transgain" vector, $\mathbf{a_0}$ and this results in $\mathbf{a_0^H} = Z_0 \mathbf{b_0^H}$ which gives for the load power:

$$P_L = \Re\left(\frac{1}{Z_0}\right)\mathbf{v^H}\left(\mathbf{a_0 a_0^H}\right)\mathbf{v} = \mathbf{v^H}\left(\mathbf{cc^H}\right)\mathbf{v} \tag{4.4}$$

for some "transconductance" vector, $\mathbf{c} = \sqrt{\Re\left(\frac{1}{Z_0}\right)}\mathbf{a_0}$.

Similarly for the i-th source terminal, the voltage v_i is trivially written as $v_i = \delta_i^H \mathbf{v}$ where δ_i is the i-th column of the $N \times N$ identity matrix, and the current can be written as $i_i = \mathbf{b_i^H v}$ for some effective "conductance" vector $\mathbf{b}_i$. We can then write for the power P_i generated by the source v_i as

$$P_i = \frac{1}{2}\mathbf{v^H}\left(\delta_\mathbf{i}\mathbf{b_i^H} + \mathbf{b_i}\delta_\mathbf{i}^\mathbf{H}\right)\mathbf{v} \equiv \mathbf{v^H A_i v}$$

where $A_i \doteq \frac{1}{2}\left(\delta_\mathbf{i}\mathbf{b}_\mathbf{i}^\mathbf{H} + \mathbf{b_i}\delta_\mathbf{i}^\mathbf{H}\right)$ is a positive semi-definite Hermitian matrix. This allows us to write for the total power generated by all the sources:

$$P_G = \mathbf{v}^\mathbf{H}\left(\sum_{i=1}^{N}\mathbf{A_i}\right)\mathbf{v} = \mathbf{v}^\mathbf{H}\bar{\mathbf{A}}\mathbf{v} \tag{4.5}$$

for some input power matrix, $\bar{\mathbf{A}} \equiv \sum_\mathbf{i}\mathbf{A_i}$.

Now the sum of the power P_L delivered to the load and all the power losses in all other circuit elements must equal the total power generated P_G. We can therefore write for the power losses

$$P_{loss} = \mathbf{v}^\mathbf{H}\mathbf{A}\mathbf{v} \tag{4.6}$$

for some positive semi-definite Hermitian matrix $\mathbf{A} = \mathbf{A}^\mathbf{H} \equiv \bar{\mathbf{A}} - \mathbf{c}\mathbf{c}^\mathbf{H}$.

Using (4.4) and (4.6), we write for the total power:

$$P_G = \mathbf{v}^\mathbf{H}\left(\mathbf{c}\mathbf{c}^\mathbf{H} + \mathbf{A}\right)\mathbf{v} \tag{4.7}$$

4.2 Optimizing the WPT system for maximum efficiency

Equation (4.7) is the total transmitted power in terms of our abstract representation of the WPT system. As explained earlier in chapter 1, we propose to treat the $\mathbf{A}$, $\mathbf{c}$ as unknown channel parameters and estimate them directly using real-time measurements as described in Section 4.3. For this section, we assume that these parameters are known, formulate a general optimization problem for the WPT system and make some observations about the properties of the optimal solution.

The basic idea is that we want to find a set of transmit voltages at each node that maximizes the power delivered to load given a fixed total transmit power P_G.

This is tantamount to maximizing the power transfer *efficiency* of the system defined as:

$$\eta(\mathbf{v}) \doteq \frac{\mathbf{v^H c c^H v}}{\mathbf{v^H \bar{A} v}} \equiv \frac{\mathbf{v^H c c^H v}}{\mathbf{v^H} \left(\mathbf{c c^H + A}\right) \mathbf{v}}$$

Formally, we state the WPT optimization problem as:

$$\begin{aligned} \tilde{\mathbf{v}} = \arg\max_{\mathbf{v}} \ & \mathbf{v^H c c^H v} \\ \text{such that } & \mathbf{v^H} \left(\mathbf{c c^H + A}\right) \mathbf{v} = 1 \end{aligned} \tag{4.8}$$

We now present the solution to the above optimization problem by deriving the the optimal solution, $\tilde{\mathbf{v}}$ and the maximum power transfer efficiency $\tilde{\eta} = \eta(\tilde{\mathbf{V}})$.

Theorem 4.1 *If* $\mathbf{A}$ *is singular, then the maximum achievable power transfer efficiency is unity.*

Proof: If $\mathbf{A}$ is singular, then there $\exists\ \mathbf{v_s} \neq 0$ such that

$$\mathbf{A v_s} = 0 \quad \Rightarrow \mathbf{v_s}^{\mathbf{H}} \mathbf{A v_s} = 0$$

Hence, the constraint of optimization problem (4.8) results in

$$\begin{aligned} P_G &= \mathbf{v_s}^{\mathbf{H}} \left(\mathbf{c c^H + A}\right) \mathbf{v_s} = \mathbf{v_s}^{\mathbf{H}} \mathbf{c c^H v_s} \equiv P_L \\ \Rightarrow \ & \tilde{\eta} = \eta(\mathbf{v_s}) = 1 \end{aligned}$$

and as a result, the maximum achievable power transfer efficiency is unity.

From the above theorem, we can observe that when the loss matrix $\mathbf{A}$ is singular, it is theoretically possible to achieve lossless power transfer which is physically unrealistic. Therefore in practice, we always expect the loss matrix $\mathbf{A}$ to be

non-singular, which is what we consider moving forward for computing the optimal solution $\tilde{\mathbf{v}}$.

Consider the Lagrangian of (4.8) with Lagrangian multiplier $l \in R$,

$$\begin{aligned} J(\mathbf{v}, l) &= \mathbf{v^H cc^H v} - l(\mathbf{v^H}\left(\mathbf{cc^H} + \mathbf{A}\right)\mathbf{v} - 1) \\ &= \mathbf{v^H}\left((1-l)\mathbf{cc^H} - l\mathbf{A}\right)\mathbf{v} + l \end{aligned}$$

Setting the partial derivatives of the Lagrangian to zero, we get for the optimal solution:

$$\frac{\partial J}{\partial \mathbf{v}} = \mathbf{v^H}\left((1-l)\mathbf{cc^H} - l\mathbf{A}\right) = 0 \tag{4.9}$$

$$\frac{\partial J}{\partial l} = \mathbf{v^H}\left(\mathbf{cc^H} + \mathbf{A}\right)\mathbf{v} - 1 = 0 \tag{4.10}$$

Simplifying (4.9), we get,

$$\begin{aligned} & \tilde{\mathbf{v}}^{\mathbf{H}}\left((1-l)\mathbf{cc^H} - l\mathbf{A}\right) = 0 \\ \Rightarrow \quad & (1-l)\mathbf{cc^H}\tilde{\mathbf{v}} = l\mathbf{A}\tilde{\mathbf{v}} \end{aligned} \tag{4.11}$$

Equation (4.11) describes a generalized eigenvalue problem.

Theorem 4.2 *Assuming that* $\boldsymbol{A}$ *is non-singular, the optimal solution to the problem (4.8) is given by*

$$\tilde{\boldsymbol{v}} = k\boldsymbol{A}^{-1}\boldsymbol{c} \tag{4.12}$$

where k *is a constant determined by the transmit power constraint. In addition, the maximum achievable transfer efficiency is always strictly less than 100%.*

Proof: Under the assumption that $\mathbf{A}$ is non-singular, we can rewrite (4.11) as:

$$\mathbf{A^{-1}c} = \left(\frac{l}{1-l}\right)\left(\frac{1}{\mathbf{c^H}\tilde{\mathbf{v}}}\right)\tilde{\mathbf{v}}$$

and hence, the optimizing vector $\tilde{\mathbf{v}}$ is a scalar multiple of $\mathbf{A^{-1}c}$:

$$\tilde{\mathbf{v}} = k\mathbf{A^{-1}c} \tag{4.13}$$

where k is a constant and can be computed using (4.10) as

$$k^2\mathbf{c^H A^{-1}}\left(\mathbf{cc^H} + \mathbf{A}\right)\mathbf{A^{-1}c} \equiv k^2\left(\alpha^2 + \alpha\right) = 1$$

$$\Rightarrow k = \frac{1}{\sqrt{\alpha(\alpha+1)}}$$

where $\alpha = \mathbf{c^H A^{-1}c} > 0$. Now, using (4.4) and (4.10), we have

$$\mathbf{v^H}\left(\mathbf{cc^H} + \mathbf{A}\right)\mathbf{v} \equiv P_L + \mathbf{v^H A v} = 1$$

and with $\mathbf{v} = \tilde{\mathbf{v}}$, we get

$$\bar{P}_L + \frac{\mathbf{c^H A^{-1} A A^{-1} c}}{\alpha(\alpha+1)} = 1 \Rightarrow \bar{P}_L + \frac{\alpha}{\alpha(\alpha+1)} = 1$$

$$\Rightarrow \bar{P}_L = \frac{\alpha}{1+\alpha} < 1$$

where $\bar{P}_L$ denotes the maximum delivered load power and is equivalent to efficiency as total transmit power is unity.

We now present some interesting properties of the optimal solution.

Property 4.1 ***Optimal solution in terms of*** $\bar{\mathbf{A}}$*:* *The optimal excitation voltages for maximizing efficiency can also be expressed in terms of the input power matrix,* $\bar{\mathbf{A}}$*,*

$$\tilde{\boldsymbol{v}} = \frac{1}{\beta}\bar{\mathbf{A}}^{-1}\boldsymbol{c}$$

where β represents the maximum achievable efficiency.

Proof: We use the Matrix Inversion Lemma to show the result.

Matrix Inversion Lemma: For any non-singular matrix $\mathbf{B}$ and a column vector $\mathbf{y}$,

$$\left(\mathbf{B}-\mathbf{y}\mathbf{y}^{H}\right)^{-1}=\mathbf{B}^{-1}+\frac{\mathbf{B}^{-1}\mathbf{y}\mathbf{y}^{H}\mathbf{B}^{-1}}{1-\mathbf{y}^{H}\mathbf{B}^{-1}\mathbf{y}} \tag{4.14}$$

Using the Matrix Inversion Lemma,

$$\begin{aligned}\mathbf{A}^{-1}\mathbf{c} &= (\bar{\mathbf{A}}-\mathbf{c}\mathbf{c}^{\mathbf{H}})^{-1}\mathbf{c}\\ &= \left(\bar{\mathbf{A}}^{-1}+\frac{\bar{\mathbf{A}}^{-1}\mathbf{c}\mathbf{c}^{\mathbf{H}}\bar{\mathbf{A}}^{-1}}{1-\mathbf{c}^{\mathbf{H}}\bar{\mathbf{A}}^{-1}\mathbf{c}}\right)\mathbf{c}\\ &= \bar{\mathbf{A}}^{-1}\mathbf{c}\left(1+\frac{\mathbf{c}^{\mathbf{H}}\bar{\mathbf{A}}^{-1}\mathbf{c}}{1-\mathbf{c}^{\mathbf{H}}\bar{\mathbf{A}}^{-1}\mathbf{c}}\right)=\frac{1}{1-\beta}\bar{\mathbf{A}}^{-1}\mathbf{c}\end{aligned} \tag{4.15}$$

where $\beta=\mathbf{c}^{\mathbf{H}}\bar{\mathbf{A}}\mathbf{c}$. Now, using (4.15)

$$\begin{aligned}\alpha=\mathbf{c}^{\mathbf{H}}\mathbf{A}^{-1}\mathbf{c}=\frac{\mathbf{c}^{\mathbf{H}}\bar{\mathbf{A}}^{-1}\mathbf{c}}{1-\beta}=\frac{\beta}{1-\beta}\Rightarrow\alpha\left(\alpha+1\right)=\frac{\beta}{\left(1-\beta\right)^{2}}\\ \Rightarrow k=\frac{1}{\sqrt{\alpha\left(\alpha+1\right)}}=\frac{1-\beta}{\sqrt{\beta}}\end{aligned} \tag{4.16}$$

Hence, using (4.13), (4.15) and (4.16), the optimal solution can be written as

$$\tilde{\mathbf{v}}=\frac{1-\beta}{\sqrt{\beta}}\frac{1}{1-\beta}\bar{\mathbf{A}}^{-1}\mathbf{c}=\frac{1}{\sqrt{\beta}}\ \bar{\mathbf{A}}^{-1}\mathbf{c} \tag{4.17}$$

and the maximum induced voltage and power in the load coil are given by

$$\tilde{v}_0=\mathbf{a_0}^{H}\tilde{\mathbf{v}}=\sqrt{\Re(Z_0)}\mathbf{c}^{H}\tilde{\mathbf{v}}=\sqrt{\Re(Z_0)}\frac{1}{\sqrt{\beta}}\ \mathbf{c}^{H}\bar{\mathbf{A}}^{-1}\mathbf{c}=\sqrt{\beta\ \Re(Z_0)}\Rightarrow\ \bar{P}_L=\beta$$

Property 4.2 *When transmit coils are weakly coupled, beamforming solution is optimal.*

Proof: Consider N transmit that are uncoupled to each other, but are strongly coupled to the receiver. Since, the transmit coils are weakly coupled to each other, the matrix $\bar{\mathbf{A}}$ is highly diagonal as the non-diagonal element, $\mathbf{A}_{ij}$ of input power matrix which represents the power consumed in the i-th coil when coil j is excited is negligible. Hence, for some $r_i,\ \rho_i > 0,\ \text{and}\ \phi_i \in [-\pi, \pi)\ \forall i$,

$$\bar{\mathbf{A}} = \begin{pmatrix} r_1 & & & \\ & r_2 & & \\ & & \ddots & \\ & & & r_N \end{pmatrix} \Rightarrow \bar{\mathbf{A}}^{-1} = \begin{pmatrix} \frac{1}{r_1} & & & \\ & \frac{1}{r_2} & & \\ & & \ddots & \\ & & & \frac{1}{r_N} \end{pmatrix}$$

and

$$\mathbf{c} = \left[\rho_1 e^{j\phi_1},\ \rho_2 e^{j\phi_2}, \ldots,\ \rho_N e^{j\phi_N}\right]^T$$

The optimal transmit voltage vector can be computed using (4.17),

$$\tilde{\mathbf{v}} = \frac{1}{\sqrt{\beta}} \begin{pmatrix} \frac{1}{r_1} & & & \\ & \frac{1}{r_2} & & \\ & & \ddots & \\ & & & \frac{1}{r_N} \end{pmatrix} \begin{bmatrix} \rho_1 e^{j\phi_1} \\ \rho_2 e^{j\phi_2} \\ \vdots \\ \rho_N e^{j\phi_N} \end{bmatrix} = \frac{1}{\sqrt{\beta}} \begin{bmatrix} \frac{\rho_1}{r_1} e^{j\phi_1} \\ \frac{\rho_2}{r_2} e^{j\phi_2} \\ \vdots \\ \frac{\rho_N}{r_N} e^{j\phi_N} \end{bmatrix}$$

and the maximum voltage in the load coil, $\tilde{v}_0$ is

$$\begin{aligned} \tilde{v}_0 &= \mathbf{a_0^H}\tilde{\mathbf{v}} = \sqrt{\Re(Z_0)}\mathbf{c_0^H}\tilde{\mathbf{v}} \\ &= k_1 \begin{bmatrix} \rho_1 e^{-j\phi_1} & \rho_2 e^{-j\phi_2} & \ldots & \rho_N e^{-j\phi_N} \end{bmatrix} \begin{bmatrix} \frac{\rho_1}{r_1} e^{j\phi_1} \\ \frac{\rho_2}{r_2} e^{j\phi_2} \\ \vdots \\ \frac{\rho_N}{r_N} e^{j\phi_N} \end{bmatrix} \\ &= k_1 \sum_{i=1}^{N} \frac{\rho_i^2}{r_i} \end{aligned}$$

where $k_1 = \frac{\sqrt{\Re(Z_0)}}{\beta}$, is a constant.

It can be seen that the induced voltage in the receiver coil has the zero phase from each individual transmit coil, hence, proving the optimality of beamforming.

Property 4.3 ***Effect of synchronization of various transmit coils:*** *It is not necessary to phase synchronize the various transmit coils, however,they still need to be frequency synchronized.*

Proof: Let the applied voltage on each transmit coil be u_i and as the clocks are not synchronized the voltage that appears across each coil, the *real* voltage is denoted by v_i and is related to the applied voltage u_i, as

$$u_i = e^{j\phi_i} v_i, \quad \phi_i \in [-\pi, \pi) \ \forall i \in 1, 2, ..., N$$

and hence,

$$\mathbf{u} = \mathbf{D}\mathbf{v} \quad \Rightarrow \mathbf{v} = \mathbf{D}^{\mathbf{H}}\mathbf{u} \tag{4.18}$$

where

$$[\mathbf{D}]_{ij} = \begin{cases} e^{j\phi_m} & \text{if } i = j = m \\ 0 & \text{else} \end{cases}$$

and $\mathbf{D}^{-1} = \mathbf{D}^{\mathbf{H}}$. The load power can be expressed in terms of apparent voltages using (4.4) as,

$$P_L = \mathbf{v}^{\mathbf{H}} \left(\mathbf{c}\mathbf{c}^{\mathbf{H}}\right) \mathbf{v} = \mathbf{u}^{\mathbf{H}}\mathbf{D} \left(\mathbf{c}\mathbf{c}^{\mathbf{H}}\right) \mathbf{D}^{\mathbf{H}}\mathbf{u} = \mathbf{u}^{\mathbf{H}} \left(\tilde{\mathbf{c}}\tilde{\mathbf{c}}^{\mathbf{H}}\right) \mathbf{u} \tag{4.19}$$

where $\tilde{\mathbf{c}} = \mathbf{D}\mathbf{c}$. The total transmit power given by (4.5) and can be written in terms of apparent voltages using (4.18) as,

$$P_G = \mathbf{v}^{\mathbf{H}}\bar{\mathbf{A}}\mathbf{v} = \mathbf{u}^{\mathbf{H}}\mathbf{D}\bar{\mathbf{A}}\mathbf{D}^{\mathbf{H}}\mathbf{u} = \mathbf{u}^{\mathbf{H}}\tilde{\mathbf{A}}\mathbf{u} \tag{4.20}$$

where $\tilde{\mathbf{A}} = \mathbf{D}\bar{\mathbf{A}}\mathbf{D}^{\mathbf{H}}$.

The optimization problem of maximizing the power transfer efficiency can be written in terms of $\mathbf{u}$ using (4.19) and (4.20) as follows:

$$\tilde{\mathbf{u}} = \arg\max_{\mathbf{u}} \ \mathbf{u^H \tilde{c} \tilde{c}^H u}$$
$$\text{such that } \mathbf{u^H \tilde{A} u} = 1 \tag{4.21}$$

The above optimization problem is similar to the optimization problem described by (4.8) whose optimal solution is given by (4.17). Hence, the optimal solution to the problem (4.21) is given by:

$$\tilde{\mathbf{u}} = \frac{1}{\sqrt{\beta_2}} \tilde{\mathbf{A}}^{-1} \tilde{\mathbf{c}} \ ; \quad \beta_2 = \tilde{\mathbf{c}}^{\mathbf{H}} \tilde{\mathbf{A}}^{-1} \tilde{\mathbf{c}} \tag{4.22}$$

Using (4.19) and (4.20),

$$\tilde{\mathbf{A}}^{-1} \tilde{\mathbf{c}} = \left(\mathbf{D} \bar{\mathbf{A}} \mathbf{D}^{\mathbf{H}}\right)^{-1} \mathbf{D c} = \mathbf{D} \bar{\mathbf{A}}^{-1} \mathbf{D}^{\mathbf{H}} \mathbf{D c} = \mathbf{D} \bar{\mathbf{A}}^{-1} \mathbf{c}$$
$$\Rightarrow \beta_2 = \tilde{\mathbf{c}}^{\mathbf{H}} \tilde{\mathbf{A}}^{-1} \tilde{\mathbf{c}} = \mathbf{c}^{\mathbf{H}} \mathbf{D}^{\mathbf{H}} \mathbf{D} \bar{\mathbf{A}}^{-1} \mathbf{c} = \mathbf{c}^{\mathbf{H}} \bar{\mathbf{A}}^{-1} \mathbf{c} = \beta$$

Hence, using (4.17) in (4.22)

$$\tilde{\mathbf{u}} = \frac{1}{\sqrt{\beta}} \tilde{\mathbf{A}}^{-1} \tilde{\mathbf{c}} = \frac{1}{\sqrt{\beta}} \mathbf{D} \bar{\mathbf{A}}^{-1} \mathbf{c} = \frac{1}{\sqrt{\beta}} \sqrt{\beta} \mathbf{D} \tilde{\mathbf{v}}$$

or in other words,

$$\tilde{\mathbf{u}} = \mathbf{D} \tilde{\mathbf{v}}$$

4.3 A practical procedure to estimate the model parameters

First, we present a simple, practical method to estimate the unknown "channel" parameters $\mathbf{A}$, $\mathbf{c}$ using a set of simple measurements, and later, present a more robust estimation procedure based on the least-squares principle. The estimation

procedure in both the methods require measurements only at the input terminals and the load and does not involve any measurements anywhere else in the circuit.

4.3.1 Simple estimation procedure

The basic idea is that the sources will apply a sequence of voltage vectors $\mathbf{v}[k],\ k = 1, 2, \ldots K$. The sources measure the resulting current vectors $\mathbf{i}[k]$, and the load measures the resulting voltages $v_0[k]$ and currents $i_0[k]$. (The currents $i_0[k]$ are of course related to the voltages $v_0[k]$ through Ohm's law and if the load impedance Z_0 is known, then only the voltage measurements $v_0[k]$ are needed.) Given at least N linear independent excitations $\mathbf{v}[k]$ and the resulting observations, we can calculate the parameters $\mathbf{A},\ \mathbf{c}$.

Specifically, consider the set of N excitations $\mathbf{v}[k] = \delta_k,\ k = 1 \ldots N$ where δ_k is the k-th column of the identity matrix $\mathbf{I}_N$. This means that for the first set of observations, transmitter 1 is excited with a unit voltage while transmitters $k = 2 \ldots N$ are short-circuited, for the second set of observations, transmitter 2 alone is excited and so on. Using the measurement of $v_0[k]$, the k-th element c_k of the vector $\mathbf{c}$ is obtained as $c_k = \sqrt{\Re\left(\frac{1}{Z_0}\right)} v_0^*[k]$ using the definition in (4.4), and similarly, using the current measurements $i_j[k]$ for each of the input terminals $j = 1 \ldots N$, the k-th element $b_{j,k}$ of each of the vectors $\mathbf{b}_j,\ j = 1 \ldots N$ can be obtained as $b_{j,k} = \mathbf{i}_j^*[k]$. Using the N set of measurements $k = 1 \ldots N$, the vectors $\mathbf{c},\ \mathbf{b}_i$ can all be obtained and the matrix $\bar{\mathbf{A}}$ can then be calculated from its definition as $\bar{\mathbf{A}} \equiv \frac{1}{2} \sum_{i=1}^{N} \left(\delta_\mathbf{i} \mathbf{b}_\mathbf{i}^\mathbf{H} + \mathbf{b}_\mathbf{i} \delta_\mathbf{i}^\mathbf{H}\right)$.

4.3.2 Robust estimation procedure

We now present a more generalized and robust procedure to estimate the parameters using real-time periodic measurements in an adaptive manner based on the least mean squares principle.

Let n denote the measurement index and at each measurement index, the input currents and output voltage/current are measured by applying input voltages across the transmit coils. When at least $n = N$ number of linearly independent voltage vectors are applied across transmitter coils, we can start estimating the model parameters. When the voltage vector $\mathbf{v}[n] = [v_1[n], v_2[n], ..., v_N[n]]^T$ is applied across the transmit coils at n-th iteration, the resulting current measured in each transmit coil and the load voltage are denoted by $\mathbf{i}[n] = [i_1[n], i_2[n], ..., i_N[n]]^T$ and $v_0[n]$ respectively. To estimate the model parameters, we form the following matrices

$$\mathbf{V} = \big[\mathbf{v}[1],\ \mathbf{v}[2], \ldots, \mathbf{v}[n]\big] \quad \text{and} \quad \mathbf{J} = \big[\mathbf{i}[1], \mathbf{i}[2], \ldots, \mathbf{i}[n]\big] \tag{4.23}$$

and output voltage vector

$$\mathbf{v_0} = \big[v_0[1],\ v_0[2], \ldots, v_0[n]\big] \tag{4.24}$$

where the n-th column of the above matrices denotes the measurements corresponding to the n-th iteration. We assume that

$$\mathbf{J}_{N\times n} = \mathbf{G}_{N\times N}\mathbf{V}_{N\times n}$$

for some "conductance" matrix $\mathbf{G}$ which is a function of the total input power matrix,

$\bar{\mathbf{A}}$. The least squares estimate of the matrix $\mathbf{G}$ denoted by $\hat{\mathbf{G}}$ is given by

$$\begin{aligned} \hat{\mathbf{G}} &= \arg\min_{\mathbf{G}} \quad ||\mathbf{J} - \mathbf{G}\mathbf{V}||_2 \\ &= \mathbf{J}\mathbf{V}^H \left(\mathbf{V}\mathbf{V}^H\right)^{-1} \end{aligned} \tag{4.25}$$

assuming that $\mathbf{V}$ has full row-rank, which can be ensured by the choice of excitation voltage we choose to apply across each of the transmit coil. Also, the least squares estimate of the transgain vector $\mathbf{a_0}$, denoted by $\hat{\mathbf{a}}_\mathbf{0}$ is given by

$$\hat{\mathbf{a}}_\mathbf{0} = \arg\min_{\mathbf{a}_0} \quad \left|\left|\mathbf{v_0} - \mathbf{a_0^H}\mathbf{V}\right|\right|_2$$

and

$$\hat{\mathbf{a}}_\mathbf{0}^\mathbf{H} = \mathbf{v_0}\mathbf{V}^H \left(\mathbf{V}\mathbf{V}^H\right)^{-1} \quad \Rightarrow \quad \hat{\mathbf{a}}_\mathbf{0} = \left(\mathbf{V}\mathbf{V}^H\right)^{-1} \mathbf{V}\mathbf{v_0}^H \tag{4.26}$$

Relation between G and $\bar{\mathbf{A}}$

We now derive the relation between the conductance matrix, $\mathbf{G}$ and the input power matrix $\bar{\mathbf{A}}$. We know that

$$\begin{aligned} \mathbf{A}_i &= \frac{1}{2}\left(\delta_i \mathbf{b}_i^H + \mathbf{b}_i \delta_i^h\right) \\ &= \frac{1}{2}\left(\delta_i \delta_i^H \mathbf{G}^H + \mathbf{G}\delta_i \delta_i^H\right) \end{aligned}$$

as $i_i = \mathbf{b_i^H}\mathbf{v} = \left(\mathbf{G}\delta_i\right)^H \mathbf{v}$. As a result,

$$\begin{aligned} \mathbf{A} &= \sum_i \mathbf{A_i} = \frac{1}{2}\left(\sum_i \delta_i \delta_i^H\right)\mathbf{G}^H + \frac{1}{2}\mathbf{G}\left(\sum_i \delta_i \delta_i^H\right) \\ &= \frac{\mathbf{G}^H + \mathbf{G}}{2} \end{aligned} \tag{4.27}$$

as the elements of $\mathbf{\Delta} = \left(\sum_i \delta_i \delta_i^H\right)$ are given by

$$[\mathbf{\Delta}]_{pq} = \begin{cases} 1 & \text{if } p = q \\ 0 & \text{else} \end{cases}$$

where $[\mathbf{\Delta}]_{pq}$ represent the p-th row and q-th column element of matrix $\mathbf{\Delta}$ and hence, $\sum_i \delta_i \delta_i^H = \mathbf{I}$.

Iterative method to update the estimates

We now present an iterative algorithm to update the estimate of conductance matrix, $\hat{\mathbf{G}}$ and transgain vector, $\hat{\mathbf{a}}_\mathbf{0}$ when a new measurement is made. We denote the least squares estimate of the conductance matrix after the n-th measurement by

$$\hat{\mathbf{G}}[n] = \mathbf{J}[n]\mathbf{V}^H[n]\left(\mathbf{V}[n]\mathbf{V}^H[n]\right)^{-1}$$

and transgain vector by

$$\hat{\mathbf{a}}^\mathbf{H}[n] = \mathbf{v_0}[n]\mathbf{V}^H[n]\left(\mathbf{V}[n]\mathbf{V}^H[n]\right)^{-1}$$

When a new measurement is made, the $(n+1)$-th least squares estimate of the conductance matrix and transgain vector are given by,

$$\begin{aligned} \hat{\mathbf{G}}[n+1] &= \mathbf{V}[n+1]\mathbf{V}^H[n+1]\left(\mathbf{V}[n+1]\mathbf{V}^H[n+1]\right)^{-1} \\ &= \hat{\mathbf{G}}[n] + \mathbf{e_1}[n+1]\mathbf{k}^\mathbf{H}[n+1] \qquad (4.28) \\ \hat{\mathbf{a}}^\mathbf{H}[n+1] &= \mathbf{v_0}[n+1]\mathbf{V}^H[n+1]\left(\mathbf{V}[n+1]\mathbf{V}^H[n+1]\right)^{-1} \\ &= \hat{\mathbf{a}}^\mathbf{H}[n] + \mathbf{e_2}[n+1]\mathbf{k}^\mathbf{H}[n+1] \qquad (4.29) \end{aligned}$$

where $\mathbf{e_1}[\mathbf{n}] = \left(\mathbf{i}[n] - \hat{\mathbf{G}}[n-1]\mathbf{v}[n]\right)$ and $\mathbf{e_2}[\mathbf{n}] = \left(\mathbf{v_0}[n] - \hat{\mathbf{a}}^H[n-1]\mathbf{v}[n]\right)$ measures the error in the input currents and output voltage. The gain of the estimator, denoted

by $\mathbf{k}$ is given by

$$\mathbf{k}[\mathbf{n}] = \frac{\left(\mathbf{V}[n-1]\mathbf{V}^H[n-1]\right)^{-1}\mathbf{v}[n]}{1+\mathbf{v}^{\mathbf{H}}[n]\left(\mathbf{V}[n-1]\mathbf{V}^H[n-1]\right)^{-1}\mathbf{v}[n]} \tag{4.30}$$

Hence, the least squares estimate for the transgain vector can be used to find the least square estimate of the transconductance vector, $\hat{\mathbf{c}}[n]$ as

$$\hat{\mathbf{c}}[n] = \sqrt{\Re\left(\frac{1}{Z_0}\right)}\hat{\mathbf{a}}_{\mathbf{0}}[n] \tag{4.31}$$

A derivation of the above is provided in Appendix.

We propose an algorithm to compute the optimal transmit voltage at each node given any measurement index, n, based on (4.17), (4.27), (4.28), (4.30) and (4.31). The algorithm is described in pseudocode form in Algorithm 4.1.

Note: We update the pseudo-inverse

$$\mathbf{P}[n] = \left(\mathbf{V}[n]\mathbf{V}^{\mathbf{H}}[n]\right)^{-1} \tag{4.32}$$

based on the Matrix Inversion Lemma and the specific equation for this case is also derived in Appendix.

4.4 Experimental validation

First, we conducted a number of simple experiments involving two transmitter coils and a single receiver coil to validate our approach and later, we performed a macro scale experiment involving four transmit coils and two receiver coils to analyze the optimal solution and the gains we expect as compared to other known methods in the literature, especially, the equal power beamforming solution which is widely used [42].

Algorithm 4.1 Iterative algorithm for computing the optimal solution

1: Excite coil 1 i.e., set $\mathbf{v}[1] = [1, 0, ..., 0]^T$

2: Measure input current vector $\mathbf{i}[1] = [i_1[1], i_2[1], ..., i_N[1]]^T$ and load voltage, $v_0[1]$

3: **repeat**

4: Repeat steps 1,2 for all transmit coils by exciting one coil at a time.

5: **until**

6: Construct matrices, $\mathbf{J}[N] = [\mathbf{i}[1], \mathbf{i}[2], ..., \mathbf{i}[N]]$, $\mathbf{V}[N] = [\mathbf{v}[1], \mathbf{v}[2], ..., \mathbf{v}[N]]$ and vector, $\mathbf{v_0}[N] = [v_0[1], v_0[2], ..., v_0[N]]$.

7: Estimate $\hat{\mathbf{G}}[N] \leftarrow \mathbf{J}[N]\mathbf{V^{-1}}[N]$ and $\hat{\mathbf{c}}^{\mathbf{H}}[N] \leftarrow \sqrt{\Re\left(\frac{1}{Z_0}\right)}\mathbf{v_0}[N]\mathbf{V^{-1}}[N]$

8: Compute $\bar{\mathbf{A}} \leftarrow 0.5\left(\hat{\mathbf{G}}[N] + \hat{\mathbf{G}}^{\mathbf{H}}[N]\right)$ and $\tilde{\mathbf{v}} \leftarrow \bar{\mathbf{A}}^{\mathbf{-1}}\hat{\mathbf{c}}[N]$

9: Set $\mathbf{P}[N] \leftarrow \left(\mathbf{V}[N]\mathbf{V}^{\mathbf{H}}[N]\right)^{-1}$

10: Set n $\leftarrow N + 1$.

11: **repeat**

12: Apply $\mathbf{v}[\mathbf{n}]$ and measure $\mathbf{i}[\mathbf{n}]$, $\mathrm{v}_0[\mathrm{n}]$.

13: Set $\mathbf{e_1}[\mathbf{n}] \leftarrow \left(\mathbf{i}[n] - \hat{\mathbf{G}}[n-1]\mathbf{v}[n]\right)$ and $\mathbf{e_2}[\mathbf{n}] \leftarrow \left(v_0[n] - \hat{\mathbf{a}}^{\mathbf{H}}[n-1]\mathbf{v}[n]\right)$

14: Calculate the gain : $\mathbf{k}^{\mathbf{H}}[n] \leftarrow \frac{\mathbf{P}[n-1]\mathbf{v}[n]}{1+\mathbf{v}^{\mathbf{H}}[n]\mathbf{P}[n-1]\mathbf{v}[n]}$

15: Set $\hat{\mathbf{G}}[n] \leftarrow \hat{\mathbf{G}}[n-1] + \mathbf{e_1}[n]\mathbf{k}^{\mathbf{H}}[n]$ and $\bar{\mathbf{A}} \leftarrow 0.5\left(\mathbf{G}[n] + \mathbf{G}^{\mathbf{H}}[n]\right)$

16: Set $\hat{\mathbf{c}}^{\mathbf{H}}[n] \leftarrow \sqrt{\Re\left(\frac{1}{Z_0}\right)}\left(\hat{\mathbf{a}}^{\mathbf{H}}[n-1] + \mathbf{e_2}[n]\mathbf{k}^{\mathbf{H}}[n]\right)$

17: Set $\mathbf{P}[n] \leftarrow \mathbf{P}[n-1]\left(\mathbf{I} - \frac{\mathbf{v}[n]\mathbf{v}^{\mathbf{H}}[n]\mathbf{P}[n-1]}{1+\mathbf{v}^{\mathbf{H}}[n]\mathbf{P}[n]\mathbf{v}[n]}\right)$

18: Compute $\tilde{\mathbf{v}} \leftarrow \bar{\mathbf{A}}^{\mathbf{-1}}\hat{\mathbf{c}}[n]$

19: Set n $\leftarrow$ n + 1

20: **until** $\mathrm{n} \leq \mathrm{n_{max}}$

4.4.1 Experiments with two transmit and one receive coil

We now present results from our first set of experiments involving two transmit and one receive coil. All three coils in this experiment were obtained from a commercial off-the-shelf catalog [43] and were designed to work with the Qi charging standard. We chose an operating frequency of 200 kHz for this experiment and added low-loss $0.1\mu F$ ceramic capacitors to each coil so they would all self-resonant at this frequency albeit with a modest Q factor. We drive each transmit coil with a signal generator and use a buffer amplifier to mitigate the effect of 50 Ω output impedance of the signal generator. We use a resistive load of 1 Ω and measure the short-circuit current across a transmit coil by measuring the voltage across a 1 Ω test resistor.

Figure 4.2 shows a buffer amplifier circuit that drives each transmit coil. The

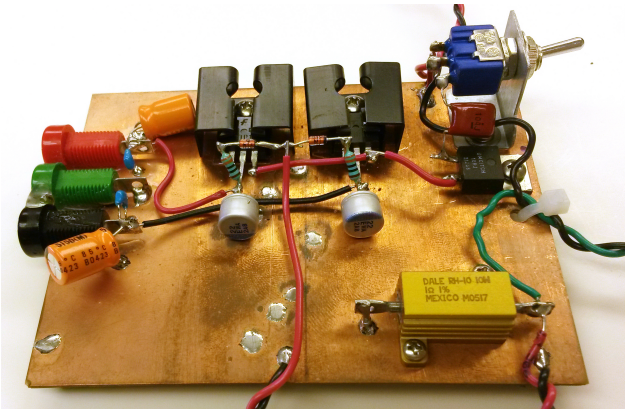

Figure 4.2: A buffer amplifier circuit for driving each transmit coil

switch in the ON position connects each coil to the signal source via the buffer am-

plifier and in the OFF position connects the coil to the ground via a 1 Ω test resistor that helps us measure the short-circuit current. Our goal in these experiment is *not* to demonstrate a WPT system with high efficiency. Instead, our goal is construct a simple experimental setup where the efficiency, even if it is small in absolute terms, is shown to be correctly optimized using our model. We specifically consider three cases, namely,

1. Weakly coupled transmit coils
2. Parasitic transmit coil
3. Strongly coupled transmit coils

The experimental setup is shown in Fig. 4.3 and the orientation and distance between these coils is varied to get the three different cases. The coupling coefficient between the two transmit coils is denoted by M_{12} and M_{1R}, M_{2R} denote the coupling coefficient between transmit coil 1 and coil 2 to the receiver respectively. A simple circuit model for this setup is also shown in Fig. 4.4; of course this simple circuit model is unlikely to be very accurate, and instead of analyzing this circuit directly, we use the simple estimation procedure outlined in section 4.3.1 to measure the model parameters, $\bar{\mathbf{A}}$ and $\mathbf{c}$.

Case1: Weakly Coupled Transmit Coils

Consider two transmit coils that are weakly coupled to each other but which are strongly coupled to the receiver individually, i.e., M_{12} is significantly smaller compared to M_{1R} and M_{2R}. The above configuration was accomplished by placing the two

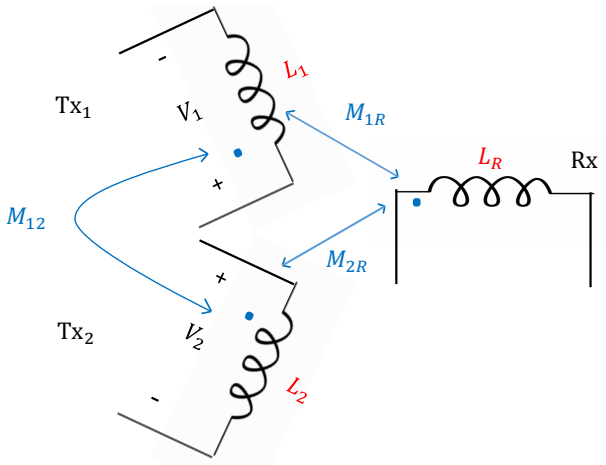

Figure 4.3: Illustration of the experimental setup for wireless power transfer to a receiver (Rx) from two transmitters (Tx1 and Tx2)

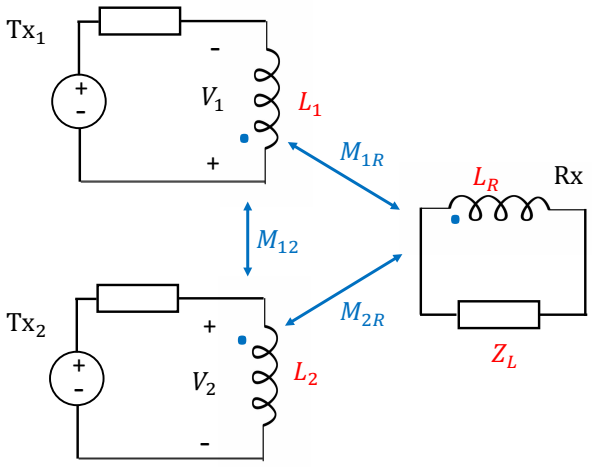

Figure 4.4: A simple circuit model for the wireless power transfer experiment with two transmitters

transmit coils side-by-side and placing the receiver coil in between the transmit coils at a separation of 3 cm and facing the transmit coils. The experimental measurements of phasor currents and voltages when single transmit coil is excited to estimate the model parameters are shown in Table 4.1.

Table 4.1: Measurements for weakly coupled transmit coils

V_1 (mV)	V_2(mV)	i_1(mA)	i_2 (mA)	v_0(mV)
mag	mag	mag, phase	mag, phase	mag, phase
393.6	0	26.3, 55.3°	2.84, 131.2°	43.0, -13.5°
0	406.2	3.1, 130.1°	24.7, 55.6°	43.2, 167.4°

From this set of measurements, we calculated the parameters $\bar{\mathbf{A}}$, $\mathbf{c}$ using the method described in Section 4.3.1. Since, the transmit coils are weakly coupled, we expect the $\bar{\mathbf{A}}$ to be highly diagonal, which is what we observe below:

$$\bar{\mathbf{A}} = 0.01 \begin{bmatrix} 3.6 & 0.6\angle 177.7 \\ 0.6\angle -177.7 & 3.3 \end{bmatrix}; \quad \mathbf{c} = 0.11 \begin{bmatrix} 1\angle 10.5 \\ 1\angle -170 \end{bmatrix}$$

The optimal transmit voltage vector calculated using (4.13) is

$$\tilde{\mathbf{v}} = k \begin{bmatrix} 1\angle 0^\circ \\ 1.1\angle 179^\circ \end{bmatrix} \text{V}$$

We can observe from Table 4.1 that the transmit coils induce roughly the same amount of voltage in the receiver coil when they are individually excited, resulting in the transmit coils to have comparable coupling coefficients to the receiver coil. Hence, the optimal solution also has roughly the same amount of transmit voltage on each

individual coil. Also, the phase of the induced voltage on the receiver due to coil 1 is 0.38°and due to coil 2 is 0.40°, confirming the optimality of the beamforming solution from property 4.2, since the transmit coils are weakly coupled to each other. The magnitude of the received voltage was measured to be 784mV when the optimal voltage excitation was applied, resulting in measured efficiency of 61.47% which is close to theoretical predicted efficiency of 62.6%. The measured efficiency was significantly higher than the single coil efficiencies of roughly about 32% from each transmit coil.

Case 2: Parasitic Transmit Coil

Consider two transmit coils that are coupled to each other but only one of these transmit coils, say coil 2 is strongly coupled to the receiver, i.e., M_{1R} is significantly smaller as compared to M_{12} and M_{2R}. The above configuration was achieved by interchanging the role of load and transmit coil from case 1 to that of transmit and load coil for case 2 respectively. The experimental measurements of phasor currents and voltages when single transmit coil is excited to estimate the model parameters are shown in Table 4.2. The estimate of the total power matrix $\bar{\mathbf{A}}$ and $\mathbf{c}$ are given by

Table 4.2: Measurements for parasitic transmit coil

V_1 (mV)	V_2(mV)	i_1(mA)	i_2 (mA)	v_0(mV)
mag	mag	mag, phase	mag, phase	mag, phase
470	0	26.1, 62.6°	25.6, -125.8°	4.4, 62.4°
0	203.6	12.1, -126.3°	36.1, 55.7°	23, -112.1°

$$\bar{\mathbf{A}} = 0.01 \begin{bmatrix} 2.2 & 2.6\angle -174.7 \\ 2.6\angle 174.7 & 8 \end{bmatrix}; \quad \mathbf{c} = 0.1 \begin{bmatrix} 0.14\angle 93.6 \\ 1.24\angle -102.4 \end{bmatrix}$$

and the optimal set of transmit voltages computed using (4.13) is

$$\tilde{\mathbf{v}} = k \begin{bmatrix} 1\angle 0^\circ \\ 1.1\angle -12.5^\circ \end{bmatrix} \text{V}$$

It can be observed that the induced voltage in the receiver coil is very small when transmit coil 1 is excited alone, confirming the very weak coupling between coil 1 and the receiver coil. As a result, it seems reasonable to drive coil 2 alone to maximize received power. However, the optimal solution suggests something very different from just driving coil 2 alone. This is because when coil 2 is excited alone, the strong coupling between the two transmit coils ensures that the induced current in coil 1 is not negligible and hence, there is some power lost in coil 1 reducing the overall efficiency. Therefore, we would still want to drive coil 1 so that the current drawn from the source can be used to cancel some of the induced current from coil 2 that results in reducing the power lost in coil 1 and therefore, improving the overall efficiency of the WPT system.

By using the optimal excitation voltages to drive the two transmit coils, we observe that the current delivered by exciting coil 1 though it is weakly coupled to the receiver results in canceling approximately 70% of induced current from coil 2. The optimal solution results in measured efficiency of 23% which is significantly better than 16% efficiency obtained by just exciting coil 2 alone. The measured efficiencies again match closely to the predicted 25% optimal efficiency and 19% efficiency obtained by exciting coil 2 alone.

Case 3: Strongly Coupled Transmit Coils

Consider the experimental setup where all the three coils are coupled to each other and this configuration was achieved by placing the three coils on the sides of an equilateral triangle; intuitively in this setup, the coupling between any two of the three coils is comparable, so the transmitters are coupled to each other as well as to the receiver.

Table 4.3: Measurements for strongly coupled transmit coils

V_1 (mV)	V_2(mV)	i_1(mA)	i_2 (mA)	v_0(mV)
mag	mag	mag, phase	mag, phase	mag, phase
277	0	40, 61°	15, -78°	18, 32°
0	280	14, -82°	37, 62°	22, -38°

Table 4.3 shows the results of a set of experiments where the phasor voltages and currents in the coils are measured while exciting the two transmit coils individually. From this set of measurements, we calculated the parameters $\bar{\mathbf{A}}$, $\mathbf{c}$ as described in Section 4.3, and the optimal voltage excitation from (4.13). The optimal solution in this case is calculated to be

$$\tilde{\mathbf{v}} = k \begin{bmatrix} 1\angle 0^\circ \\ 1.4\angle 128^\circ \end{bmatrix} \text{V}$$

It can be seen from Table 4.3 that the transmit coils have strong and almost equal coupling to the receiver coil because they induce roughly equal voltage in the receiver coil when they are separately excited. The optimal solution $\tilde{\mathbf{v}}$ also has roughly equal

magnitudes for the voltage to be applied on both the transmitter coils. Remarkably, however, the phase of the optimal induced voltage at the receiver coil due to coil Tx1 is approximately -40° and due to coil Tx2 is approximately 20°; in other words, the phases of optimal induced voltages are around 60° apart at the receiver which makes the optimal solution very far from the phase coherent beamforming solution.

The measured power transfer efficiencies also confirm the predictions of our model very well. Specifically, the calculated optimal solution $\tilde{\mathbf{v}}$ is able to significantly improve the efficiency as compared to single coil efficiency, as well as the naive phase coherent beamforming solution. The efficiency of coil Tx1 is measured to be approximately 6% and coil Tx2 approximately 10%, while the efficiency achieved by exciting two transmit coils with the optimal voltage vector was measured to be approximately 26%. By contrast, the efficiency achieved by the phase coherent beamforming solution was measured to be only about 20% which is significantly worse than the optimal solution. These measured efficiency numbers are also very close to the theoretical predicted efficiencies of 27% and 21% for the optimal and beamforming solutions respectively calculated using the estimated values of the parameters $\mathbf{A}$, $\mathbf{c}$.

4.4.2 Experiments with four transmit and two receive coils

Now, we present the experimental results with four transmit and two receive coils. We offer an analysis of the measurements obtained from the experiments conducted at the Purdue University. We performed two sets of experiments. In the first set of experiments, each of the four transmitter coils is excited one at a time and

the resulting voltages and currents are measured. In the second set of experiments, the transmit coils are excited *two* at a time resulting in $\binom{4}{2} = 6$ sets of voltage and current measurements.

In this set of experiments, we use current sources rather than voltage sources to drive the coils as measuring the open-circuit voltages on the transmit coils is much easier than measuring short-circuit currents, which is the case when we use voltage sources. With the help of duality, we can translate the above estimation procedure for measuring the model parameters to deal with current sources and also, derive the necessary optimal excitation currents to maximize efficiency. As a result of duality, using (4.4) we can express load power in terms of input currents, $\mathbf{i}$ as,

$$P_L = \mathbf{i^H} \left(\mathbf{cc^H}\right) \mathbf{i} \tag{4.33}$$

for some *trans-impedance* vector, $\mathbf{c} = \sqrt{\Re\left(Z_0\right)}\mathbf{b_0}$, where the load current $i_0 = \mathbf{b_0^H i}$. Also, using (4.7) the input power can also be expressed in terms of input currents, $\mathbf{i}$ as,

$$P_G = \mathbf{i^H \bar{B} i} \tag{4.34}$$

Similar to (4.17), the optimal current excitation vector that maximizes efficiency is given by

$$\tilde{\mathbf{i}} = k\ \bar{\mathbf{B}}^{-1}\mathbf{c} \tag{4.35}$$

We briefly outline the simple estimation procedure presented in section 4.3.1 to estimate the model parameter with current sources instead of voltage sources. As a result of duality, the load current when the k-th coil is excited alone with unit

current, determines the k-th element of transgain vector $\mathbf{b_0}$. Similarly, using the voltage measurements across input terminals, $v_j[k]$ for each of the input terminals $j = 1 \dots N$, the k-th element $a_{j,k}$ of each of the vectors $\mathbf{a}_j$, $j = 1 \dots N$ can be obtained as $a_{j,k} = \mathbf{v}_j^*[k]$. Using the N set of measurements $k = 1 \dots N$, the vectors $\mathbf{c}$, $\mathbf{a}_i$ can all be obtained and the matrix $\bar{\mathbf{B}}$ can then be calculated from its definition as $\bar{\mathbf{B}} \equiv \frac{1}{2} \sum_{i=1}^{N} \left(\delta_{\mathbf{i}} \mathbf{a}_{\mathbf{i}}^{\mathbf{H}} + \mathbf{a_i} \delta_{\mathbf{i}}^{\mathbf{H}} \right)$.

Since there are two receive coils, we use $\mathbf{b_{0,1}}$ and $\mathbf{b_{0,2}}$ to denote the current gain vectors between transmit coil array and receiver coil 1 and 2 respectively, i.e.,

$$i_{0,1} = \mathbf{b}_{\mathbf{0,1}}^{\mathbf{H}} \mathbf{i} \quad \text{and} \quad i_{0,2} = \mathbf{b}_{\mathbf{0,2}}^{\mathbf{H}} \mathbf{i} \tag{4.36}$$

and calculate the trans-impedance gain as,

$$\mathbf{c_1} = \sqrt{\Re\left(Z_{0,1}\right)}\, \mathbf{b_{0,1}} \quad \text{and} \quad \mathbf{c_2} = \sqrt{\Re\left(Z_{0,2}\right)}\, \mathbf{b_{0,2}} \tag{4.37}$$

where $Z_{0,1}$ and $Z_{0,2}$ are the load resistances in receiver coil 1 and 2 respectively.

We use the single coil excitation measurements to measure the model parameters and analyze the efficiency of WPT system and use the two coil excitation measurements to verify our results. We compare the optimal efficiency against two other methods, namely,

1. Equal power beamforming: This is the most widely used method in the literature on WPT systems with multiple transmitters [42] in which the phase of the excitation current is chosen to be the negative of the phase of the transgain at each transmitter. This choice of current excitation ensures that the contributions from each transmitter to the total load current are aligned in phase and

thus add up *coherently*.

2. Conjugate beamforming: We propose this method inspired by a common precoding technique in multi-antenna wireless communication systems. In this method, the excitation current is chosen to be the complex conjugate of the current gain at each node. This choice of excitation current still achieves phase coherence in the receiver coil but may be expected to achieve superior efficiency compared to equal power beamforming because it allows transmitters with weak channels to scale back their transmitted power proportionally.

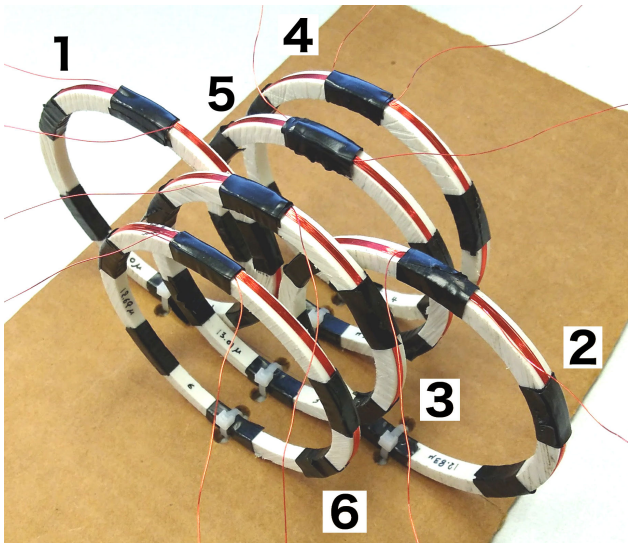

Figure 4.5: Geometrical position of four transmit and two receive coils for wireless power transfer

The measurement results when a single transmitter coil is excited are shown

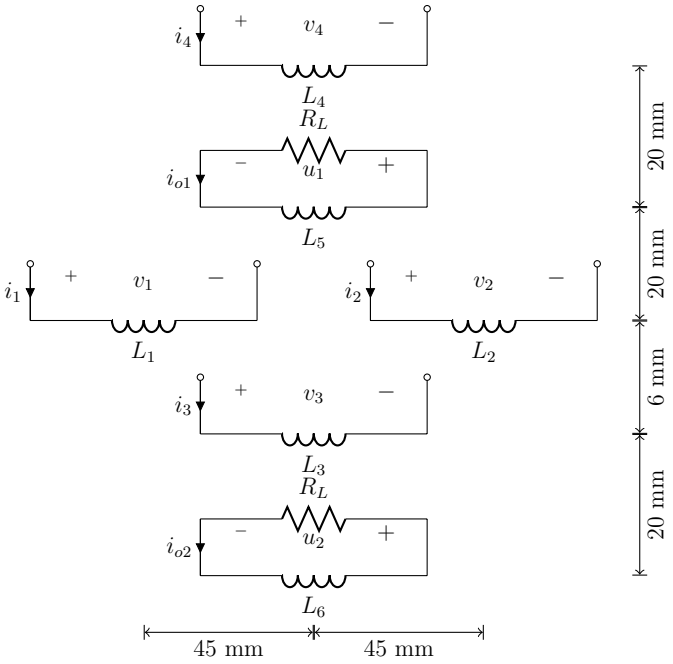

Figure 4.6: Circuit configuration of experimental setup and dimensions indicate center-to-center distances of the coils

in Table 4.4.

We use the estimation procedure described in section 4.3 with four measurements to measure the model parameters. The estimated transmitted power matrix is:

$$\bar{\mathbf{B}} = \begin{bmatrix} 0.93 & 0.02\angle 21.1^\circ & 0.13\angle -30.4^\circ & 0.1\angle -35.6^\circ \\ 0.02\angle -21.1^\circ & 1.31 & 0.12\angle -1.8^\circ & 0.1\angle -38.8^\circ \\ 0.13\angle 30.4^\circ & 0.12\angle 1.8^\circ & 1.08 & 0.16\angle 1.0^\circ \\ 0.1\angle 35.6^\circ & 0.1\angle 38.8^\circ & 0.16\angle -1.0^\circ & 0.92 \end{bmatrix}$$

and the trans-impedance vectors are:

$$\mathbf{c_1} = \begin{bmatrix} 0.12\angle 78.2^\circ \\ 0.12\angle 78.2^\circ \\ 0.28\angle 78.4^\circ \\ 0.36\angle 79.2^\circ \end{bmatrix}; \quad \mathbf{c_2} = \begin{bmatrix} 0.11\angle 77.4^\circ \\ 0.11\angle 78.4^\circ \\ 0.36\angle 78^\circ \\ 0.08\angle 75.7^\circ \end{bmatrix}$$

Table 4.4: Measurements with four-transmitters when single coil is excited

n	i_1 (mV)	i_2(mV)	i_3(mA)	i_4 (mA)	v_1(mV)	v_2(mV)
index	mag	mag	mag	mag	mag, phase	mag, phase
1	33.2	0	0	0	550.2, -86.8°	32.9, 89.0°
2	0	33.4	0	0	33.2, 89.2°	543.4, -85.4°
3	0	0	32.9	0	55.6, -86.4°	60.0, -86.1°
4	0	0	0	33.2	28.3, -85.3°	27.4, -84.7°

v_3(mV)	v_4 (mV)	$i_{0,1}$(mA)	$i_{0,2}$(mA)
mag, phase	mag, phase	mag, phase	mag, phase
51.9, -85.8°	24.9, -84.3°	0.4, -78.2°	0.4, -77.4°
60.1, -86.2°	23.4, -84.1°	0.4, -78.4°	0.4, -78.3°
551.4, -86.3°	45.5, -83.3°	0.9, -78.4°	1.2, -79.1°
45.7, -83.6°	549.5, -86.8°	1.2, -79.1°	0.3, -75.7°

We first look at maximizing the efficiency to receive coil 1 or coil 5 in Fig. 4.6 and the optimal excitation vector computed using (4.13) is

$$\tilde{\mathbf{i}}_{\mathbf{1}} = k_1 \left[1\angle 0°; 0.6\angle -3.2°; 2.2\angle -26.3°; 4.0\angle -23.8°\right]^T \text{A}$$

and the corresponding equal power ($\mathbf{i_{eq,1}}$) and conjugate beamforming excitation ($\mathbf{i_{conj,1}}$) are:

$$\mathbf{i_{eq,1}} = k_2 \left[1\angle 0°; 1\angle 0°; 1\angle 0.2°; 1\angle 10°\right]^T \text{A}$$

and

$$\mathbf{i_{conj,1}} = k_3 \left[1.0\angle 0°; 1.0\angle 0°; 2.3\angle 0.2°; 3.0\angle 10°\right]^T \text{A}$$

It can be seen from Fig. 4.6 that transmit coils 3 and 4 are co-planar to the receive coil 1 and hence, have strong coupling co-efficients to receive coil 1 as compared to transmit coils 1 and 2, which is what we observe in $\mathbf{c_1}$. Also, as transmit

coil 4 is closer to receive coil 1, they have a strong coupling coefficient between them as compared to transmit coil 3, which is also reflected in $\mathbf{c_1}$.

As a result of strong coupling between transmit coils 3 and 4 to the receive coil 1, the optimal solution is heavily weighted to these two coils. The maximum achievable efficiency is 19.1% which is significantly better than 14.1% efficiency obtained by using the well-known method of equal power beamforming [42] and marginally better than 18.3% efficiency achieved by conjugate beamforming. The phase of the received voltage due to transmit coils 1, 2, 3 and 4 are 22.5°, 18.2°, -3.2°, -1.5°respectively and it can be observed that this is different from the beamforming excitation. Note that the efficiency degradation due to the non-optimal phase excitation of the conjugate beamforming solution is small. Most of the efficiency improvement of the optimal solution as compared to equal power beamforming is due to the amplitude mismatch i.e. the power transmitted by coils that are very weakly coupled to the receiver.

This observation highlights an important oversight in previous work that has mostly taken for granted the optimality of coherent beamforming excitation. The beamforming solution seems intuitively reasonable following an analogy with beamforming from antenna arrays: coherent beamforming allows the individual induced currents from each transmitter to combine constructively at the intended receiver and therefore achieves the largest possible signal levels at the receiver *for a given set of signal levels at each transmitter*. Thus beamforming is actually optimal in a certain sense. The flaw in this reasoning is that it completely neglects the effect of coherent excitation on power losses. While it is true that the received signal is enhanced by

coherent beamforming, the power transfer *efficiency* overall may not increase proportionally depending on what it does to the power losses.

The above intuitive interpretation is also supported by our experimental results. When we attempt to transmit power to receiver 1, the receiver 2 acts as a parasitic loss element. The beamforming solution is independent of the channels from the transmitters to receiver 2 and depends only on the channels to receiver 1. In contrast, the optimal solution fully incorporates all the relevant channel information. Indeed when we observe the amount of power transferred to the undesired receiver 2, we find that the optimal solution, $\tilde{\mathbf{i}}_\mathbf{1}$ results in an efficiency of 6.9% for receiver coil 2 which is the smaller than the 8.9% efficiency obtained by using equal power and conjugate beamforming. In other words, the optimal solution has the effect of not only maximizing the power in receive coil 1 but also minimizes the power delivered to the parasitic receiver coil 2.

Now, we can also examine the case where our aim is to maximize power transfer efficiency to receive coil 2, and receiver 1 behaves as the parasitic element. The optimal solution in this case is given by

$$\tilde{\mathbf{i}}_\mathbf{2} = k_4 \left[1\angle 0^\circ; 0.6\angle -10.4^\circ; 3.4\angle -15.9^\circ; 0.4\angle -35.9^\circ\right]^T \text{A}$$

and the equal power ($\mathbf{i_{eq,2}}$) and conjugate beamforming ($\mathbf{i_{conj,2}}$) solution for receiver coil 2 are

$$\mathbf{i_{eq,2}} = k_5 \left[1\angle 0^\circ; 1\angle 10^\circ; 1\angle 0.6^\circ; 1\angle -1.7^\circ\right]^T \text{A}$$

and

$$\mathbf{i_{conj,2}} = k_6 \left[1.0\angle 0^\circ; 1.0\angle 10^\circ; 3.3\angle 0.6^\circ; 0.7\angle -1.7^\circ\right]^T \text{A}$$

It can be seen from Fig. 4.6 that transmit coil 3 is co-planar and closer to receive coil 2 and hence, has strong coupling co-efficient to receive coil 2 as compared to three other transmit coils, which is reflected in $\mathbf{c_2}$.

As a result of this strong coupling between transmit coils 3 and receive coil 2, the optimal solution is heavily weighted to transmit coil 3. The maximum achievable efficiency is 13.4% which is significantly better than 8.9% efficiency obtained by using the well-known method of equal power beamforming [42] and marginally better than 13% efficiency achieved by conjugate beamforming. The phase of the received voltage due to transmit coils 1, 2, 3 and 4 are 15.3°, 4.0°, -1.2°, -18.9°respectively and is different from the beamforming excitation. Similar to the case of maximizing efficiency to receiver coil 1, the effect of amplitude mismatch between optimal and equal power beamforming excitation has a more pronounced effect on efficiency as compared to phase mismatch between optimal excitation and beamforming. Since most of the received power is due to coil 3, the conjugate beamforming solution by virtue of having roughly the same magnitude on transmit coil 3 as that of the optimal excitation, suffers only a small efficiency degradation as compared to the optimal solution.

The optimal solution, $\tilde{\mathbf{i}}_\mathbf{2}$ results in an efficiency of 9.9% to the undesired receiver coil 1 which is again the smallest as compared to the 14.1% efficiency obtained by using equal power and 11.7% efficiency obtained by conjugate beamforming. We note that equal power beamforming solution, $\mathbf{i_{eq,2}}$ actually delivers more power to parasitic receiver coil 1 instead of the desired receive coil 2, which confirms our intuitive

explanation of the sub-optimality of beamforming.

Table 4.5: Measurements with four-transmitters when two coils are excited

i_1 (mA)	i_2 (mA)	i_3 (mA)	i_4 (mA)	v_1 (mV)	v_2 (mV)
mag, phase	mag, phase	mag, phase	mag, phase	mag, phase	mag, phase
32.9, 0°	33.2, 2.5°	0	0	525.6, -85.1°	537.2, -85.6°
32.5, 0°	0	32.6, 1.7°	0	601.5, -85.0°	45.2, -82.7°
32.7, 0°	0	0	32.8, 2.6°	577.9, -85.6°	3.5, -4.9°
0	31.4, 0°	32.6, 2.0°	0	28.2, -81.0°	597.2, -85.5°
0	32.5, 0°	0	32.8, 2.2°	4.0, 42.5°	594.6, -85.4°
0	0	32.3, 0°	32.6, 1.0°	82.4, -85.2°	86.2, -85.5°

v_3(mV)	v_4 (mV)	$i_{0,1}$(mA)	$i_{0,2}$(mA)
mag, phase	mag, phase	mag, phase	mag, phase
119.4, -85.0°	59.1, -83.9°	0.9, -77.5°	0.8, -77.0°
604.0, -85.6°	71.7, -83.0°	1.4, -77.3°	1.6, -78.0°
99.6, -83.8°	593.3, -85.6°	1.6, -78.3°	0.6, -76.3°
616.5, -85.5°	82.4, -86.4°	1.4, -77.4°	1.6, -78.0°
114.9, -84.2°	600.9, -86.0°	1.7, -78.1°	0.7, -76.3°
614.5, -85.3°	599.1, -86.5°	2.1, -78.8°	1.6, -77.9°

We made additional measurements to check the reliability of the estimated model parameters and hence, the efficiency calculations. Table 4.5 shows the phasor measurements which were obtained by simultaneously exciting two of the four transmit coils. We compute the measured efficiency as the ratio of measured load power and measured input power. Using the measurements, we calculate the total input power (P_G) and the load power (P_L) as

$$P_G = \sum_k \Re(v_k i_k^*); \qquad P_L = \Re(v_0 i_0^*) \tag{4.38}$$

We compare the measured efficiency against the predicted efficiency, where the latter is computed by using the estimated model parameters to estimate the load and total input power for the given excitation current vectors using (4.33) and (4.34) respectively.

Figure 4.8 shows the measured and predicted efficiencies in receiver coil 2 for the measurements shown in Table 4.5. We can observe that the predicted efficiency closely matches with the measured efficiency (difference being less than 2%). Similarly, for receiver coil 1 with the measurements in Table 4.4, the predicted and measured efficiencies are shown in Fig. 4.7 and in this case too, the predicted efficiency matches the measured efficiency for most of the measurements (to within an error of 2%) expect one measurement (index 9), where the error is slightly higher at 4%.

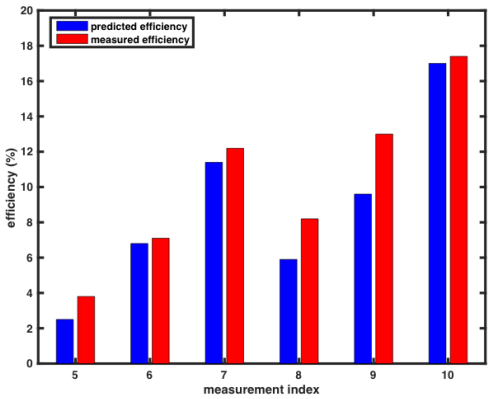

Figure 4.7: Predicted and measured efficiency for receiver coil 1 when two transmit coils are simultaneously excited

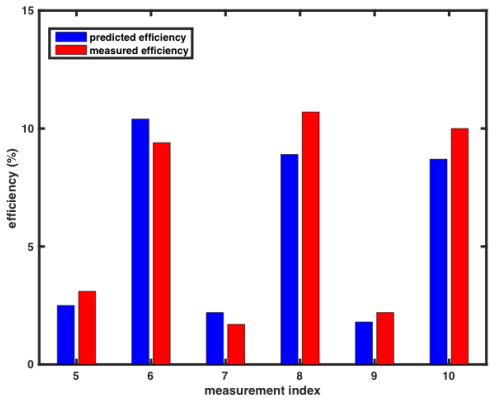

Figure 4.8: Predicted and measured efficiency for receiver coil 2 when two transmit coils are simultaneously excited

Hence, we conclude that the measurements are quite stable and we also observed that the measurements are highly repeatable.

CHAPTER 5
CONCLUSION AND FUTURE RESEARCH

5.1 Summary

In this work, we addressed the problems of precoder design for maximizing the two Figures of Merits, communication capacity and received power from a wideband distributed transmit array to a receiver node. We showed that these two FOMs are equivalent for the narrowband case; however, they result in vastly different optimality criterion for precoders in the wideband case. In chapter 2, we presented the optimality criterion for both the capacity and power maximizing precoders and established that

1. the maximum sum-rate capacity of a MAC channel always provides a strict lower bound on the capacity achieved by distributed beamforming.
2. at high SNR, the equal power beamforming precoder achieves the maximum capacity.
3. at low SNR, the precoder that maximizes the received power also maximizes the capacity.

In chapter 3, we presented fixed point algorithms to compute the precoders that maximize the two FOMs and showed that with the help of feedback from cooperating receiver we could implement these algorithms in a distributed manner assuming prior CSI knowledge at each node. We also presented simulation results that learn the precoders using these fixed point algorithms and compared the gains against simple alternatives like equal-power beamforming.

The idea of maximizing received power suggests a natural application of wireless charging. However, the large propagation losses associated with radiative fields makes antennas unattractive for building wireless power transfer systems and hence, most of the practical WPT systems use near-field inductive coupling to transfer power. In Chapter 4, we described a novel abstract model for optimizing the efficiency of a WPT system with multiple transmitters to a single receiver coil. We also presented a simple and also a robust estimation procedure to measure the model parameters and an iterative algorithm to update these parameters. We also conducted numerous experiments and demonstrated the potential efficiency increases achieved with this approach.

5.2 Open problems

We now present some future research directions that are a natural extension of this work.

1. Wideband Precoder Estimation without Prior CSI using aggregate feedback: In Chapter 3, we established the fact that availability of aggregate feedback from a receiver helps in implementing the fixed point algorithms that compute the capacity or received power maximizing precoder in a distributed manner with prior channel information at each transmitting node. Also, in [44], we presented an approach based on aggregate feedback to directly learn the precoder without prior channel knowledge in the narrowband scenario, where each node in the array applies a sequence of pseudo-random perturbations to their array weights

and observe their combined effects on the received signal by which each node can learn its own precoder to the receiver over time.

Note: In the case of narrowband beamforming, learning the precoding weights is equivalent to learning the self CSI. Since we decompose the wideband channel to N narrowband sub-channels, we can beamform on all the sub-channels simultaneously and learn the CSI by learning the precoding weights on these N sub-channels.

With the above observation in mind, we can learn the wideband precoder using a two-stage process: in the first stage, the array nodes use a number of time-slots to obtain self CSI using only aggregate feedback and in the second stage, take advantage of fixed point algorithms to compute the precoders that maximize the capacity or received power. Both stages rely only on the same aggregate feedback from the receiver.

One potential future work is to develop algorithms that merge the two stages to learn the precoder into a single step process, i.e. the array nodes need not wait until they have sufficiently accurate self CSI to begin the precoder estimation. Also, the method proposed in [44] to learn the channel is very slow as the channel learning process relies on the principle of the weak law of large numbers. Another potential future work is to develop algorithms that help us learn the channels more quickly using aggregate feedback.

2. WPT systems with multiple receive coils: Our abstract model for WPT can be easily generalized to model multiple receiver coils. Using multiple receive

coils, we can choose to maximize power transferred to certain receiver coils and minimize power delivered to other receiver coils. These systems are of tremendous interest in biomedical applications where we can use one receive coil to charge the implant devices by maximizing power delivered to this coil and use other receive coils to reduce power delivered to sensitive tissues around the implant devices in the human body.

3. Communication in WPT systems: Our abstract circuit model assumes that the receiver coils can communicate back to the transmit coil array. Exploring methods for communication protocols and achievable capacity in the near-field communication range are of high importance for helping us build a real-time WPT system.

Appendix 1

Proof of Lemma 2.1

Lemma 2.1 *The input power distribution that maximizes the sum-rate capacity of a narrowband cooperative Gaussian MAC channel is also Gaussian, whose covariance matrix has rank 1. Additionally, beamforming maximizes the capacity of this channel.*

Proof: Consider n nodes with narrowband channels to the receiver and with i-th node transmitting a message signal, $\mathrm{x_i}$. The input covariance matrix is,

$$E[\mathbf{x}\mathbf{x}^{\mathbf{H}}] = \begin{bmatrix} P_1 & \rho_{12}\sqrt{P_1P_2} & \dots & \rho_{1n}\sqrt{P_1P_n} \\ \rho_{12}^*\sqrt{P_1P_2} & P_2 & \dots & \rho_{2n}\sqrt{P_2P_n} \\ \vdots & \vdots & \vdots & \vdots \\ \rho_{1n}^*\sqrt{P_1P_n} & \rho_{2n}^*\sqrt{P_2P_n} & \dots & P_n \end{bmatrix} \tag{1}$$

where $\mathbf{x} = [\mathrm{x_1}, \mathrm{x_2}, ..., \mathrm{x_n}]^T$ and ρ_{ij} is the correlation coefficient between x_i and x_j. Also, the maximum transmit power at each node is denoted by P_i, i.e., $E[|x_i|^2] \leq P_i$. The received signal is given by:

$$y = h_1x_1 + h_2x_2 + ... + h_nx_n + z \tag{2}$$

where h_i is the complex channel gain from i-th node to the receiver and $z \sim N(0, \sigma^2)$ is AWGN.

The maximum sum rate capacity of the channel is given by [41]:

$$C = \underset{p(x_1,x_2,...,x_n)}{\operatorname{argmax}} \ \mathcal{I}(x_1, x_2, ..., x_n; y) \tag{3}$$

and the mutual information is given by

$$\begin{aligned}\mathcal{I}(x_1, x_2, ..., x_n; y) &= h(y) - h(y|x_1, x_2, ..., x_n) \\ &= h(y) - h(z) \\ &= h(y) - \frac{1}{2}\log(2\pi e\sigma^2) \\ &\leq \frac{1}{2}\log(2\pi e\sigma_y^2(\boldsymbol{\rho})) - \frac{1}{2}\log(2\pi e\sigma^2) \qquad (4)\end{aligned}$$

with equality iff $y \sim N\left(0, \sigma_y^2(\boldsymbol{\rho})\right)$, where we explicitly denote the dependence of received signal power on correlation coefficients by $\sigma_y^2(\boldsymbol{\rho})$. Since the channel is AWGN, the input capacity maximizing distribution is also the Gaussian distribution

To maximize capacity given by (3), we need to maximize the mutual information given by (4), which can be achieved by maximizing the received signal power, $\sigma_y^2(\boldsymbol{\rho})$. The power in the received signal is given by,

$$\begin{aligned}\sigma_y^2(\boldsymbol{\rho}) = E[|y|^2] &= E\left[|h_1x_1 + h_2x_2 + ... + h_nx_n + z|^2\right] \\ &= \sum_{i=1}^{n} |h_i|^2 E[x_i^2] + 2\sum_{\substack{i=1;j=1 \\ i>j}}^{n} \Re\left(h_ih_j^* E[x_ix_j^*]\right) + \sigma^2 \\ &= \sum_{i=1}^{n} |h_i|^2 P_i + 2\sum_{\substack{i=1;j=1 \\ i>j}}^{n} \Re\left(h_ih_j^*\rho_{ij}\right)\sqrt{P_iP_j} + \sigma^2 \\ &= \sum_{i=1}^{n} |h_i|^2 P_i + 2\sum_{\substack{i=1;j=1 \\ i>j}}^{n} \Re\left(e^{j\Delta\phi_{ij}}\rho_{ij}\right)|h_i||h_j|\sqrt{P_iP_j} + \sigma^2 \\ &\leq \left(|h_1|\sqrt{P_1} + |h_2|\sqrt{P_2} + ... + |h_n|\sqrt{P_n}\right)^2 + \sigma^2 \qquad (5)\end{aligned}$$

with equality iff $\rho_{ij} \equiv e^{-j\Delta\phi_{ij}} \quad \forall i, j$, where

$$h_i = |h_i|e^{j\phi_i} \quad \text{and} \quad \Delta\phi_{ij} = \phi_i - \phi_j \qquad (6)$$

With $\rho_{ij} \equiv e^{-j\Delta\phi_{ij}} \quad \forall i,j$ and using (6),

$$E[\mathbf{x}\mathbf{x}^{\mathbf{H}}] = \begin{bmatrix} P_1 & e^{-j\Delta\phi_{12}}\sqrt{P_1P_2} & \dots & e^{-j\Delta\phi_{1n}}\sqrt{P_1P_n} \\ e^{j\Delta\phi_{12}}\sqrt{P_1P_2} & P_2 & \dots & e^{-j\Delta\phi_{2n}}\sqrt{P_2P_n} \\ \vdots & \vdots & \vdots & \vdots \\ e^{j\Delta\phi_{1n}}\sqrt{P_1P_n} & e^{-\Delta\phi_{2n}}\sqrt{P_2P_n} & \dots & P_n \end{bmatrix}$$

$$= \begin{bmatrix} e^{-j\phi_1}\sqrt{P_1} \\ e^{-j\phi_2}\sqrt{P_2} \\ \vdots \\ e^{-j\phi_n}\sqrt{P_n} \end{bmatrix} \begin{bmatrix} e^{j\phi_1}\sqrt{P_1} & e^{j\phi_2}\sqrt{P_2} & \dots & e^{j\phi_n}\sqrt{P_n} \end{bmatrix}$$

i.e., the co-variance matrix has rank 1.

Additionally, we note that choosing the message signals that satisfy the above covariance matrix results in received power given by (5) which is the power achieved by the beamforming solution, hence, proving the optimality of beamforming solution in the case of cooperative Gaussian MAC channel.

Proof of Theorem

Theorem 2.2 *Let $C_{\max}(\boldsymbol{H})$ and $C_{\text{eq}}(\boldsymbol{H})$ denote the maximum capacity with distributed beamforming and equal power beamforming respectively. Then,*

$$\text{Lim}_{\gamma\to\infty} \frac{C_{\max}(\gamma\boldsymbol{H})}{C_{\text{eq}}(\gamma\boldsymbol{H})} = 1$$

Proof: The capacity of distributed beamforming is given by:

$$C = \sum_{k=1}^{K} \log\left(1 + \left(\sum_{i=1}^{n} g_i(f_k)h_i(f_k)\right)^2\right)$$

We use $C(\gamma)$ (drop the explicit dependence on channel gains, $\mathbf{H}$) to denote the achievable capacity when the channels are scaled by a factor of $\sqrt{\gamma}$ and is given by

$$C(\gamma) = \sum_{k=1}^{K} \log\left(1 + \gamma\left(\sum_{i=1}^{n} g_i(f_k)h_i(f_k)\right)^2\right)$$

and the scaling constant $\sqrt{\gamma}$ can be varied to change the SNR.

The optimal precoder that maximizes the capacity of the scaled channel is denoted by $\tilde{g}_i(f_k)$ and because of the power constraint, we have

$$\tilde{g}_i(f_k) \leq 1 \quad \forall i,k \tag{7}$$

The equal power beamforming precoder distributes unit power equally in all K subcarriers, i.e, $g_i^{(eq)}(f_k) = \frac{1}{\sqrt{K}}$, and the capacity of equal power beamforming is given by

$$C_{\text{eq}}(\gamma) = \sum_{k=1}^{K} \log\left(1 + \gamma\left(\sum_{i=1}^{n} \frac{1}{\sqrt{K}} h_i(f_k)\right)^2\right) = \sum_{k=1}^{K} \log\left(1 + \frac{\gamma}{K}\left(\sum_{i=1}^{n} h_i(f_k)\right)^2\right)$$

Consider the ratio of maximum achievable capacity and capacity achieved by equal power beamforming and by definition, this ratio is always greater than or equal to 1, i.e.,

$$\frac{C_{\max}(\gamma)}{C_{\text{eq}}(\gamma)} = \frac{\sum_{k=1}^{K} \log\left(1 + \gamma\left(\sum_{i=1}^{n} \tilde{g}_i(f_k) h_i(f_k)\right)^2\right)}{\sum_{k=1}^{K} \log\left(1 + \frac{\gamma}{K}\left(\sum_{i=1}^{n} h_i(f_k)\right)^2\right)} \geq 1 \tag{8}$$

Define,

$$T(f_k) = \left(\sum_{i=1}^{n} \tilde{g}_i(f_k) h_i(f_k)\right)^2 \quad \text{and} \quad M(f_k) = \frac{1}{K}\left(\sum_{i=1}^{n} h_i(f_k)\right)^2 \tag{9}$$

We note that using Cauchy-Swartz inequality and (7),

$$T(f_k) \leq \left(\sum_{i=1}^{n} \tilde{g}_i^2(f_k)\right)\left(\sum_{i=1}^{n} h_i^2(f_k)\right) \leq n\left(\sum_{i=1}^{n} h_i^2(f_k)\right) \tag{10}$$

and as the channel gains, $\mathbf{H}$ are finite, $\exists$ constants $0 \leq B < \infty$ and $0 \leq L < \infty$ such that

$$T(f_k) \leq B \quad \text{and} \quad M(f_k) \leq L \tag{11}$$

As a result of (11), using (9) in (8),

$$\begin{aligned}
\lim_{\gamma\to\infty}\frac{C_{\max}(\gamma)}{C_{\text{eq}}(\gamma)} &= \lim_{\gamma\to\infty}\frac{\sum_{k=1}^{K}\log\left(1+\gamma T(f_k)\right)}{\sum_{k=1}^{K}\log\left(1+\gamma M(f_k)\right)} \\
&= \lim_{\gamma\to\infty}\frac{\sum_{k=1}^{K}\log\left(\gamma\left(T(f_k)+\frac{1}{\gamma}\right)\right)}{\sum_{k=1}^{K}\log\left(\gamma\left(M(f_k)+\frac{1}{\gamma}\right)\right)} \\
&= \lim_{\gamma\to\infty}\frac{K\log(\gamma)+\sum_{k=1}^{K}\log\left(T(f_k)+\frac{1}{\gamma}\right)}{K\log(\gamma)+\sum_{k=1}^{K}\log\left(M(f_k)+\frac{1}{\gamma}\right)} \\
&= \lim_{\gamma\to\infty}\frac{K+\frac{\sum_{k=1}^{K}\left(\log\left(T(f_k)+\frac{1}{\gamma}\right)\right)}{\log(\gamma)}}{K+\frac{\sum_{k=1}^{K}\left(\log\left(M(f_k)+\frac{1}{\gamma}\right)\right)}{\log(\gamma)}}=1
\end{aligned}$$

Hence,

$$\lim_{\gamma\to\infty}\frac{C_{\max}(\gamma)}{C_{\text{eq}}(\gamma)}=1$$

Proof of Theorem

Theorem 2.3 *With distributed beamforming, let $C_{\text{pow}}(\boldsymbol{H})$ denote the achievable capacity with power maximizing precoder and $C_{\max}(\boldsymbol{H})$ denote the maximum achievable capacity . Then,*

$$\text{Lim}_{\gamma\to 0}\ \frac{C_{\text{pow}}(\gamma\boldsymbol{H})}{C_{\max}(\gamma\boldsymbol{H})}=1$$

Proof: The capacity, $C(\gamma)$ and received power, $P_R(\gamma)$ when the channels are scaled by a factor of $\sqrt{\gamma}$ are given by

$$C(\gamma)=\sum_{k=1}^{K}\log\left(1+\gamma\left(\sum_{i=1}^{n}g_i(f_k)h_i(f_k)\right)^2\right);\ P_R(\gamma)=\gamma\sum_{k=1}^{K}\left(\sum_{i=1}^{n}g_i(f_k)h_i(f_k)\right)^2$$

and let the power maximizing precoder and the capacity maximizing precoder of the scaled channels be denoted by $g_{i,\gamma}^{(c)}(f_k)$ and $g_i^{(p)}(f_k)$, respectively, and because of the

power constraint, we have

$$g_{i,\gamma}^{(c)}(f_k) \leq 1 \quad \text{and} \quad g_i^{(p)}(f_k) \leq 1 \quad \forall i,k \tag{12}$$

Note: Since, the power maximizing precoder is scale-independent from Property 2.4 in section 2.3.1, $g_{i,\gamma}^{(p)}(f_k) = g_i^{(p)}(f_k)$.

The achievable capacity with the power maximizing precoder is given by

$$C_{\text{pow}}(\gamma) = \sum_{k=1}^{K} \log\left(1 + \gamma S_{\text{p}}^2(f_k)\right) \tag{13}$$

where $S_{\text{p}} = \sum_{i=1}^{n} g_i^{(p)}(f_k) h_i(f_k)$, and the maximum achievable capacity is,

$$C_{\max} = \sum_{k=1}^{K} \log\left(1 + \gamma S_{\text{c}}^2(f_k)\right) \tag{14}$$

where $S_{\text{c}} = \sum_{i=1}^{n} g_{i,\gamma}^{(c)}(f_k) h_i(f_k)$.

Consider,

$$R(\gamma) \equiv \frac{C_{\text{pow}}(\gamma)}{C_{\max}(\gamma)} \tag{15}$$

and by definition, $R(\gamma) \leq 1$.

Now, using (13) and (14)

$$\begin{aligned} \lim_{\gamma \to 0} R(\gamma) &= \lim_{\gamma \to 0} \frac{\sum_{k=1}^{K} \log\left(1 + \gamma S_{\text{p}}^2(f_k)\right)}{\sum_{k=1}^{K} \log\left(1 + \gamma S_{\text{c}}^2(f_k)\right)} \\ &= \lim_{\gamma \to 0} \frac{\sum_{k=1}^{K} \log\left(1 + \gamma S_{\text{p}}^2(f_k)\right)}{\gamma \sum_{k=1}^{K} S_{\text{p}}^2(f_k)} \frac{\gamma \sum_{k=1}^{K} S_{\text{c}}^2(f_k)}{\sum_{k=1}^{K} \log\left(1 + \gamma S_{\text{c}}^2(f_k)\right)} \frac{\sum_{k=1}^{K} S_{\text{p}}^2(f_k)}{\sum_{k=1}^{K} S_{\text{c}}^2(f_k)} \end{aligned} \tag{16}$$

Using L'Hospital's Rule,

$$\lim_{\gamma \to 0} \frac{\sum_{k=1}^{K} \log\left(1 + \gamma S_{\text{p}}^2(f_k)\right)}{\gamma \sum_{k=1}^{K} S_{\text{p}}^2(f_k)} = \lim_{\gamma \to 0} \frac{1}{\sum_{k=1}^{K} S_{\text{p}}^2(f_k)} \sum_{k=1}^{K} \left(\frac{S_{\text{p}}^2(f_k)}{1 + \gamma \sum_{k=1}^{K} S_{\text{p}}^2(f_k)} \right) = 1 \tag{17}$$

and similarly,

$$\lim_{\gamma \to 0} \frac{\gamma \sum_{k=1}^{K} S_{\text{c}}^2(f_k)}{\sum_{k=1}^{K} \log\left(1 + \gamma S_{\text{c}}^2(f_k)\right)} = 1 \tag{18}$$

Hence, using (17) and (18) in (16), we have

$$\begin{aligned}\lim_{\gamma\to 0} R(\gamma) &= \frac{\sum_{k=1}^{K} S_{\text{pow}}^2(f_k)}{\sum_{k=1}^{K} S_{\text{cap}}^2(f_k)} \\ &= \frac{\sum_{k=1}^{K}\left(\sum_{i=1}^{n} g_i^{(p)}(f_k)h_i(f_k)\right)^2}{\sum_{k=1}^{K}\left(\sum_{i=1}^{n} g_{i,\gamma}^{(c)}(f_k)h_i(f_k)\right)^2} \\ &= \frac{P_R^{(\max)}}{P_R^{(\text{cap})}} \geq 1 \end{aligned} \tag{19}$$

where $P_R^{(\max)}$ and $P_R^{(\text{cap})}$ are the maximum received power and the received power with capacity maximizing precoder, respectively. Hence, from (15) and (19), we have

$$\lim_{\gamma\to 0} R(\gamma) \equiv \lim_{\gamma\to 0} \frac{C_{\text{pow}}(\gamma)}{C_{\max}(\gamma)} = 1$$

Proposition: Let $g_i^{(c)}(f_k)$ and $g_i^{(p)}(f_k)$ denote the capacity and power maximizing precoders at a subchannel frequency f_k respectively. Then,

$$\lim_{\gamma\to 0} \frac{g_{i,\gamma}^{(c)}(f_k)}{g_i^{(p)}(f_k)} = 1$$

where $g_{i,\gamma}^{(c)}(f_k)$ and $g_i^{(p)}(f_k)$ denote the capacity and power maximizing precoder when the channels are scaled by a factor, $\sqrt{\gamma}$.

The above can be shown using (19) as the equality holds only when $P_R^{(\max)} = P_R^{(\text{cap})}$.

From the above Corollary, we state that the precoders that maximize the capacity and received power are equivalent at low SNR.

Appendix 2

Iterative updates for the conductance matrix and transgain vectors

The least squares estimate of the conductance matrix, $\hat{\mathbf{G}}[n]$ and transgain vector $\hat{\mathbf{a}}^{\mathbf{H}}[n]$ when a set of "n" measurements are

$$\begin{aligned} \hat{\mathbf{G}}[n] &= \mathbf{J}[n]\mathbf{V}^H[n]\left(\mathbf{V}[n]\mathbf{V}^H[n]\right)^{-1} \\ \text{and } \hat{\mathbf{a}}^{\mathbf{H}}[n] &= \mathbf{v_0}[n]\mathbf{V}^H[n]\left(\mathbf{V}[n]\mathbf{V}^H[n]\right)^{-1} \end{aligned} \tag{20}$$

where $\mathbf{V}[n] = [\mathbf{v}[1], \mathbf{v}[2], ..., \mathbf{v}[n]]$ and $\mathbf{J}[n] = [\mathbf{i}[1], \mathbf{i}[2], ..., \mathbf{i}[n]]$. After the $(n+1)$-th measurement, when the voltage vector, $\mathbf{v}[n+1]$ is applied across the transmit coils, the measured input currents and output voltage are denoted by $\mathbf{i}[n+1]$ and $v_0[n+1]$, respectively. The matrix of applied voltages and measured currents are

$$\mathbf{V}[n+1] = [\mathbf{V}[n] \;\; \mathbf{v}[\mathbf{n+1}]] \;\text{ and }\; \mathbf{J}[n+1] = [\mathbf{J}[n] \;\; \mathbf{i}[\mathbf{n+1}]] \tag{21}$$

and vector of measured output voltages is

$$\mathbf{v_0}[n+1] = [v_0[1], v_0[2], ..., v_0[n+1]] \tag{22}$$

From (21),

$$\begin{aligned} \mathbf{V}[n+1]\mathbf{V}^H[n+1] &= [\mathbf{V}[n] \;\; \mathbf{v}[\mathbf{n+1}]] \begin{bmatrix} \mathbf{V}^H[n] \\ \mathbf{v}^{\mathbf{H}}[n+1] \end{bmatrix} \\ &= \mathbf{V}[n]\mathbf{V}^H[n] + \mathbf{v}[n+1]\mathbf{v}^{\mathbf{H}}[n+1] \end{aligned}$$

and we observe the following :

1. Using the Matrix Inversion Lemma,

$$\begin{aligned}\left(\mathbf{V}[n+1]\mathbf{V}^H[n+1]\right)^{-1} &= \left(\mathbf{V}[n]\mathbf{V}^H[n]+\mathbf{v}[n+1]\mathbf{v}^{\mathbf{H}}[n+1]\right)^{-1} \\ &= \left(\mathbf{V}[n]\mathbf{V}^H[n]\right)^{-1} \\ &\quad \left(\mathbf{I}-\frac{\mathbf{v}[n+1]\mathbf{v}^{\mathbf{H}}[n+1]\left(\mathbf{V}[n]\mathbf{V}^H[n]\right)^{-1}}{1+\mathbf{v}^{\mathbf{H}}[n+1]\left(\mathbf{V}[n]\mathbf{V}^H[n]\right)^{-1}\mathbf{v}[n+1]}\right) \quad (23)\end{aligned}$$

Note: The above equation can be used to update the pseduo-inverse as follows:

$$\begin{aligned}\mathbf{P}[n+1] &= \left(\mathbf{V}[n+1]\mathbf{V}^H[n+1]\right)^{-1} \\ &= \mathbf{P}[n]\left(\mathbf{I}-\frac{\mathbf{v}[n+1]\mathbf{v}^{\mathbf{H}}[n+1]\mathbf{P}[n]}{1+\mathbf{v}^{\mathbf{H}}[n+1]\mathbf{P}[n]\mathbf{v}[n+1]}\right)\end{aligned}$$

2. Also, from (21)

$$\begin{aligned}\mathbf{J}[n+1]\mathbf{V}^H[n+1] &= \left[\mathbf{J}[n] \;\; \mathbf{i}[n+1]\right]\begin{bmatrix}\mathbf{V}^H[n] \\ \mathbf{v}^{\mathbf{H}}[n+1]\end{bmatrix} \\ &= \mathbf{J}[n]\mathbf{V}^H[n]+\mathbf{i}[n+1]\mathbf{v}^{\mathbf{H}}[n+1] \quad (24)\end{aligned}$$

and from (22),

$$\begin{aligned}\mathbf{v_0}[n+1]\mathbf{V}^H[n+1] &= \left[\mathbf{v_0}[n] \;\; v_0[n+1]\right]\begin{bmatrix}\mathbf{V}^H[n] \\ \mathbf{v}^{\mathbf{H}}[n+1]\end{bmatrix} \\ &= \mathbf{v_0}[n]\mathbf{V}^H[n]+v_0[n+1]\mathbf{v}^{\mathbf{H}}[n+1] \quad (25)\end{aligned}$$

3. We also observe that,

$$\begin{aligned}
&\mathbf{v^H}[n+1]\left(\mathbf{V}[n]\mathbf{V}^H[n]\right)^{-1}\left(\mathbf{I}-\frac{\mathbf{v}[n+1]\mathbf{v^H}[n+1]\left(\mathbf{V}[n]\mathbf{V}^H[n]\right)^{-1}}{1+\mathbf{v^H}[n+1]\left(\mathbf{V}[n]\mathbf{V}^H[n]\right)^{-1}\mathbf{vi}[n+1]}\right)\\
&\quad=\frac{\mathbf{v^H}[n+1]\left(\mathbf{V}[n]\mathbf{V}^H[n]\right)^{-1}}{1+\mathbf{v^H}[n+1]\left(\mathbf{V}[n]\mathbf{V}^H[n]\right)^{-1}\mathbf{v}[n+1]}\\
&\quad+\frac{\mathbf{v^H}[n+1]\left(\mathbf{V}[n]\mathbf{V}^H[n]\right)^{-1}\left(\mathbf{v^H}[n+1]\left(\mathbf{V}[n]\mathbf{V}^H[n]\right)^{-1}\mathbf{v}[n+1]\right)}{1+\mathbf{v^H}[n+1]\left(\mathbf{V}[n]\mathbf{V}^H[n]\right)^{-1}\mathbf{v}[n+1]}\\
&\quad-\frac{\left(\mathbf{v^H}[n+1]\left(\mathbf{V}[n]\mathbf{V}^H[n]\right)^{-1}\mathbf{v}[n+1]\right)\mathbf{v^H}[n+1]\left(\mathbf{V}[n]\mathbf{V}^H[n]\right)^{-1}}{1+\mathbf{v^H}[n+1]\left(\mathbf{V}[n]\mathbf{V}^H[n]\right)^{-1}\mathbf{v}[n+1]}\\
&\quad=\frac{\mathbf{v^H}[n+1]\left(\mathbf{V}[n]\mathbf{V}^H[n]\right)^{-1}}{1+\mathbf{v^H}[n+1]\left(\mathbf{V}[n]\mathbf{V}^H[n]\right)^{-1}\mathbf{v}[n+1]}
\end{aligned}\tag{26}$$

First, we deal with the least square estimate of the conductance matrix and the $(n+1)$-th estimate is given by,

$$\hat{\mathbf{G}}[\mathbf{n+1}]=\mathbf{J}[n+1]\mathbf{V}^H[n+1]\left(\mathbf{V}[n+1]\mathbf{V}^H[n+1]\right)^{-1}$$

and using (24), (23), (20), (26), in that order

$$\begin{aligned}
\hat{\mathbf{G}}[n+1] &= \left(\mathbf{J}[n]\mathbf{V}^H[n]+\mathbf{i}[n+1]\mathbf{v^H}[n+1]\right)\left(\mathbf{V}[n]\mathbf{V}^H[n]\right)^{-1}\\
&\qquad\left(\mathbf{I}-\frac{\mathbf{v}[n+1]\mathbf{v^H}[n+1]\left(\mathbf{V}[n]\mathbf{V}^H[n]\right)^{-1}}{1+\mathbf{v^H}[n+1]\left(\mathbf{V}[n]\mathbf{V}^H[n]\right)^{-1}\mathbf{v}[n+1]}\right)\\
&= \left(\hat{\mathbf{G}}[n]+\mathbf{i}[n+1]\mathbf{v^H}[n+1]\left(\mathbf{V}[n]\mathbf{V}^H[n]\right)^{-1}\right)\\
&\qquad\left(\mathbf{I}-\frac{\mathbf{v}[n+1]\mathbf{v^H}[n+1]\left(\mathbf{V}[n]\mathbf{V}^H[n]\right)^{-1}}{1+\mathbf{v^H}[n+1]\left(\mathbf{V}[n]\mathbf{V}^H[n]\right)^{-1}\mathbf{v}[n+1]}\right)\\
&= \hat{\mathbf{G}}[n]\left(\mathbf{I}-\frac{\mathbf{v}[n+1]\mathbf{v^H}[n+1]\left(\mathbf{V}[n]\mathbf{V}^H[n]\right)^{-1}}{1+\mathbf{v^H}[n+1]\left(\mathbf{V}[n]\mathbf{V}^H[n]\right)^{-1}\mathbf{v}[n+1]}\right)\\
&\qquad+\frac{\mathbf{i}[n+1]\mathbf{v^H}[n+1]\left(\mathbf{V}[n]\mathbf{V}^H[n]\right)^{-1}}{1+\mathbf{v^H}[n+1]\left(\mathbf{V}[n]\mathbf{V}^H[n]\right)^{-1}\mathbf{v}[n+1]}\\
&= \hat{\mathbf{G}}[n]+\left(\mathbf{i}[n+1]-\hat{\mathbf{G}}[n]\mathbf{v}[n+1]\right)\\
&\qquad\frac{\mathbf{v^H}[n+1]\left(\mathbf{V}[n]\mathbf{V}^H[n]\right)^{-1}}{1+\mathbf{v^H}[n+1]\left(\mathbf{V}[n]\mathbf{V}^H[n]\right)^{-1}\mathbf{v}[n+1]}
\end{aligned}\tag{27}$$

Similarly, we can derive the update equation for the transgain vector as follows: The least square estimate of the transgain vector at the $(n+1)$-th iteration it is given by,

$$\hat{\mathbf{a}}^{\mathbf{H}}[\mathbf{n+1}] = \mathbf{v_0}[n+1]\mathbf{V}^H[n+1]\left(\mathbf{V}[n+1]\mathbf{V}^H[n+1]\right)^{-1}$$

and using (25), (23), (20), (26), in that order

$$\begin{aligned}
\hat{\mathbf{a}}^{\mathbf{H}}[n+1] &= \left(\mathbf{v_0}[n]\mathbf{V}^H[n] + v_0[n+1]\mathbf{v}^{\mathbf{H}}[n+1]\right)\left(\mathbf{V}[n]\mathbf{V}^H[n]\right)^{-1} \\
&\qquad \left(\mathbf{I} - \frac{\mathbf{v}[n+1]\mathbf{v}^{\mathbf{H}}[n+1]\left(\mathbf{V}[n]\mathbf{V}^H[n]\right)^{-1}}{1+\mathbf{v}^{\mathbf{H}}[n+1]\left(\mathbf{V}[n]\mathbf{V}^H[n]\right)^{-1}\mathbf{v}[n+1]}\right) \\
&= \left(\hat{\mathbf{a}}^{\mathbf{H}}[n] + v_0[n+1]\mathbf{v}^{\mathbf{H}}[n+1]\left(\mathbf{V}[n]\mathbf{V}^H[n]\right)^{-1}\right) \\
&\qquad \left(\mathbf{I} - \frac{\mathbf{v}[n+1]\mathbf{v}^{\mathbf{H}}[n+1]\left(\mathbf{V}[n]\mathbf{V}^H[n]\right)^{-1}}{1+\mathbf{v}^{\mathbf{H}}[n+1]\left(\mathbf{V}[n]\mathbf{V}^H[n]\right)^{-1}\mathbf{v}[n+1]}\right) \\
&= \hat{\mathbf{a}}^{\mathbf{H}}[n]\left(\mathbf{I} - \frac{\mathbf{v}[n+1]\mathbf{v}^{\mathbf{H}}[n+1]\left(\mathbf{V}[n]\mathbf{V}^H[n]\right)^{-1}}{1+\mathbf{v}^{\mathbf{H}}[n+1]\left(\mathbf{V}[n]\mathbf{V}^H[n]\right)^{-1}\mathbf{v}[n+1]}\right) \\
&\qquad + \frac{v_0[n+1]\mathbf{v}^{\mathbf{H}}[n+1]\left(\mathbf{V}[n]\mathbf{V}^H[n]\right)^{-1}}{1+\mathbf{v}^{\mathbf{H}}[n+1]\left(\mathbf{V}[n]\mathbf{V}^H[n]\right)^{-1}\mathbf{v}[n+1]} \\
&= \hat{\mathbf{a}}^{\mathbf{H}}[n] + \left(v_0[n+1] - \hat{\mathbf{a}}^{\mathbf{H}}[n]\mathbf{v}[n+1]\right) \\
&\qquad \frac{\mathbf{v}^{\mathbf{H}}[n+1]\left(\mathbf{V}[n]\mathbf{V}^H[n]\right)^{-1}}{1+\mathbf{v}^{\mathbf{H}}[n+1]\left(\mathbf{V}[n]\mathbf{V}^H[n]\right)^{-1}\mathbf{v}[n+1]} \quad (28)
\end{aligned}$$

Hence, the update equations (27) and (28) can be re-written as

$$\hat{\mathbf{G}}[n+1] = \hat{\mathbf{G}}[n] + \mathbf{e_1}[n+1]\mathbf{k}^{\mathbf{H}}[n+1];\ \hat{\mathbf{a}}^{\mathbf{H}}[n+1] = \hat{\mathbf{a}}^{\mathbf{H}}[n] + \mathbf{e_2}[n+1]\mathbf{k}^{\mathbf{H}}[n+1]$$

where the *error* in current and output voltage measurement are given by

$$\mathbf{e_1}[n+1] = \mathbf{i}[n+1] - \hat{\mathbf{G}}[n]\mathbf{v}[n+1] \text{ and } \mathbf{e_2}[n+1] = v_0[n+1] - \hat{\mathbf{a}}^{\mathbf{H}}[n]\mathbf{v}[n+1]$$

and the gain of the estimator is,

$$\mathbf{k}[n+1] = \frac{\left(\mathbf{V}[n]\mathbf{V}^H[n]\right)^{-1}\mathbf{v}[n+1]}{1+\mathbf{v}^{\mathbf{H}}[n+1]\left(\mathbf{V}[n]\mathbf{V}^H[n]\right)^{-1}\mathbf{v}[n+1]}$$

REFERENCES

[1] W. Yu, W. Rhee, S. Boyd, and J. M. Cioffi, "Iterative water-filling for gaussian vector multiple-access channels," *IEEE Transactions on Information Theory*, vol. 50, no. 1, pp. 145–152, 2004.

[2] S. Goguri, R. Mudumbai, D. R. Brown III, S. Dasgupta, and U. Madhow, "Capacity maximization for distributed broadband beamforming," in *appear in Acoustics, Speech, and Signal Processing, 2016. Proceedings.(ICASSP16). IEEE International Conference on*, 2016.

[3] U. Madhow, D. R. Brown, S. Dasgupta, and R. Mudumbai, "Distributed massive mimo: Algorithms, architectures and concept systems," in *Information Theory and Applications Workshop (ITA), 2014*. IEEE, 2014, pp. 1–7.

[4] R. Mudumbai, G. Barriac, and U. Madhow, "On the feasibility of distributed beamforming in wireless networks," *Wireless Communications, IEEE Transactions on*, vol. 6, no. 5, pp. 1754–1763, 2007.

[5] R. G. Gallager, *Information theory and reliable communication*. Springer, 1968, vol. 2.

[6] R. Mudumbai, D. R. Brown III, U. Madhow, and H. V. Poor, "Distributed transmit beamforming: challenges and recent progress," *Communications Magazine, IEEE*, vol. 47, no. 2, pp. 102–110, 2009.

[7] P. Bidigare, U. Madhow, R. Mudumbai, and D. Scherber, "Attaining fundamental bounds on timing synchronization," in *2012 IEEE International Conference on Acoustics, Speech and Signal Processing (ICASSP)*, March 2012, pp. 5229–5232.

[8] R. Mudumbai, J. Hespanha, U. Madhow, and G. Barriac, "Distributed transmit beamforming using feedback control," *IEEE Transactions on Information Theory*, vol. 56, no. 1, pp. 411–426, Jan 2010.

[9] C. Lin, V. V. Veeravalli, and S. P. Meyn, "A random search framework for convergence analysis of distributed beamforming with feedback," *IEEE Transactions on Information Theory*, vol. 56, no. 12, pp. 6133–6141, 2010.

[10] D. R. Brown, R. David, and P. Bidigare, "Improving coherence in distributed miso communication systems with local accelerometer measurements," in *Information Sciences and Systems (CISS), 2015 49th Annual Conference on*. IEEE, 2015, pp. 1–6.

[11] A. Kumar, R. Mudumbai, S. Dasgupta, M. M. U. Rahman, D. R. B. III, U. Madhow, and T. P. Bidigare, "A scalable feedback mechanism for distributed nullforming with phase-only adaptation," *IEEE Transactions on Signal and Information Processing over Networks*, vol. 1, no. 1, pp. 58–70, March 2015.

[12] M. M. Rahman, H. E. Baidoo-Williams, R. Mudumbai, and S. Dasgupta, "Fully wireless implementation of distributed beamforming on a software-defined radio platform," in *Proceedings of the 11th international conference on Information Processing in Sensor Networks*. ACM, 2012, pp. 305–316.

[13] P. Bidigare, M. Oyarzyn, D. Raeman, D. Chang, D. Cousins, R. O'Donnell, C. Obranovich, and D. Brown, "Implementation and demonstration of receiver-coordinated distributed transmit beamforming across an ad-hoc radio network," in *Signals, Systems and Computers (ASILOMAR), 2012 Conference Record of the Forty Sixth Asilomar Conference on*, Nov 2012, pp. 222–226.

[14] F. Quitin, M. M. U. Rahman, R. Mudumbai, and U. Madhow, "A scalable architecture for distributed transmit beamforming with commodity radios: Design and proof of concept," *Wireless Communications, IEEE Transactions on*, vol. 12, no. 3, pp. 1418–1428, 2013.

[15] D. Scherber, P. Bidigare, R. O'Donnell, M. Rebholz, M. Oyarzun, C. Obranovich, W. Kulp, D. Chang, and D. R. Brown, "Coherent distributed techniques for tactical radio networks: Enabling long range communications with reduced size, weight, power and cost," in *Military Communications Conference, MILCOM 2013-2013 IEEE*. IEEE, 2013, pp. 655–660.

[16] B. Peiffer, R. Mudumbai, A. Kruger, A. Kumar, and S. Dasgupta, "Experimental demonstration of a distributed antenna array pre-synchronized for retrodirective transmission," in *Information Sciences and Systems (CISS), 2016 50th Annual Conference on*, March 2016, pp. 1–6.

[17] B. Peiffer, R. Mudumbai, S. Goguri, K. Anton, and S. Dasgupta, "Experimental demonstration of nullforming from a fully-wireless distributed array," in *2016 IEEE Global Conference on Signal and Information Processing,submitted*.

[18] D. J. Love, R. W. Heath Jr, and T. Strohmer, "Grassmannian beamforming for multiple-input multiple-output wireless systems," *Information Theory, IEEE Transactions on*, vol. 49, no. 10, pp. 2735–2747, 2003.

[19] R. Mudumbai, B. Wild, U. Madhow, and K. Ramchandran, "Distributed beamforming using 1 bit feedback: from concept to realization," in *Proceedings of the 44th Allerton conference on communication, control and computation*, 2006, pp. 1020–1027.

[20] P. Bidigare, D. R. Brown III, U. Madhow, R. Mudumbai, A. Kumar, B. Peiffer, and S. Dasgupta, "Wideband distributed transmit beamforming using reciprocity with endogenous relative calibration," in *Asilomar Conference on Signals, Systems, and Computers, 2015 IEEE*. IEEE, 2015.

[21] H. Rahul, S. S. Kumar, and D. Katabi, "Megamimo: Scaling wireless capacity with user demand," *Proc. of ACM SIGCOMM 2012*, 2012.

[22] H. V. Balan, R. Rogalin, A. Michaloliakos, K. Psounis, and G. Caire, "Airsync: Enabling distributed multiuser mimo with full spatial multiplexing," *IEEE/ACM Transactions on Networking (TON)*, vol. 21, no. 6, pp. 1681–1695, 2013.

[23] R. Irmer, H. Droste, P. Marsch, M. Grieger, G. Fettweis, S. Brueck, H.-P. Mayer, L. Thiele, and V. Jungnickel, "Coordinated multipoint: Concepts, performance, and field trial results," *Communications Magazine, IEEE*, vol. 49, no. 2, pp. 102–111, 2011.

[24] M. F. Gencel, M. E. Rasekh, and U. Madhow, "Scaling wideband distributed transmit beamforming via aggregate feedback," in *2015 IEEE International Conference on Communications (ICC)*. IEEE, 2015, pp. 2356–2362.

[25] P. Viswanath, D. N. Tse, and V. Anantharam, "Asymptotically optimal waterfilling in vector multiple-access channels," *Information Theory, IEEE Transactions on*, vol. 47, no. 1, pp. 241–267, 2001.

[26] S. Goguri, D. Ogbe, R. Mudumbai, D. Love, S. Dasgupta, and P. Bidigare, "Maximizing wireless power transfer using distributed beamforming," in *Signals, Systems and Computers, 2016 50th Asilomar Conference on*. IEEE, 2016, pp. 1775–1779.

[27] "System description wireless power transfer," *Wireless Power Consortium Standards*, Apr. 2011.

[28] Z. N. Low, R. A. Chinga, R. Tseng, and J. Lin, "Design and test of a high-power high-efficiency loosely coupled planar wireless power transfer system," *IEEE Transactions on Industrial Electronics*, vol. 56, no. 5, pp. 1801–1812, 2009.

[29] G. Wang, W. Liu, M. Sivaprakasam, and G. A. Kendir, "Design and analysis of an adaptive transcutaneous power telemetry for biomedical implants," *IEEE Transactions on Circuits and Systems I: Regular Papers*, vol. 52, no. 10, pp. 2109–2117, 2005.

[30] S. A. Ahson and M. Ilyas, *RFID handbook: applications, technology, security, and privacy*. CRC press, 2008.

[31] A. Kurs, A. Karalis, R. Moffatt, J. D. Joannopoulos, P. Fisher, and M. Soljačić, "Wireless power transfer via strongly coupled magnetic resonances," *science*, vol. 317, no. 5834, pp. 83–86, 2007.

[32] A. P. Sample, D. T. Meyer, and J. R. Smith, "Analysis, experimental results, and range adaptation of magnetically coupled resonators for wireless power transfer," *IEEE Transactions on Industrial Electronics*, vol. 58, no. 2, pp. 544–554, 2011.

[33] R. Johari, J. V. Krogmeier, and D. J. Love, "Analysis and practical considerations in implementing multiple transmitters for wireless power transfer via coupled magnetic resonance," *IEEE Transactions on Industrial Electronics*, vol. 61, no. 4, pp. 1774–1783, 2014.

[34] D. Ahn and S. Hong, "Effect of coupling between multiple transmitters or multiple receivers on wireless power transfer," *IEEE Transactions on Industrial Electronics*, vol. 60, no. 7, pp. 2602–2613, 2013.

[35] *Electronic Code of Federal Regulations, Part 15: Radio Frequency Devices, F. C. Commission*, vol. Title 47: Telecommunication (47CFR15), 2014.

[36] N. Oodachi, K. Ogawa, H. Kudo, H. Shoki, S. Obayashi, and T. Morooka, "Efficiency improvement of wireless power transfer via magnetic resonance using transmission coil array," in *Antennas and Propagation (APSURSI), 2011 IEEE International Symposium on*. IEEE, 2011, pp. 1707–1710.

[37] I.-J. Yoon and H. Ling, "Investigation of near-field wireless power transfer under multiple transmitters," *IEEE Antennas and Wireless Propagation Letters*, vol. 10, pp. 662–665, 2011.

[38] B. H. Waters, B. J. Mahoney, V. Ranganathan, and J. R. Smith, "Power delivery and leakage field control using an adaptive phased array wireless power system," *IEEE Transactions on Power Electronics*, vol. 30, no. 11, pp. 6298–6309, 2015.

[39] M. Kiani and M. Ghovanloo, "The circuit theory behind coupled-mode magnetic resonance-based wireless power transmission," *IEEE Transactions on Circuits and Systems I: Regular Papers*, vol. 59, no. 9, pp. 2065–2074, Sept 2012.

[40] S. Goguri, R. Mudumbai, and A. Kruger, "Optimizing wireless power transfer with multiple transmitters," in *Information Sciences and Systems (CISS), 2017 51st Annual Conference on, accepted for publication*, 2017.

[41] T. M. Cover and J. A. Thomas, *Elements of Information Theory (Wiley Series in Telecommunications and Signal Processing)*. Wiley-Interscience, 2006.

[42] B. Zhao, N.-C. Kuo, and A. M. Niknejad, "A gain boosting array technique for weakly-coupled wireless power transfer," *IEEE Transactions on Power Electronics*, 2016.

[43] "Product page and spec sheet," [online] http://katalog.we-online.de/pbs/datasheet/760308111.pdf.

[44] S. Goguri, B. Peiffer, R. Mudumbai, and S. Dasgupta, "A class of scalable feedback algorithms for beam and null-forming from distributed arrays," in *Signals, Systems and Computers, 2016 50th Asilomar Conference on*. IEEE, 2016, pp. 1447–1451.